College of ENGINEERING
VILLANOVA UNIVERSITY

Center for Advanced Communications

Villanova University

FINAL REPORT

(6/1/2004 – 6/1/2005)

High Rate Multiuser Cooperative Diversity Systems

Submitted to

Office of Naval Research

Grant No. N00014-04-1-0617

Principal Investigators

Yimin Zhang (PI)
Moeness Amin (Co-PI)

Contributors

Prof. Yimin Zhang
Prof. Moeness Amin
Dr. Genyuan Wang
Ms. Morgan Watson
Mr. Gjergji Kurti

August 2005

Table of Contents

1. Executive Summary

This report presents a comprehensive summary of the research work performed under ONR funding, grant No. N00014-04-1-0167 over the period of June 1, 2004 to June 1, 2005.

The contributors to the research over the span of the funding period are Prof. Yimin Zhang (PI), Prof. Moeness Amin (Co-PI), Dr. Genyuan Wang (Post-Doctoral Fellow), and Mr. Gjergji Kurti (Graduate Student) from Villanova University. Ms. Morgan Watson from NAVSEA Philadelphia has worked closely with the research team at Villanova University and has provided valuable insights into several issues vital to the progress and advances in research.

The results obtained in this project have been disseminated in three submitted journal articles and seven peer-reviewed conference papers. Section 2 lists, with complete citations, all publications acknowledging the ONR support. This list is also used to point the reader to the technical material and the pertinent papers in the report underlying each subsection. Section 3 of this final report includes selected key papers, representing our efforts in different areas covering cooperative diversity, space-time coding, and channel modeling, and spatial correlation study in the sea surface environment. Each of these papers is cast as a subsection with its own abstract, introduction, figure numbers, equation numbers, conclusions, and references.

1.1 Main Contributions

The fundamental objective of this research project is to develop novel cooperative wireless network schemes and practical coding designs that provide unmanned surface vehicles (USV) swarm reliable wireless links with the overall data throughput and the communication quality significantly exceeding those of existing non-cooperative systems. Towards this end, we have made contributions in three areas: (1) We have developed a cooperation protocol that effectively constructs distributed space-time codes for cooperative diversity systems. Depending on application environments, the proposed protocol can be used to construct different distributed space-time codes. For example, high data rate distributed codes can be used to improve the communication efficiency when the channel state information (CSI) is available at the receivers, whereas differential distributed space-time codes can be used to avoid channel estimations in the absence of CSI. (2) We have developed full-rate, large diversity product space-time codes with non-vanishing minimum determinant. The proposed space-time codes are an important component in high-efficiency distributed space-time code construction. (3) We have studied the channel modeling and spatial correlation between different antennas in sea surface environments. The results are important in assessing the performance of cooperative diversity systems in sea surface environments as well as in designing array antenna configurations.

1.2 Cooperative Diversity Techniques

We have developed a protocol for cooperative systems that permits effective use of various multiple-input-multiple-output (MIMO) space-time coding schemes. Based on high-rate MIMO space-time codes and differential space-time codes, the proposed protocol allows the development of high-rate distributed space-time codes and differential distributed space-time codes, respectively, depending on the channel state information (CSI) availability, for the use of USV network systems. A multiuser scenario is considered where all users have their own

information to send, and desire to cooperate with each other in order to maintain reliable communication links and to send the information to the receiver at a high data rate. When the CSI is available at the receivers, this protocol enables the use of high-rate full-diversity space-time codes for the construction of high efficiency distributed space-time codes. On the other hand, when CSI is unavailable at the receivers, differential distributed space-time modulations can be constructed based on the proposed protocol.

Publications [1, 2, 3, 7, 8, 9].

1.3 Space-Time Code Development

Designs of space-time code with full rate, large diversity product, and non-vanishing minimum determinant of codewords continue to attract great attentions. However, in most available determinant non-vanishing space-time codes for three, four and six transmit antennas, the average powers at each layer are different, resulting high peak to average power ratio. In this paper, a new cyclic algebraic space-time design scheme is proposed and the optimal codes in this class are provided by using some specific cyclic field extensions. The class of cyclic algebraic space-time codes not only include the available non-vanishing determinant cyclotomic space-time codes for three, four and six transmit antennas, but also have the desirable property that the optimal codes can be achieved with the same average power at each layer.

Publications [4, 10].

1.4 Channel Modeling and Spatial Correlation Study in Sea Surface Environment

We have studied the propagation environment and technology applicable to multi-sensor communications in USV networks located in a rough sea environment. We first investigated the statistical model of the propagation environment, where we provided the analytical expressions of the wave height, the probability of having line-of-sight (LOS) between two USVs in terms of the weather condition and antenna height, and the spatial correlation of the propagation channels related to different antennas. We have then investigated the fading reduction capability of multiple-input-multiple-output (MIMO) systems and the performance in general Ricean channels assuming different spatial channel correlation values.

Publications [5, 6].

2. List of Publications

[1]* Y. Zhang, G. Wang, M. Watson, and M. G. Amin, "Cooperative wireless network for unmanned surface vehicles," *AUVSI Unmanned Systems*, Anaheim, CA, August 2004.

[2] G. Wang, Y. Zhang, and M. G. Amin, "Cooperation diversity using differential distributed space-time codes," *Joint Conference of Asia-Pacific Conference on Communications and International Symposium on Multi-Dimensional Mobile Communications*, Beijing, China, August 2004.

[3] Y. Zhang, "Differential modulation schemes for decode-and-forward cooperative diversity," *IEEE International Conference on Acoustics, Speech, and Signal Processing*, Philadelphia, PA, March 2005.

[4] G. Wang, J.-K. Zhang, Y. Zhang, and K. M. Wong, "Space-time code designs with non-vanishing determinants for three, four and six transmit antennas," *IEEE International Conference on Acoustics, Speech, and Signal Processing*, Philadelphia, PA, March 2005.

[5]* G. Kurti, Y. Zhang, M. Watson, and M. G. Amin, "Multi-sensor communications in unmanned surface vehicle networks," *Intelligent Ship Symposium*, Villanova, PA, June 2005.

[6] G. Kurti, Y. Zhang, M. G. Amin, and M. Watson, "Spatial correlation for unmanned surface vehicles," *IEEE AP-S International Symposium*, Washington, DC, July 2005.

[7]* Y. Zhang, G. Wang, and M. G. Amin, "Imperfectly synchronized cooperative network using distributed space-frequency coding," *IEEE Vehicular Technology Conference*, Dallas, TX, September 2005. (accepted)

[8]* G. Wang, Y. Zhang, and M. G. Amin, "Differential distributed space-time modulation for cooperative networks," submitted to *IEEE Transactions on Wireless Communications*.

[9] G. Wang, Y. Zhang, and M. G. Amin, "Space-time cooperation diversity using high-rate codes," submitted to *Wireless Personal Communications*.

[10]* G. Wang, J.-K. Zhang, Y. Zhang, M. G. Amin, and K. M. Wong, "Space-time code designs with non-vanishing determinants based on cyclic field extension families," submitted to *IEEE Transactions on Information Theory*.

Publications with * are included in "Section 3: Selected Publications."

3. Selected Publications

3.1 Cooperative wireless network for unmanned surface vehicles

3.2 Differential distributed space-time modulation for cooperative networks

3.3 Imperfectly synchronized cooperative network using distributed space-frequency coding

3.4 Space-time code designs with non-vanishing determinants for three, four and six transmit antennas

3.5 Multi-Sensor Communications in Unmanned Surface Vehicle Networks

Cooperative Wireless Network for Unmanned Surface Vehicles

Yimin Zhang[†], *Genyuan Wang*[†], *Morgan Watson*[‡], and *Moeness G. Amin*[†]

[†] Center for Advanced Communications
Villanova University, Villanova, PA 19085
e-mail: {yimin.zhang,genyuan.wang,moeness.amin}@villanova.edu
http://www.villanova.edu/

[‡] NAVSEA
4700 S. Broad Street, Philadelphia, PA 19112-1403
e-mail: WatsonMA@nswccd.navy.mil

Abstract

As part of Future Naval Capabilities (FNC), the Navy is envisioned to be a lean, distributed force of reconfigurable and multi-mission capable platforms. At the heart of this vision, cascading unmanned surface vehicles (USVs) into a "SWARM" of connectivity nodes offers great flexibility and modularity. The USVs must be able to provide a network of communication data relays, a common tactical picture and mapping for situational awareness. The vehicles must also possess robust communications resistant to jamming, fading and interference while acquiring a high speed data exchange for processing and fusion of information. Reliable wireless network with high data throughput is essential in various military wireless communication systems. While the multiple-input multiple-output (MIMO) communication schemes have the potential to exceed the single-input single-output (SISO) Shannon capacity bound, equipping a large number of antennas in a USV is practically impossible. To increase the diversity gain beyond the number of physical antennas, cooperative wireless networks that exploit cooperation among multiple terminals become essential. This paper proposes novel cooperative wireless networking schemes and practical coding designs that provide the USV Swarm reliable wireless links with the overall data throughput and the communication quality significantly exceeding those of the existing non-cooperative systems.

I. Introduction

As part of Future Naval Capabilities (FNC), the Navy is envisioned to be a lean, distributed force of reconfigurable and multi-mission capable platforms. At the heart of this vision, cascading unmanned surface vehicles (USVs) into a "SWARM" of connectivity nodes offers great flexibility and modularity. USVs are on the threshold of playing key roles in the digital battlespace. Within the context of a larger group of unmanned

This work is supported in part by the ONR under Grant No. N00014-04-1-0617.

systems, USVs have been in use for years or are in the late stages of development. Relatively, Unmanned Air Vehicles (UAVs) are commonplace in many military operations as both weapons and reconnaissance platforms. Unmanned Ground Vehicles (UGVs) are being developed for high-risk operations such as surveillance, while Unmanned Underwater Vehicles (UUVs) are new and in development.

USVs are envisioned to be a multi-mission, rapidly configurable, long endurance unmanned platform providing offboard sensor and weapon capability to perform critical missions like Intelligence, surveillance, reconnaissance, Anti-Submarine Warfare, mine countermeasures, communications and navigation. The technical challenges during these USV missions are to provide optimal performance while subjected to adverse motions, multi-vehicle control, data fusion, obstacle avoidance as well as robust and reliable communications. More importantly, an autonomous environment where electromagnetic radiation is increased, brings with it the possibility of fading, jamming and interference. This paper addresses methods for maximizing communication and reducing fading and interference. In particular, this paper focuses on novel high-rate full-diversity cooperative diversity schemes for wireless communication systems through the use of space-time codes. The proposed systems enable simultaneous transmission of data from all cooperative terminals, providing high diversity gain and potentially high data rate beyond the limit of non-cooperative systems.

In combating channel impairment problem caused from multipath fading, receive diversity techniques using different space branches at the receiver have been shown effective for many years. When the channel is fast time-varying, time diversity is also an option. Recently, transmit diversity schemes add the capability of diversity to the transmitter to spread the information across the transmit antennas [1], [2]. As a result, the information capacity of wireless communication systems increases dramatically by employing multiple transmit and receive antennas [3]. A wireless system consisting of multiple transmit and receive antennas is referred to as a multi-input multi-output (MIMO) system, whereas a system with multiple transmit antennas and a single received antenna is referred to as a multi-input single-output (MISO) system. When the correlation among different channel

path gains is low, a MIMO/MISO system can achieve higher diversity gain and higher data rates, compared to a single transmit antenna system, without increasing premium bandwidth or power [3], [4].

When the channel state information (CSI) is available at the receiver, several space-time codes have been developed to achieve high data rate, while maintaining a high diversity gain [14], [15], [16], [17], [18]. In particular, a space-time code is said to achieve full-rate when the data rate (i.e., the number of transmitted symbols per time slot) reaches the number of transmit antennas. Use of the full-rate full-diversity space-time codes allows simultaneous signal transmission without reducing date rates.

In certain situations, for example, when the fading channel environment is rapidly time-varying, the CSI may not available or cannot be reliably estimated. Differential space-time codes are useful which imply differential coding between two adjacent space-time code matrices. In this case, the decoding at the receiver is independent of the underlying channels [22], [23], [24], [25], [26], [27], [28].

It may often be impractical, however, for a transmitter in the underlying USV networks to be equipped with multiple antennas. For example, the physical limitation of a USV makes it only ready to host a single antenna, particularly when the frequency is relatively low. In addition, depending on the fading characteristics, for example, when shadowing effect occurs, the use of multiple antennas may not be effective to combat the attenuation. To increase the reliability and throughput of a system in such situations, cooperative diversity exploiting cooperation among multiple terminals is a promising techniques. It was first introduced in [5], [6] and further developed by others (e.g., [7], [8], [9], [10]). In a multi-user environment, cooperative diversity allows mobile terminals to achieve high transmit diversity gain beyond the limitation of the number of transmitter antennas at each terminal. It has been shown that cooperative diversity can improve the communication capacity and enhance the robustness of wireless link when a single channel is not reliable.

In this paper, we develop a protocol for cooperative systems that permits effective use of various MIMO space-time coding schemes [11], [12]. Based on the aforementioned high-rate MIMO space-time codes and differential space-time codes, the proposed pro-

tocol allows the development of high-rate distributed space-time codes and differential distributed space-time codes, respectively, depending on the CSI availability, for the use of USV network systems. A multiuser scenario is considered where all users have their own information to send, and desire to cooperate with each other in order to maintain reliable communication links and to send the information to the receiver at a high data rate.

II. Cooperative Diversity

A. Concept

To illustrate the concept of cooperative diversity in a wireless network, consider a simple model as depicted in Fig. 1(a). The user cooperates with other users and serves as a relay terminal for them. Therefore, each transmit user receives an attenuated and noisy version of the partner's transmitted signal and relays it to the destination or other relays. The destination receives a noisy version of the sum of the attenuated signals from all users. Denote the number of users as M. The received signal at the destination during one symbol period t is expressed in baseband model as

$$y_0(t) = \sum_{i}^{M} h_{i0} x_i(t) + n_0(t), \tag{1}$$

whereas the signal received at relay k is

$$y_k(t) = \sum_{i \neq k} h_{ik} x_i(t) + n_k(t). \tag{2}$$

We used subscript 0 for the destination terminal for notational convenience. In (1) and (2), $x_i(t)$ is the signal transmitted by user i, for $i = 1, 2, \cdots, M$, and $n_k(t)$ are the additive channel noise terms at the destination ($k = 0$) and the relay receivers ($k = 1, 2, \cdots, M$), respectively. It is assumed that a terminal does not receive signal from other parties when it is transmitting. The fading channels, h_{ik}, remain constant over a period of several time slots (the length of one or two codewords depending on the protocols), and when observed over time, they form independent stationary ergodic stochastic processes, resulting in frequency non-selective fading.

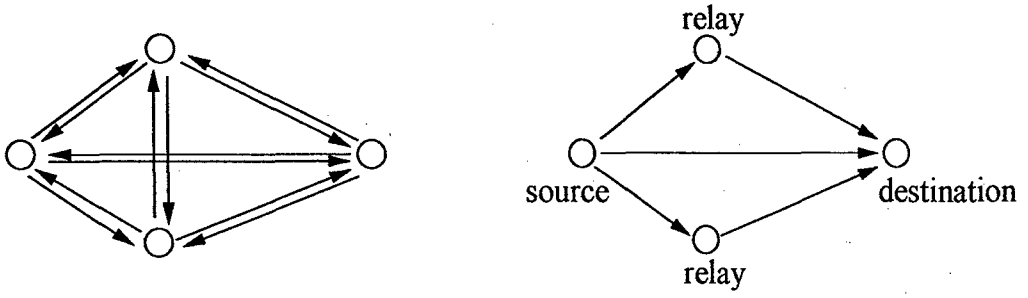

(a) System model. (b) Data transmission through relays.

Fig. 1. System model illustration.

The cooperation process can be divided into two phases (refer to Fig. 1(b)). In the first phase (broadcast phase), the information is transmitted from a source user to the relay terminals, and the destination may also receive a copy of the same information. In the second phase (relay phase), the relay terminals transmit the signal to the destination.

B. Amplify-and-Forward and Decode-and-Forward Algorithms

Depending on how the relay terminals relay the signals from other terminals, there are two major algorithms, namely, amplify-and-forward and decode-and-forward. In the amplify-and-forward algorithm, a relay terminal amplifies the attenuated and noisy signals it receives and retransmits them to the destination and other possible relay terminals. The operation at the relay terminal is limited to amplification and, in some cases, some simple computations such as complex conjugation which is required in certain orthogonal codes including Alamouti's. On the other hand, when the decode-and-forward algorithm is used, the information is first decoded at a relay terminal, and then retransmitted from the delay terminal after proper coding. At the expense of introducing additional complexity at the relay terminals, the decode-and-forward algorithm allows the removal of relay noise (i.e., the noise the relay terminals receive), and provides the flexibility of encoding the information at the relay phase so that higher spectral efficiency can be achieved [8], [21].

It is clear that the decode-and-forward algorithm requires higher complexity and, in some applications, may cause security concerns because a relay terminal decodes the information it relays and, therefore, it is technically possible for a relay terminal to monitor other users'

information. It is contrast to the amplify-and-forward algorithm, where a relay terminal does not decode the information it relays. In addition, the decode-and-forward algorithms requires the CSI for effective decoding, unless the modulation schemes used do not require CSI for decoding (such as the differential modulation schemes to be discussed later).

C. Protocols

Several cooperative diversity protocols have been investigated. The early protocols used repetition-based approaches, which is illustrated in Fig. 2(a). After the source broadcasts its information to the destination and the relays, all relays repeats this information in a sequential order. Therefore, a diversity gain of up to M is achieved at the expense of reducing the degrees of freedom by a factor of M. Arbitrary permutations of these allocations in time and frequency does not alter the performance, as long as causality is preserved and each of the subchannels contains a fraction of $1/M^2$ of the total degrees of freedom (DOFs) in the channel. Such protocols does not require decoding and encoding at the relay terminals and, therefore, is suitable for the amplify-and-forward algorithm. The most significant disadvantage of such protocol is their low throughput rates. As is clear from Fig. 2(a), transmission between different nodes at each time slot utilizes a fraction of $1/M$ of the total DOFs in the channel.

Recently, more effective protocols have been developed to take advantages of the advances of MIMO space-time codes. For example, in [8], [21], proposed space-time cooperation protocols illustrated in Figs. 2(b) and (c). These protocols provide more effective bandwidth use, particularly when the number of cooperative users is large. These protocols allow the use of a fraction of up to $1/2$ of the total DOFs in the channel. The protocols require decoding of other users' information and, therefore, should be incorporated with the decode-and-forward algorithm. As addressed earlier, the use of the decode-and-forward algorithm not only significantly increases the complexity of the terminals that is highly undesirable, it may also raise security concern in some applications.

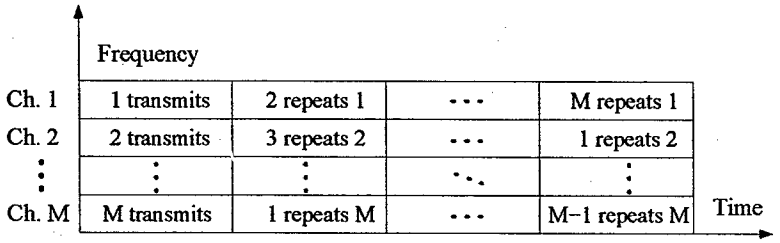

(a) repetition-based diversity scheme

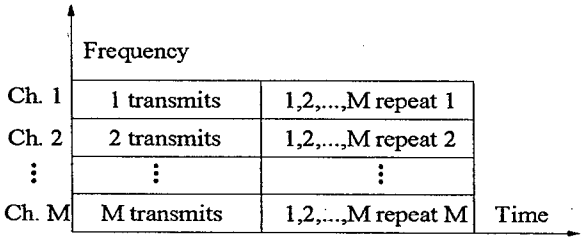

(b) space-time cooperation scheme I

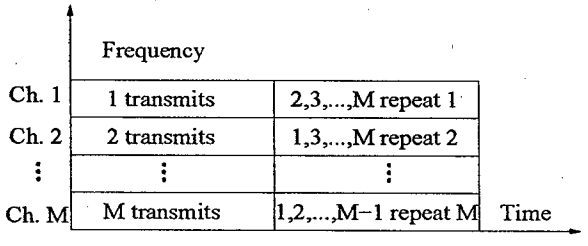

(c) space-time cooperation scheme II

Fig. 2. Cooperative diversity schemes.

III. Proposed High-Rate Full-Diversity Cooperation Protocol

Figure 3 shows the proposed cooperation protocol. There are M users present, each is equipped with a single antenna that can be used for transmit and receive. When considering user i as the source user, the other $M-1$ ones act as the relay users for user i. At the source user, a set of $M \times M$ multi-layer cyclotomic space-time codewords, $\mathbf{X}_i$, are formed from the source information sequence. Before the codeword is modified for the cooperative diversity use, the data rate is full (i.e., $R = M$). However, because the $M-1$ relays do not have the information to be relayed, the source user must first broadcast this information to the relays.

In this protocol, through the first $M-1$ time blocks, the ith row of the $M \times M$ codeword is transmitted during the ith time block from each source transmitter, where $i = 1, \cdots, M-1$. In the Mth time block, the full codeword is transmitted from the M

virtual antennas (i.e., one source transmit antenna and $M-1$ relay antennas).

The proposed method is amendable for the use of both amplify-and-forward and decode-and-forward algorithms. When the former one is considered, this protocol does not require decoding and encoding at the relay terminals while it takes the advantage of high data rate and high diversity gain. In this case, each of the $M-1$ relay terminals receives one different row of the codeword transmitted from the source user through the broadcast phase (i.e., during the first $M-1$ time blocks), and the row is retransmitted in the relay phase which spans the Mth time block. The use of amplify-and-forward algorithm does not require the relays to have the CSI. It is evident that, in the proposed scheme, unit degree of freedom is achieved, compared to $1/M$ (repetition-based diversity scheme in Fig. 2(a)) and $1/2$ (space-time cooperation schemes I and II in Figs. 2(b) and (c)) decode-based diversity scheme in Fig. 2(a)) in the aforementioned space-time cooperation schemes.

When the decode-and-forward algorithm is considered, the $M-1$ relay users can decode the signal from the information transmitted through the first $M-1$ time slots. The signal will be retransmitted after encoding during the Mth time slot either from all the M users (space-time cooperation scheme I) or from the $M-1$ relays (space-time cooperation scheme II). Unless differential or other non-coherent coding schemes (to be introduced later) are exploited, the use of decode-and-forward algorithm requires each relay to have the CSI of the channel between the source and itself. Such decoding and encoding can effectively eliminate the relay noise when the channel between the source user and the relay terminals are reliable to the extent that the information can be correctly detected at each relay.

It is emphasized that, because the codeword $\mathbf{X}_i$ is full rank, the relay users can decode the signal with a full or partial set of the M rows of the $M \times M$ codeword. This permits flexible protocol design to further increase the data rates by truncating the broadcast phase when the channels between the source user and the relay terminals are highly reliable. This comes at the expense of requiring additional complexity to both the physical (PHY) and media access control (MAC) layers in order to monitor the channel quality and decoding performance, and to adaptively control the resource allocations in the broadcast phase.

From a 2×2 MIMO space-time codeword $\mathbf{X}_i$, the protocols equivalently transmit the

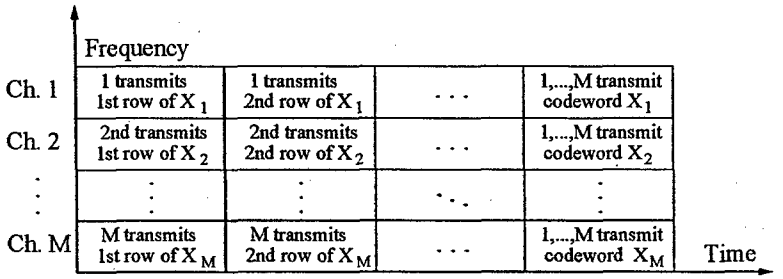

Fig. 3. The proposed space-time cooperation scheme.

following 2×4 codeword $\mathbf{X}'$, i.e.,

$$\mathbf{X}_i = \begin{bmatrix} x_i(1) & x_i(2) \\ x_i(3) & x_i(4) \end{bmatrix} \quad \Rightarrow \quad \mathbf{X}'_i = \sqrt{g'} \begin{bmatrix} x_i(3) & x_i(4) & x_i(1) & x_i(2) \\ 0 & 0 & \hat{x}_i(3) & \hat{x}_i(4) \end{bmatrix}, \tag{3}$$

where $\hat{x}_i(t)$ is a replica of $x_i(t)$ and g' is a power normalization factor. When the amplify-and-forward algorithm is used, $\hat{x}_i(t)$ is a complex scaled and noisy version of $x_i(t)$. The scale comes from the channel attenuation and the amplification in the relay terminal, whereas the channel noise is added before the amplification. When the decode-and-forward algorithm is used, the scale and noise can be removed, given the channels between the source and the relay terminals are reliable.

When we assume $\hat{x}_i(t)$ is the exact replica of $x_i(t)$, we can equivalently consider the resulting codeword as,

$$\mathbf{X}_i = \begin{bmatrix} x_i(1) & x_i(2) \\ x_i(3) & x_i(4) \end{bmatrix} \quad \Rightarrow \quad \mathbf{X}'_i = \sqrt{g'} \begin{bmatrix} x_i(3) & x_i(4) & x_i(1) & x_i(2) \\ 0 & 0 & x_i(3) & x_i(4) \end{bmatrix}. \tag{4}$$

A code like $\mathbf{X}'_i$ in (4) is referred to as the distributed space-time code corresponding to the space-time code $\mathbf{X}_i$.

IV. High-Efficiency Space-Time Cooperation Schemes

In this section, we consider effective space-time cooperation schemes when the CSI is available at the receivers. We first review the general criteria of MIMO space-time code design and some class of high-rate full-diversity space-time codes. We then propose a new space-time cooperation protocol that can effectively incorporate the high-rate full-diversity space-time codes and is applicable to both amplify-and-forward and decode-and-forward algorithms.

A. Space-Time Codes in MIMO Systems

Assume a transmitter that has N_t transmit antennas, and consider that the following $N_t \times N_t$ square codeword

$$\mathbf{C} = \begin{bmatrix} c_1^1 & c_2^1 & \cdots & c_{N_t}^1 \\ c_1^2 & c_2^2 & \cdots & c_{N_t}^2 \\ \vdots & \vdots & \ddots & \vdots \\ c_1^{N_t} & c_2^{N_t} & \cdots & c_{N_t}^{N_t} \end{bmatrix}$$

is transmitted. In a codeword, the rows of the coding matrix stand for "space" (i.e., antennas), and the columns stand for "time". When codeword $\mathbf{E}$ is transmitted, the probability that a maximum-likelihood receiver decides erroneously in favor of another signal codeword $\mathbf{E}$ in independent fading channels is bounded by [4]

$$P(\mathbf{C} \to \mathbf{E}) \leq \left(\prod_{i=1}^{r} \lambda_i \right)^{-N_r} (E_s/4N_0)^{-rN_r}, \tag{5}$$

where r is the rank of $\mathbf{D_{CE}} = \mathbf{C} - \mathbf{E}$, λ_i, $i = 1, \cdots, r$ are the r nonzero eigenvalues of $\mathbf{D_{CE}}\mathbf{D_{CE}^H}$, N_r is the number of receive antennas, E_s is the average transmitted symbol energy, and N_0 is the noise variance of $N_0/2$ in each of its two dimensions.

There are several criteria for MIMO space-time code design. The most commonly used ones are the rank criterion, determinant criterion, and symbol rate criterion. In (5), the rank r determines the order with which the codeword error rate (CER) decreases with the input signal-to-noise ratio (SNR) when the SNR goes to infinite. Maximizing the diversity product $\prod_{i=1}^{r} \lambda_i$ also reduces the CER. The symbol rate is defined as $R = M/T$ symbols per channel use (PCU) if an information sequence of M information symbols is mapped to a space-time codeword $\mathbf{X}$ with T time slots (i.e., each codeword is a $N_t \times M$ matrix). It is said that a space-time code achieves full rate if its symbol rate is $R = N_t$ symbols PCU for a transmit array of N_t antennas.

B. High-Rate Full-Diversity Space-Time Codes

With these design criteria in mind, several space-time codes have been developed that achieve full data rate and full diversity gain. For example, multi-layer cyclotomic space-time codes have been proposed which bear high or even full data rate information [13], [14], [15], [16], [17], [19].

Consider a simple situation where two transmit antennas are present. The following two-layer code provides data rate of two (i.e., full rate $R = 2$),

$$\mathbf{V} = \begin{bmatrix} \rho_1 v_1^{(1)} & \rho_2 v_1^{(2)} \\ \rho_2 v_2^{(2)} & \rho_1 v_2^{(1)} \end{bmatrix}, \tag{6}$$

where $v_i^{(l)}$, $i = 1, 2$, $l = 1, 2$, are the ith point in the cyclotomic lattice of the lth layer, and ρ_i are some complex numbers (see [19] for the determination of values of ρ_i). For each of the two users, $i = 1, 2$, the codeword matrix in (6) is mapped to the following data matrix to be transmitted,

$$\mathbf{X}_i = \begin{bmatrix} x_i(1) & x_i(2) \\ x_i(3) & x_i(4) \end{bmatrix} = \sqrt{g}\mathbf{V} = \sqrt{g} \begin{bmatrix} \rho_1 v_1^{(1)} & \rho_2 v_1^{(2)} \\ \rho_2 v_2^{(2)} & \rho_1 v_2^{(1)} \end{bmatrix}, \tag{7}$$

where g is a factor to normalize the averaging codeword energy. The multi-layer cyclotomic space-time codes are full-rate, and are shown in [19] to be of full diversity gain and optimal diversity product. These codes have full-rate and full-diversity features and, when used instead of the original data stream in an independent MIMO fading channel environment, improvements in system performance and power efficiency can be expected.

V. Differential Cooperation Schemes

The previous section considered effective space-time cooperation schemes when the CSI is available at the receivers. Such information is obtained usually through channel estimation, either using training (pilot) signals or utilizing blind methods. However, channel estimation is often complicated and may reduce the transmission efficiency if pilot signals are used. In addition, there is an issue of reliability and practicality if the channels experience fast fading. This section develops differential cooperation schemes based on the differential space-time codes. By eliminating the needs of channel estimation, such schemes are useful in such situations in which the CSI are either unknown or cannot be reliably estimated.

We first review the differential space-time codes developed for MIMO systems, and then show the feasibility of extending them to the space-time cooperation applications.

A. Differential Space-Time Codes

Differential space-time codes are useful in dealing with rapid MIMO fading environments. Differential coding is applied between two adjacent space-time code matrices so that the decoding at the receiver is independent of the underlying channels [22], [23], [24], [25], [26], [27], [28].

For example, denote $\mathcal{G}$ as a set of K different unitary matrices used for differential coding, $k = 1, \cdots, K$, and

$$\mathcal{G} = \{\mathbf{U}_k, k = 1, \cdots, K\}. \tag{8}$$

The information steam is mapped to one of the K space-time codewords $\mathbf{U}_k$ in $\mathcal{G}$. To send the message $\mathbf{G}(t) \in \mathcal{G}$ at time t, the transmitter sends $\mathbf{C}(t)$ where

$$\mathbf{C}(t) = \mathbf{C}(t-1)\mathbf{G}(t), \quad \mathbf{C}(0) = \mathbf{I}, \tag{9}$$

with $\mathbf{C}(t-1)$ denoting the matrix transmitted over the time block $t-1$ and $\mathbf{I}$ being the identity matrix. The differential space-time coding scheme works well in time-varying channels, provided that the channels do not change significantly over two adjacent code matrices.

B. Differential Space-Time Cooperation Schemes

We now consider the feasibility of extending the differential space-time codes to cooperation networks. For simplicity, we consider a two-user case in the absence of relay noise, and user 2 is a terminal to relay user 1's information. The following 2×4 distributed differential space-time code $\mathbf{C}'(t)$ is generated from a 2×2 differential space-time code $\mathbf{C}(t)$:

$$\mathbf{C}(t) = \begin{bmatrix} c_1(t) & c_2(t) \\ c_3(t) & c_4(t) \end{bmatrix} \quad \Rightarrow \quad \mathbf{C}'(t) = \begin{bmatrix} c_3(t) & c_4(t) & c_1(t) & c_2(t) \\ 0 & 0 & c_3(t) & c_4(t) \end{bmatrix}. \tag{10}$$

Note here that we use t to denote the time index for a codeword. Corresponding to (9), the relationship between two adjacent distributed codewords, $\mathbf{C}'(t)$ and $\mathbf{C}'(t-1)$, and the information code matrix $\mathbf{G}'(t)$ is

$$\mathbf{C}'(t) = \mathbf{C}'(t-1)\mathbf{G}'(t), \quad \mathbf{G}'(t) = \begin{bmatrix} \mathbf{G}(t) & \mathbf{O} \\ \mathbf{O} & \mathbf{G}(t) \end{bmatrix}. \tag{11}$$

Denote $\mathbf{h}(t) = [h_1(t) \;\; h_2(t)]$ whose components are assumed to remain almost constant for any two adjacent codewords but are assumed to be independent and stationary ergodic stochastic processes (i.e., $\mathbf{h}(t) = \mathbf{h}(t-1)$). Then, the 1×4 received signal row vector at the destination is expressed as

$$\begin{aligned} \mathbf{y}(t) &= \mathbf{h}(t)\mathbf{C}'(t) = \mathbf{h}(t)\mathbf{C}'(t-1)\mathbf{G}'(t) = \mathbf{h}(t-1)\mathbf{C}'(t-1)\mathbf{G}'(t) \\ &= [\mathbf{h}(t-1)\mathbf{C}'(t-1)]\,\mathbf{G}'(t) = \mathbf{y}(t-1)\mathbf{G}'(t). \end{aligned} \tag{12}$$

Therefore, it becomes evident that the differential distributed space-time coding schemes can be applied to a cooperative network because $\mathbf{G}'(t)$ and, equivalently, $\mathbf{G}(t)$, can be recovered from $\mathbf{y}(t)$ and $\mathbf{y}(t-1)$, without knowing the CSI.

VI. Numerical Results

In this section, we show some numerical results to support our findings. The first set of simulations considers a set of 2×2 cyclotomic space-time codes as the prototype for the development of the distributed space-time codes. The prototype codeword has 256 constellations over two time slots. For comparison, Alamouti's codes with the same information rate are also considered. All the channels are assumed to be independent and identically distributed (i.i.d.) random Gaussian processes with zero mean and unit variance. The relay noise is not considered in the simulations.

Figure 4(a) compares the CER performance of the cooperative diversity schemes using the Alamouti's and the cyclotomic codes. The SNR is defined as the ratio of the averaged codeword energy to the noise energy over the same period. It is seen that, the cyclotomic codes outperforms the Alamouti's by about 1.5 dB.

The second set compares different detection methods for the Alamouti's codes, where the QPSK modulation is used. As evidenced in Fig. 4(b), the expense of using differential detection is the 3 dB noise amplification.

VII. Conclusion and Remarks

We have proposed a novel cooperative protocol and several distributed space-time codes for application to wireless networking in unmanned surface vehicles (USVs). The proposed protocol is applicable to both amplify-and-forward and decode-and-forward algorithms.

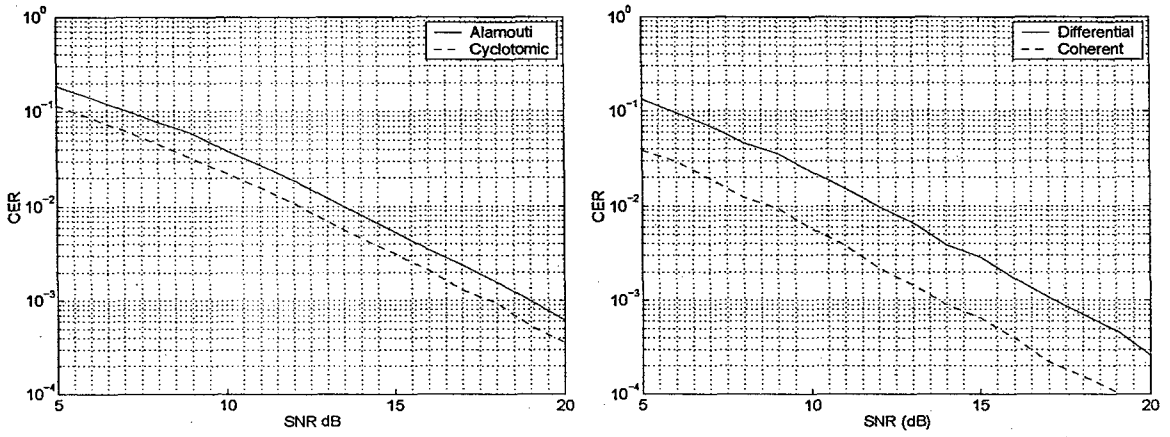

(a) Comparison of prototype codes (b) Comparison of detection methods

Fig. 4. CER performance of different distributed space-time schemes and detection methods.

The two proposed distributed space-time coding schemes are useful, respectively, when the CSI is or is not available. The advantage of the proposed methods were confirmed through numerical simulations.

The swarm of USV architecture has similarities to the sensor network and ad hoc networks. While our contribution in this paper focused on the effective data transmission, other developments in several fronts of these areas can be applied. For example, routing algorithm is another important issue to be considered [29]. The information sensed at different nodes are usually correlated and distributed source coding, originated from Slepian and Wolf's work [30], can be used to reduce the total amount of data without compromising the information [31], [32]. The importance of such data compression is particularly significant when large amount of data, e.g., acoustic imaging information, is to be transmitted. However, unlike typical sensor network application where energy consumption is of great concern, it is of secondary priority in the USV networking applications.

References

[1] S. M. Alamouti, "A simple transmitter diversity scheme for wireless communications," *IEEE J. Select. Areas Commun.*, vol. 16, pp. 1451–1458, Oct. 1998.

[2] A. F. Naguib, N. Seshadri, A. R. Calderbank, "Increasing data rate over wireless channels: space-time coding and signal processing for high data rate wireless communications," *IEEE Signal Proc. Mag.*, vol. 17, no. 3, pp. 76–92, May 2000.

[3] G. J. Foschini and M. J. Gans, "On limits of wireless communications in a fading environment when

using multiple antennas," *Wireless Personal Commun.*, vol. 6, no. 3, pp. 311–335, March 1998.

[4] V. Tarokh, H. Jafarkhani, and A. R. Calderbank, "Space-time block codes from orthogonal designs," *IEEE Trans. Inform. Theory*, vol. 45, no. 5, July 1999.

[5] A. Sendonaris, E. Erkip, and B. Aazhang, "Increasing uplink capacity via user cooperation diversity," *Proc. IEEE Int. Symp. Info. Theory*, Cambridge, MA, p. 156, Aug. 1998.

[6] A. Sendonaris, E. Erkip, and B. Aazhang, "User cooperative diversity – Part I and Part II," submitted to *IEEE Trans. Commun.*

[7] J. N. Laneman, D. N. C. Tse, and G. W. Wornell, "Cooperative diversity in wireless networks: effective protocols and outrage behavior," *IEEE Trans. Inform. Theory*, accepted for publication.

[8] J. N. Laneman and G. W. Wornell, "Distributed Space-Time Coded Protocols for Exploiting Cooperative Diversity in Wireless Networks", *IEEE Trans. Inform. Theory*, vol. 49, no. 10, pp. 2415–2425, Oct. 2003.

[9] P. A. Anghel, G. Leus, and M. Kaveh, "Multi-user space-time coding in a cooperative networks," *Proc. IEEE ICASSP*, Hong Kong, May 2003.

[10] Y. Hua, Y. Mei, and Y. Chang, "Parallel wireless mobile relays with space-time modulations," *Proc. IEEE Workshop on Statistical Signal Processing*, St. Louis, MO, Sept. 2003.

[11] G. Wang, Y. Zhang, and M. G. Amin, "Space-time cooperation diversity using high-rate codes," *Int. Symp. on Antennas and Propagation*, Sendai, Japan, Aug. 2004.

[12] G. Wang, Y. Zhang, and M. G. Amin, "Cooperation diversity using differential distributed space-time codes," *Joint Conf. of Asia-Pacific Conf. on Communications and Int. Symp. on Multi-Dimensional Mobile Communications*, Beijing, China, Aug. 2004.

[13] M. O. Damen, A. Tewfik, and J.-C. Belfiore, "A construction of a space-time code based on the theory of numbers," *IEEE Trans. Inform. Theory*, vol. 48, no. 3, pp. 753–760, March 2002.

[14] H. El Gamal and M. O. Damen, "Universal space-time coding," *IEEE Trans. Inform. Theory*, vol. 49, pp. 1097–1119, May 2003.

[15] M. O. Damen, and N. C. Beaulieu, "On two high rate algebraic space-time codes," *IEEE Trans. Inform. Theory*, vol. 49, pp. 1059–1063, April 2003.

[16] M. O. Damen, H. El Gamel, and N. C. Beaulieu, "Linear threaded algebraic space-time constellations," *IEEE Trans. Inform. Theory*, vol. 49, no. 10, pp. 2372–2388, Oct. 2003.

[17] X. Ma and G. B. Giannakis, "Full-diversity full rate complex-field space-time coding," *IEEE Trans. Signal Processing*, vol. 51, no. 11, Nov. 2003.

[18] G. Wang, H. Liao, H. Wang, and X-G. Xia, "Systematic and optimal cyclotomic space-time code designs based on high dimensional lattices," *Proc. Globecom*, San Fransicso, CA, Dec. 2003.

[19] G. Wang and X-G. Xia, "Optimal multi-layer cyclotomic space-time code designs with highest product diversity gain and full rate," submitted to *IEEE Trans. Inform. Theory.*

[20] J.-C. Belfiore, G. Rekaya, and E. Viterbo, "The Golden code: a 2×2 full-rate space-time code with non-vanishing determinants," submitted to *IEEE Trans. Inform. Theory.*

[21] M. Janani, A. Hedayat, T. E. Hunter, and A. Nosratinia, "Coded cooperative in wireless commu-

nications: space-time transmission and iterative decoding," *IEEE Trans. Signal Processing*, vol. 52, no. 2, pp. 362–371, Feb. 2004.

[22] B. L. Hughes, "Differential space-time modulation," *IEEE Trans. Inform. Theory*, vol. 46, pp. 2567–2578, Nov. 2000.

[23] B. M. Hochwald and W. Sweldens, "Differential unitary space-time modulation," *IEEE Trans. Commun.*, vol. 48, pp. 2041–2052, Dec. 2000.

[24] V. Tarokh and H. Jafarkhani, "A differential detection scheme for transmit diversity," *IEEE J. Select. Areas Commun.*, vol. 18, pp. 1169–1174, July 2000.

[25] X.-B. Liang and X.-G. Xia, "On the nonexistence of rate-one generalized complex orthogonal designs," *IEEE Trans. Inform. Theory*, vol. 49, no. 11, pp. 2984–2988, Nov. 2003.

[26] Z. Liu, G. B. Giannakis, and B. L. Hughes, "Double differential space-time block coding for time-varying fading channels," *IEEE Trans. Commun.*, vol. 49, pp. 1529–1539, Sept. 2001.

[27] A. Shokrollahi, B. Hassibi, B. M. Hochwald, and W. Sweldens, "Representation theory for high-rate multiple-antenna code design," *IEEE Trans. Inform. Theory*, vol. 47, pp. 2335–2367, Sept. 2001.

[28] H. Li and J. Li, "Differential and coherent decorrelating multiuser receivers for space-time-coded CDMA systems," *IEEE Trans. Signal Processing*, vol. 50, no. 10, pp. 2529–2537, Oct. 2002.

[29] C. A. Santivanez and R. Ramanathan, "Scalability of routing in ad hoc networks: Principles and practice," in X. Cheng, X. Huang, and D.-Z. Du (ed.), *Ad Hoc Wireless Networking*, Kluwer, 2003.

[30] D. Slepian and J. K. Wolf, "Noiseless coding of correlated information sources," *IEEE Trans. Inform. Theory*, vol. 19, pp. 471–480, July 1973.

[31] S. Pradhan, J. Kusuma, and L. Ramchandran, "Distributed compression in a sense microsensor netowkr," *IEEE Signal Processing Magazine*, vol. 19, pp. 51–60, March 2002.

[32] Z. Xiong, A. D. Liveris, and S. Cheng, "Distributed source coding for sensor networks," *IEEE Signal Processing Magazine*, to appear.

Differential Distributed Space-Time Modulation for Cooperative Networks

Genyuan Wang, Yimin Zhang, and Moeness Amin

Abstract

In this paper, we develop a protocol for the construction of cooperative networks when the channel state information is not available at the transmitters and the receivers. In the proposed protocol, differential space-time codewords are generated at the source terminal. In the broadcast phase, each row of the differential space-time codeword is transmitted to a different relay, whereas in the relay phase, the relaying terminals retransmit the codeword through simple amplify-and-forward algorithm. The performance of the cooperative diversity system is analyzed for a two-user case for different channel environments in terms of the diversity gain and the diversity product. The optimization of the power allocation between source and relay terminals is considered for the maximization of the diversity product. When the same modulation scheme is used, the performance of differential detection is degraded by 3 dB noise enhancement compared with coherent detection.

Keywords

Cooperative diversity, MIMO, space-time coding, differential coding.

This work is supported in part by the ONR under Grant No. N00014-04-1-0617 and NSF under Grant No. EEC-0203459.

The authors are with the Center for Advanced Communications, College of Engineering, Villanova University, Villanova, PA 19085, USA (e-mail: {genyuan.wang, yimin.zhang, moeness.amin} @villanova.edu). Phone: 610-519-4544, Fax: 610-519-4436.

I. Introduction

The multi-input-multi-output (MIMO) technology, incorporating appropriate space-time coding schemes, allows considerable increase of the information capacity in fading channels [1]–[4]. Without increasing premium bandwidth or transmit power, a MIMO system can achieve higher diversity gains and data rates, compared to single-input or/and single-output system counterparts.

It is often impractical, however, for a transmitter to host a large number of antennas for a desirable diversity gain, especially for small size transceivers operating at relatively low frequencies. In addition, delivery of information from a transmitter to a receiver can be compromised when they are distant apart, or when the wireless channel links are highly impairing. This difficulty arises in a wide class of wireless networks, such as local area networks (LANs), sensor networks, and ad hoc networks. For these applications, cooperative diversity exploiting cooperation among multiple terminals proves desirable.

The cooperative diversity techniques have recently attracted considerable attentions. In responding to the increasing needs of effective and reliable wireless networks in various applications, the development of cooperative diversity techniques has benefitted from the recent advances of space-time codes, transmit diversity, and MIMO technologies. Recent research work has shown system feasibility and provided capacity analyses of different cooperative diversity techniques (see for example, [5]–[21]). These methods assume that channel state information (CSI) is available at the receivers, although few assume CSI knowledge at the transmitters.

CSI knowledge at the receivers is usually obtained through channel estimation, either using training (pilot) signals or utilizing blind methods. However, channel estimation is often complicated and may reduce the transmission efficiency, if pilot signals are used. In addition, the estimation becomes unreliable and impractical in fast fading environments [22]. In such situations, MIMO systems often adopt differential space-time coding schemes which use differential codes between two adjacent space-time code matrices so that the

decoding at the receiver is independent of the fading channels [22]–[30].

As the cooperative diversity schemes involve both broadcast and relay phases, multiple cooperative terminals should be considered. The propagation channels are, therefore, more complicated than those encountered in MIMO scenarios [31]. Accordingly, the consideration of system design without assuming knowledge of CSI at a receiver becomes a practical requirement.

So far, several differential cooperative diversity schemes have been developed for applications in the absence of CSI knowledge at the receivers. A repetition-based differential amplify-and-forward scheme is proposed in [32] for a single-relay scenario, where differentially encoded BPSK signals are used. In [33], a differential modulation scheme is proposed for two-user cooperative diversity systems, where the relay terminals uses QPSK modulation to transmit two BPSK streams. The information of one user stays in the in-phase axis (I-axis) while that of the other user stays in the quadrature-phase axis (Q-axis). In [34], a non-coherent decode-and-forward scheme is developed for binary frequency shift keying (BFSK) modulations.

In this paper, we develop a new distributed space-time modulation scheme for cooperative systems that require no knowledge of the CSI at both transmitters and receivers. In the proposed protocol, differential space-time codewords are generated at the source terminal, and each row of a codeword is relayed by a different relay terminal. Fundamentally, any differential space-time codes can be employed in the proposed scheme, whereas the relay terminals implement a simple amplify-and-forward relaying algorithm. An entry of the user's differential space-time codeword is not based on any specific modulation such as PSK or FSK. The performance of the cooperative diversity system is analyzed for a two-user case for different channel environments in terms of the diversity gain and the diversity product. The optimization of the power allocation between source and relay terminals are considered for the maximization of the diversity product. Roughly, the performance of differential detection is degraded by 3 dB noise enhancement compared with the coherent

detection, when the same modulation scheme is used.

In this paper, we consider memoryless channels and assume that the terminals transmitting the same distributed space-time codeword are synchronized at the destination receiver. When the channels are not perfectly synchronized, the synchronization error between the terminals can be considered as channel dispersion effect [35]. The effect of channel dispersion in cooperative network as well as the effective approaches using equalization and orthogonal frequency division multiplexing (OFDM) techniques have been considered in [35], [36], [37].

This paper is organized as follows. In Section II, the system model is introduced. In Section III, we review the existing cooperative protocols, and then propose a new protocol which is effective to transmit distributed information when the CSI is unavailable at the receivers. The differential space-time cooperative structure is shown in Section IV and the performance analysis is provided in Section V. Numerical results are provided in Section VI.

II. System Model

To illustrate the concept of cooperative diversity in a wireless network, consider a simple narrowband communication model as depicted in Fig. 1(a). Each user cooperates with the other users and serves as a relay terminal for them. Therefore, each user receives an attenuated and noisy version of the partners' transmitted signal and relays it to the destination or other relays. The destination terminal receives a noisy version of the sum of the attenuated signals from all users (see Fig. 1(b)). Denote the number of users as M. The received signal at the destination during the lth symbol period is expressed in the baseband model as

$$y(l) = \sum_{i=1}^{M} \gamma_{i0} h_{i0}(l) x_i(l) + n(l), \tag{1}$$

where we used subscript 0 to denote the destination terminal for notational convenience. In (1), $x_i(l)$ is the source or relaying signal transmitted by the ith user, for $i = 1, 2, \cdots, M$,

γ_{i0} is the large-scale attenuation factor of the channel between the ith terminal and the destination, whereas $h_{i0}(l)$ represents the respective unit-variance small-scale time-varying statistics of the channel. In addition, $n_0(l)$ is the additive channel noise term at the destination.

It is assumed that a relay terminal does not receive signals from other users when it is transmitting. Therefore, the signal received at relay terminal k is expressed as

$$r^{(k)}(l) = \sum_{i \neq k} \gamma_{ik} h_{ik}(l) x_i(l) + n_r^{(k)}(l). \tag{2}$$

where γ_{ik} and $h_{ik}(l)$, respectively, represent the large-scale attenuation factor and the small-scale time-varying statistics of the channel between user terminals i and k, and $n_r^{(k)}(l)$ is the additive channel noise term at the relay receiver k, where $i, k = 1, 2, \cdots, M$.

Depending on how the relay terminals relay the signals from other users, two major schemes can be devised, namely, amplify-and-forward and decode-and-forward. In this paper, we focus on the simpler amplify-and-forward scheme which requires the least complexity at the relay terminals.

III. Cooperation Protocols

A. Existing Protocols

Several cooperative diversity protocols have been investigated. The early protocols used repetition-based approaches, which is illustrated in Fig. 2(a) [8], [19]. After source terminal i broadcasts a block of information symbols (e.g., $\mathbf{s}_i(l) = [s_i(l), s_i(l+1), \cdots, s_i(l+L-1)]$, where L is the length of the data block) to the destination and the relay terminals, all relay terminals repeat the same data (i.e., $\mathbf{s}_i(l) = [s_i(l), s_i(l+1), \cdots, s_i(l+L-1)]$) in a sequential order.

Recently, more effective protocols have been developed to take advantages of the advances of MIMO space-time codes. For example, [8] and [19] proposed space-time cooperation protocols which are illustrated in Fig. 2(b) and (c). In the broadcast phase, the source terminal i broadcasts a block of information symbols (e.g., $\mathbf{s}_i(l) = [s_i(l), s_i(l+$

$1), \cdots, s_i(l+L-1)]$) to the destination and the relay terminals. In the relay phase, for scheme I depicted in Fig. 2(b), the source and the relay terminals transmit different rows of a space-time codeword $\mathbf{X}_i(\nu)$, which is constructed from $\mathbf{s}_i(l)$, where ν denote the index of a coded data block. Space-time cooperative scheme II is very similar to scheme I. The only difference between them lies in the fact that in scheme I, the source terminal takes part in the relay phase, whereas in scheme II it does not. Such protocols provide more effective bandwidth use, particularly when the number of cooperative users is large.

B. Proposed Protocol

Most existing cooperative protocols assume that the CSI is known at the receivers. In this section, we develop a protocol that is applicable to space-time cooperation, where the CSI is unavailable at the receivers. The proposed protocol performs differential distributed space-time coding and information detection using the relatively simple amplify-and-forward algorithm. Fig. 3 depicts the proposed protocol. When considering user i as the source user, the other $M-1$ ones act as its relays. At the source terminal, an $M \times M$ space-time codewords, $\mathbf{X}_i(\nu)$, is formed from the source information symbols. Each of the $M-1$ relay terminals receives a different row of the codeword $\mathbf{X}_i(\nu)$ that is transmitted from the source user through the broadcast phase (i.e., during the first $M-1$ time blocks). All the M rows of $\mathbf{X}_i(\nu)$ are transmitted from the M terminals in the relay phase which spans the Mth time block. It is noted that the destination listens to the source during the broadcast phase, whereas it listens to the source and the relay terminals during the relay phase.

Consider the simple case of two users, i.e., $M = 2$. The source terminal forms a 2×2 MIMO space-time codeword $\mathbf{X}_i(\nu)$ from the source information symbols $\mathbf{s}_i(l) = [s_i(l), s_i(l+1), \cdots, s_i(l+L-1)]$. Then, using the cooperative protocol, the source and relay terminals equivalently transmit the following 2×4 codeword $\hat{\mathbf{X}}_i'(\nu)$ in the cooperative

diversity system, i.e.,

$$\mathbf{X}_i(\nu) = \begin{bmatrix} x_i(\nu,1) & x_i(\nu,2) \\ x_i(\nu,3) & x_i(\nu,4) \end{bmatrix} \quad \Rightarrow \quad \hat{\mathbf{X}}_i'(\nu) = \begin{bmatrix} x_i(\nu,3) & x_i(\nu,4) & x_i(\nu,1) & x_i(\nu,2) \\ 0 & 0 & \hat{x}_i(\nu,3) & \hat{x}_i(\nu,4) \end{bmatrix}, \tag{3}$$

where $\hat{x}_i(\nu,\tau)$ is the complex scaled and noisy version of $x_i(\nu,\tau)$. In the above space-time codewords, the columns specify the time dimension, whereas the rows specify the space dimension (i.e., antennas or relay terminals).

IV. Differential Cooperation Schemes

In this section, we first briefly review the differential space-time codes developed for MIMO systems, and then show the feasibility of employing them in the space-time cooperation applications through the proposed protocol.

A. Differential Space-Time Codes

In order to deal with rapid MIMO fading environments where the CSI is unavailable at the receiver, differential space-time codes can be used. For essence, differential coding between two adjacent space-time code matrices is used so that the decoding at the receiver can be performed without the knowledge of channels [22]–[30]. Differential space-time codes are most commonly used in the form of unitary matrices [22], [27].

Let $\mathcal{G} = \{\mathbf{G}_i, i = 1, \cdots, N\}$ be a set of $M \times M$ unitary matrices (i.e., $\mathbf{G}_i\mathbf{G}_i^H = \mathbf{G}_i^H\mathbf{G}_i = \mathbf{I}_M$, where $\mathbf{I}_M$ is the $M \times M$ identity matrix), and $\mathbf{C}(0)$ is an $M \times M$ matrix. $\log_2 N$ information bits are mapped to one of the N unitary matrices $\mathbf{G}_i$ in $\mathcal{G}$. To send the message $\mathbf{G}(\nu) \in \mathcal{G}$ over time block ν, the transmitter sends $\mathbf{C}(\nu)$ where

$$\mathbf{C}(\nu) = \mathbf{C}(\nu-1)\mathbf{G}(\nu) = \mathbf{C}(0)\prod_{\tau=1}^{\nu}\mathbf{G}(\tau). \tag{4}$$

Matrix $\mathbf{C}(\nu)$ takes the following general format

$$\mathbf{C}(\nu) = \begin{bmatrix} c_{11}(\nu) & c_{12}(\nu) & \cdots & c_{1M}(\nu) \\ c_{21}(\nu) & c_{22}(\nu) & \cdots & c_{2M}(\nu) \\ \vdots & \vdots & \ddots & \vdots \\ c_{M1}(\nu) & c_{M2}(\nu) & \cdots & c_{MM}(\nu) \end{bmatrix}. \tag{5}$$

The spectral efficiency of this code is $(1/M)\log_2 N$ bits per channel use. When the channels corresponding to different transmit antennas are independent and identically distributed (i.i.d.), $\mathbf{C}(\nu)$ is often designed to take the form of unitary matrices for improved system capacity [23], [24], [26]. That is,

$$\mathbf{C}(\nu)\mathbf{C}^H(\nu) = \mathbf{I}_M. \tag{6}$$

In this case, $\mathbf{C}(0)$ is chosen as unitary.

The differential space-time coding scheme works well in time-varying channels, provided that the channels do not change significantly over a period of two adjacent codewords, i.e., $\mathbf{h}(\nu-1) = \mathbf{h}(\nu)$, where $\mathbf{h}(\nu) = [h_{10}(\nu), \cdots, h_{M0}(\nu)]$ is a vector channel with the ith element representing the channel coefficient between the ith transmit antenna and the destination receiver. Denote the signals received at the receiver corresponding to the $(\nu-1)$th and νth codewords as

$$\mathbf{y}(\nu-1) = \mathbf{h}(\nu-1)\mathbf{C}(\nu-1) + \mathbf{n}(\nu-1)$$

and

$$\mathbf{y}(\nu) = \mathbf{h}(\nu)\mathbf{C}(\nu) + \mathbf{n}(\nu),$$

then we have

$$\mathbf{y}(\nu) = \mathbf{h}(\nu-1)\mathbf{C}(\nu-1)\mathbf{G}(\nu) + \mathbf{n}(\nu) = [\mathbf{y}(\nu-1) - \mathbf{n}(\nu-1)]\mathbf{G}(\nu) + \mathbf{n}(\nu). \tag{7}$$

Because $\mathbf{G}(\nu)$ is unitary, $-\mathbf{n}(\nu-1)\mathbf{G}(\nu)$ can be considered as additional noise term with the same variance as $\mathbf{n}(\nu)$. Therefore, the information $\mathbf{G}(\nu)$ can be recovered from $\mathbf{y}(\nu-1)$ and $\mathbf{y}(\nu)$ through the above relationship at the expense that the equivalent noise power is doubled.

B. Differential Space-Time Cooperative Schemes

We now consider the feasibility of extending the differential space-time codes to cooperative networks. For the clarity of the presentation of the proposed method, we ignore the

noise effect in this section. The effect of noise, and the optimization of power allocation in different antennas as well as different broadcast and relay phases, will be considered in Section V for a two-user scenario.

Assume that there are M users cooperating with each other. Without loss of generality, we only focus on the first user's information and the user index is omitted without confusion. Following the protocol depicted in Section III, $\mathbf{C}' \in \mathcal{C}^{M\times M^2}$ is constructed from the corresponding differential space-time codeword $\mathbf{C} \in \mathcal{G}$, expressed as

$$\mathbf{C}'(\nu) = \begin{bmatrix} c_{21}(\nu) & \cdots & c_{2M}(\nu) & \cdots & c_{M1}(\nu) & \cdots & c_{MM}(\nu) & c_{11}(\nu) & \cdots & c_{1M}(\nu) \\ 0 & \cdots & \cdots & \cdots & \cdots & \cdots & 0 & c_{21}(\nu) & \cdots & c_{2M}(\nu) \\ \vdots & \vdots & \vdots & \vdots & \vdots & \vdots & \vdots & \vdots & \ddots & \vdots \\ 0 & \cdots & \cdots & \cdots & \cdots & \cdots & 0 & c_{M1}(\nu) & \cdots & c_{MM}(\nu) \end{bmatrix}. \tag{8}$$

It is assumed that signals transmitted from different terminals are synchronized at the destination receiver.

Because different rows of the DSTC codeword undergo different propagation channels with different attenuations, it is desirable to allocate energy adaptively to different rows. For this purpose, (8) is generalized to

$$\mathbf{C}'(\nu) = \begin{bmatrix} \alpha_2\sqrt{P_1}c_{21}(\nu) & \cdots & \alpha_M\sqrt{P_1}c_{MM}(\nu) & \alpha_1\sqrt{P_1}c_{11}(\nu) & \cdots & \alpha_1\sqrt{P_1}\hat{c}_{1M}(\nu) \\ 0 & \cdots & 0 & \sqrt{P_2}c_{21}(\nu) & \cdots & \sqrt{P_2}c_{2M}(\nu) \\ \vdots & \vdots & \vdots & \vdots & \ddots & \vdots \\ 0 & \cdots & 0 & \sqrt{P_M}c_{M1}(\nu) & \cdots & \sqrt{P_M}c_{MM}(\nu) \end{bmatrix}, \tag{9}$$

where $P_i \geq 0$ is the transmit power of different users, $i = 1, \cdots, M$, and $\alpha_i \geq 0$ is used to adjust the transmit power at the source terminal corresponding to different codeword rows. Because $\mathbf{C}(\nu)$ is unitary, $\sum_{k=1}^{M} |c_{ik}|^2 = 1$ for $i = 1, \cdots, M$. Therefore, the total codeword power of the DSTC in (9) is $P = P_1 \sum_{i=1}^{M} \alpha_i^2 + \sum_{i=2}^{M} P_i$. The optimization of the power allocation is considered in Section V.

Next, we consider the detection of differential DSTC codeword $\mathbf{C}'(\nu)$ without using the CSI. From (4) and (9), the relationship between two adjacent differential DSTC codewords,

$\mathbf{C}'(\nu)$ and $\mathbf{C}'(\nu-1)$, and the information codeword $\mathbf{G}(\nu)$ is expressed as

$$\mathbf{C}'(\nu) = \mathbf{C}'(\nu-1)\mathbf{G}'(\nu) = \mathbf{C}'(0)\prod_{\tau=1}^{\nu}\mathbf{G}'(\tau), \tag{10}$$

where

$$\mathbf{G}'(\nu) = \mathrm{diag}\,[\,\mathbf{G}(\nu),\cdots,\mathbf{G}(\nu)\,] = \mathbf{I}_M \otimes \mathbf{G}(\nu), \tag{11}$$

with $\otimes$ denoting the Kronecker product operator. Because $\mathbf{G}(\nu)$ is unitary, it is clear that the $M^2 \times M^2$ matrix $\mathbf{G}'(\nu)$ is also unitary (i.e., $\mathbf{G}'(\nu)(\mathbf{G}'(\nu))^H = \mathbf{I}_{M^2}$).

Note that the encoding process of (10) is performed at the source terminal and, therefore, it does not require the relay terminals to perform encoding or to possess information required in the differential coding process. In addition, it is noted that the distributed space-time codeword $\mathbf{C}'(\nu)$ is, in general, not unitary. However, because $\mathbf{G}'(\nu)$ is unitary, we have

$$\mathbf{C}'(\nu)[\mathbf{C}'(\nu)]^H = \mathbf{C}'(\nu-1)\mathbf{G}'(\nu)[\mathbf{G}'(\nu)]^H[\mathbf{C}'(\nu-1)]^H = \mathbf{C}'(\nu-1)[\mathbf{C}'(\nu-1)]^H = \mathbf{C}'(0)[\mathbf{C}'(0)]^H. \tag{12}$$

Therefore, the transmit power of $\mathbf{C}'(\nu)$ is unchanged for different ν and, subsequently, the robustness of the differential code is guaranteed.

Denote $\tilde{\mathbf{h}}(\nu) = [h_{10}(\nu),\ h_{12}(\nu)h_{20}(\nu),\ \cdots,\ h_{1,M}(\nu)h_{M,0}(\nu)]$ as the $1 \times M$ channel vector whose components are assumed constant for any two adjacent codewords (i.e., $\tilde{\mathbf{h}}(\nu) = \tilde{\mathbf{h}}(\nu-1)$) and are independent and stochastic processes over time. Then, the $1 \times M^2$ received signal vector at the destination terminal is given by

$$\begin{aligned}\mathbf{y}(\nu) &= \tilde{\mathbf{h}}(\nu)\mathbf{C}'(\nu) = \tilde{\mathbf{h}}(\nu)\mathbf{C}'(\nu-1)\mathbf{G}'(\nu)\\ &= \tilde{\mathbf{h}}(\nu-1)\mathbf{C}'(\nu-1)\mathbf{G}'(\nu)\\ &= \mathbf{y}(\nu-1)\mathbf{G}'(\nu).\end{aligned} \tag{13}$$

From (13), it becomes evident that the differential detection is feasible in cooperative networks because $\mathbf{G}'(\nu)$ and, equivalently, $\mathbf{G}(\nu)$, can be recovered from $\mathbf{y}(\nu)$ and $\mathbf{y}(\nu-1)$, without the knowledge of the channel characteristics.

V. Performance Analysis

A. Signal Model

In this section, we consider the performance of the proposed system. For simplicity, we only consider a two-user scenario (ref. Fig. 4), while the extension to multi-user scenarios is straightforward. Because of the symmetry, we focus only on the transmission of user 1's information, whereas the second user is regarded as the relay.

Consider the generalized codeword $\hat{\mathbf{C}}'(\nu)$ which considers the relay noise and takes the following form

$$\hat{\mathbf{C}}'(\nu) = \begin{bmatrix} \sqrt{P_1}c_{21}(\nu) & \sqrt{P_1}c_{22}(\nu) & \alpha\sqrt{P_1}c_{11}(\nu) & \alpha\sqrt{P_1}c_{12}(\nu) \\ 0 & 0 & \sqrt{P_2}\hat{c}_{21}(\nu) & \sqrt{P_2}\hat{c}_{22}(\nu) \end{bmatrix}, \tag{14}$$

where $\hat{c}_{ik}$ denotes the attenuated and noisy version of c_{ik}, $i,k = 1,2$. The expression of $\hat{c}_{ik}$ will be implicitly given later in (17). The total energy used to transmit $\hat{\mathbf{C}}'(\nu)$ is $P = (1+\alpha^2)P_1+P_2$. Note that, while we only use a single α in the first row (compared to α_1 and α_2 in (9)), it is obvious that α, P_1, and P_2 together provide enough degrees-of-freedom to adjust the power over different terminals and different time slots.

We first consider the signal flow during time block ν which spans four time slots. In the first two time slots, $c_{21}(\nu)$ and $c_{22}(\nu)$ are transmitted from user 1's antenna. As the result, the signals received at relay terminal (user 2) and the destination receiver are expressed, respectively, as

$$[\,r_1(\nu), r_2(\nu)\,] = \sqrt{P_1}\gamma_{12}h_{12}(\nu)\,[\,c_{21}(\nu), c_{22}(\nu)\,] + [\,n_{r1}(\nu), n_{r2}(\nu)\,] \tag{15}$$

$$[\,y_1(\nu), y_2(\nu)\,] = \sqrt{P_1}\gamma_{10}h_{10}(\nu)\,[\,c_{21}(\nu), c_{22}(\nu)\,] + [\,n_1(\nu), n_2(\nu)\,], \tag{16}$$

where $n_i(\nu)$ and $n_{ri}(\nu)$ denote, respectively, the receiver noise at the destination and the relay at time slot i within time block ν.

At the second time block, $c_{11}(\nu)$ and $c_{12}(\nu)$ are transmitted from user 1's antenna, and $r_1(\nu)$ and $r_2(\nu)$ are relayed from user 2's antenna after the amplification. The received

signal at the destination receiver becomes

$$\begin{aligned}
[y_3(\nu), y_4(\nu)] &= \left[\sqrt{P_1}\gamma_{10}h_{10}(\nu), \sqrt{P_2}\gamma_{20}h_{20}(\nu)\right]\begin{bmatrix} \alpha c_{11}(\nu) & \alpha c_{12}(\nu) \\ \hat{c}_{21}(\nu) & \hat{c}_{22}(\nu) \end{bmatrix} + [n_3(\nu), n_4(\nu)] \\
&= \left[\sqrt{P_1}\gamma_{10}\, h_{10}(\nu), \sqrt{P_1P_2}\gamma_{20}\gamma_{12}h_{20}(\nu)h_{12}(\nu)g_2\right]\begin{bmatrix} \alpha c_{11}(\nu) & \alpha c_{12}(\nu) \\ c_{21}(\nu) & c_{22}(\nu) \end{bmatrix} \\
&\quad + \sqrt{P_2}\gamma_{20}h_{20}(\nu)g_2\,[n_{r1}(\nu), n_{r2}(\nu)] + [n_3(\nu), n_4(\nu)] \\
&= \left[\sqrt{P_1}\gamma_{10}\, h_{10}(\nu), \sqrt{P_2}\gamma_{20}h_{20}(\nu)h_{12}(\nu)\tilde{g}_2\right]\begin{bmatrix} \alpha c_{11}(\nu) & \alpha c_{12}(\nu) \\ c_{21}(\nu) & c_{22}(\nu) \end{bmatrix} \\
&\quad + \sqrt{\frac{P_2}{P_1}}\frac{\gamma_{20}}{\gamma_{12}}h_{20}\tilde{g}_2\,[n_{r1}(\nu), n_{r2}(\nu)] + [n_3(\nu), n_4(\nu)],
\end{aligned} \tag{17}$$

where

$$\begin{aligned}
g_2^2 &= \{E\,[|r_1(\nu)|^2 + |r_2(\nu)|^2]\}^{-1} = \{E\,[P_1\gamma_{12}^2|h_{12}(\nu)|^2 + n_{r1}^2(\nu) + n_{r2}^2(\nu)]\}^{-1} \\
&= \left[P_1\gamma_{12}^2 + 2\sigma_{rn}^2\right]^{-1} = P_1^{-1}\gamma_{12}^{-2}\left[1 + \frac{2\sigma_{rn}^2}{P_1\gamma_{12}^2}\right]^{-1}
\end{aligned} \tag{18}$$

is a power normalization factor such that the total energy transmitted from the relay terminal over the two symbols is P_2, and

$$\tilde{g}_2^2 = g_2^2 P_1\gamma_{12}^2 = \frac{P_1\gamma_{12}^2}{P_1\gamma_{12}^2 + 2\sigma_{rn}^2} \leq 1 \tag{19}$$

is the power ratio at which the relay terminal transmits desired signal in the presence of relay noise. In (18) and (19), $\sigma_{rn}^2 = E\,[|n_{r1}(\nu)|^2] = E\,[|n_{r2}(\nu)|^2]$ is the variance of the relay noise.

Equations (15) – (18) can be combined into the following format

$$\mathbf{y}(\nu) = \mathbf{h}(\nu)\mathbf{C}'(\nu) + \underbrace{\mathbf{n}(\nu) + \sqrt{\frac{P_2}{P_1}}\frac{\gamma_{20}}{\gamma_{12}}h_{20}\tilde{g}_2\mathbf{n}_r(\nu)}_{\tilde{\mathbf{n}}(\nu)}, \tag{20}$$

where

$$\begin{aligned}
\mathbf{y}(\nu) &= [y_1(\nu), y_2(\nu), y_3(\nu), y_4(\nu)] \\
\mathbf{h}(\nu) &= [\gamma_{10}h_{10}(\nu), \gamma_{20}h_{20}(\nu)h_{12}(\nu)\tilde{g}_2] \\
\mathbf{n}(\nu) &= [n_1(\nu), n_2(\nu), n_3(\nu), n_4(\nu)] \\
\mathbf{n}_r(\nu) &= [0, 0, n_{r1}(\nu), n_{r2}(\nu)],
\end{aligned}$$

and

$$\mathbf{C}'(\nu) = \begin{bmatrix} \sqrt{P_1}c_{21}(\nu) & \sqrt{P_1}c_{22}(\nu) & \alpha\sqrt{P_1}c_{11}(\nu) & \alpha\sqrt{P_1}c_{12}(\nu) \\ 0 & 0 & \sqrt{P_2}c_{21}(\nu) & \sqrt{P_2}c_{22}(\nu) \end{bmatrix}. \tag{21}$$

It is noted that, because of the relay noise, the average power that the relay terminal uses to transmit the useful information is $P_2\tilde{g}_2^2/2$ for each symbol, whereas the average power transmitted from the relay terminal is $P_2/2$ per symbol.

Similar to (20), for time block $\nu-1$, we have

$$\begin{aligned}\mathbf{y}(\nu-1) &= \mathbf{h}(\nu-1)\mathbf{C}'(\nu-1)+\mathbf{n}(\nu-1)+\sqrt{\frac{P_2}{P_1}}\frac{\gamma_{20}}{\gamma_{12}}h_{20}\tilde{g}_2\mathbf{n}_r(\nu-1)\\ &= \mathbf{h}(\nu)\mathbf{C}'(\nu-1)+\mathbf{n}(\nu-1)+\sqrt{\frac{P_2}{P_1}}\frac{\gamma_{20}}{\gamma_{12}}h_{20}\tilde{g}_2\mathbf{n}_r(\nu-1),\end{aligned} \tag{22}$$

where again $\mathbf{h}(\nu)=\mathbf{h}(\nu-1)$ is assumed. With the noise components considered, $\mathbf{y}(\nu)$ and $\mathbf{y}(\nu-1)$ are now related through the following relationship

$$\mathbf{y}(\nu)=\mathbf{y}(\nu-1)\mathbf{G}'(\nu)+\tilde{\mathbf{n}}(\nu), \tag{23}$$

where

$$\tilde{\mathbf{n}}(\nu)=\left[\mathbf{n}(\nu)+\sqrt{\frac{P_2}{P_1}}\frac{\gamma_{20}}{\gamma_{12}}h_{20}\tilde{g}_2\mathbf{n}_r(\nu)\right]-\left[\mathbf{n}(\nu-1)+\sqrt{\frac{P_2}{P_1}}\frac{\gamma_{20}}{\gamma_{12}}h_{20}\tilde{g}_2\mathbf{n}_r(\nu-1)\right]\mathbf{G}'(\nu). \tag{24}$$

Because $\mathbf{G}'(\nu)$ is unitary, it is evident from the above equation that the differential decoding doubles the noise power or, equivalently, reduces the SNR by 3 dB.

B. Maximum Likelihood Detection

The covariance matrix of the combined noise vector $\tilde{\mathbf{n}}(\nu)$ is obtained as

$$\mathbf{R}_{\tilde{\mathbf{n}}}=E[\tilde{\mathbf{n}}^H(\nu)\tilde{\mathbf{n}}(\nu)]=2\sigma_n^2\left[\mathbf{I}_4+\frac{P_2}{P_1}\frac{\gamma_{20}^2}{\gamma_{12}^2}\frac{\sigma_{rn}^2}{\sigma_n^2}\tilde{g}_2^2\mathbf{D}_2\right]=\sigma_n^2\Delta^2, \tag{25}$$

where $\sigma_n^2=E\left[|n_1(\nu)|^2\right]=E\left[|n_2(\nu)|^2\right]$ is the variance of the destination receiver noise, $\mathbf{D}_2=\text{diag}[0,\ 0,\ 1,\ 1]$, and

$$\Delta^2=2\left[\mathbf{I}_4+\frac{P_2}{P_1}\frac{\gamma_{20}^2}{\gamma_{12}^2}\frac{\sigma_{rn}^2}{\sigma_n^2}\tilde{g}_2^2\mathbf{D}_2\right]=2\left[\mathbf{I}_4+\frac{P_2\gamma_{20}^2\sigma_{rn}^2}{\sigma_n^2\left(P_1\gamma_{12}^2+2\sigma_{rn}^2\right)}\mathbf{D}_2\right]=2\left[\mathbf{I}_4+W\mathbf{D}_2\right] \tag{26}$$

is a diagonal matrix implicitly defined in the above equation, where

$$W=\frac{P_2\gamma_{20}^2\sigma_{rn}^2}{\sigma_n^2\left(P_1\gamma_{12}^2+2\sigma_{rn}^2\right)}. \tag{27}$$

The maximum likelihood detection results in the estimation of $\mathbf{G}(\nu)$ as

$$\begin{aligned}\hat{\mathbf{G}}(\nu) &= \arg\min_{\mathbf{G}} \mathrm{tr}\left\{[\mathbf{y}(\nu)\Delta^{-1} - \mathbf{y}(\nu-1)(\mathbf{I}_2 \otimes \mathbf{G})\Delta^{-1}]\,[\mathbf{y}(\nu)\Delta^{-1} - \mathbf{y}(\nu-1)(\mathbf{I}_2 \otimes \mathbf{G})\Delta^{-1}]^H\right\} \\ &= \arg\min_{\mathbf{G}} \mathrm{tr}\left\{[\mathbf{y}(\nu) - \mathbf{y}(\nu-1)(\mathbf{I}_2 \otimes \mathbf{G})]\,\Delta^{-2}\,[\mathbf{y}(\nu) - \mathbf{y}(\nu-1)(\mathbf{I}_2 \otimes \mathbf{G})]^H\right\},\end{aligned} \tag{28}$$

where "tr" denotes the trace of a matrix.

C. Performance Analysis

While the accurate performance of a differentially coded system requires the consideration of the quadratic receiving structure [22], [23], [26], it can be well approximated in high SNR situations by using an equivalent coherent receiver model (23) with known channel vector $\mathbf{y}(\nu-1)$ and enhanced noise power of $\tilde{\mathbf{n}}(\nu)$ [25].

From (25), it is clear that the variance of the combined noise term during the last two symbols is larger than that during the first two symbols. Assume that the covariance matrix $\mathbf{R}_{\tilde{\mathbf{n}}} = \sigma_n^2\Delta^2$ can be estimated at the destination receiver. Then, right multiplying Δ^{-1} to (23) results in

$$\mathbf{y}(\nu)\Delta^{-1} = \mathbf{y}(\nu-1)\mathbf{G}'(\nu)\Delta^{-1} + \tilde{\mathbf{n}}(\nu)\Delta^{-1} \tag{29}$$

or

$$\mathbf{y}'(\nu) = \mathbf{y}(\nu-1)\tilde{\mathbf{G}}(\nu) + \mathbf{n}'(\nu), \tag{30}$$

where $\mathbf{y}'(\nu) = \mathbf{y}(\nu)\Delta^{-1}$, $\tilde{\mathbf{G}}(\nu) = \mathbf{G}'(\nu)\Delta^{-1}$, and $\mathbf{n}'(\nu) = \tilde{\mathbf{n}}(\nu)\Delta^{-1}$ has a covariance matrix $\sigma_n^2\mathbf{I}_4$. Multiplying $\mathbf{y}(\nu)$ by Δ^{-1} amounts to adjusting the signal strength at the receiver so that the noise power of the four symbols becomes equal. It does not affect the total power transmitted at the source and relay terminals.

From (29) and (30), it is seen that the detection problem becomes equivalent to finding unknown unitary codeword $\mathbf{G}'(\nu)$ in known equivalent channel vector $\mathbf{y}(\nu-1)$, known noise covariance matrix $\sigma_n^2\Delta^2$, and independent and temporally white noise components. From the above two equations, we can derive the pairwise codeword error probability (CER), i.e., the probability of transmitting $\mathbf{G}' = \mathrm{diag}[\mathbf{G}, \mathbf{G}]$ and deciding in favor of another

$\mathbf{E}' = \text{diag}[\mathbf{E}, \mathbf{E}]$ at the detector, conditioned by the equivalent channel vector $\mathbf{y}(\nu-1)$. The CER is given by

$$P(\mathbf{G}' \to \mathbf{E}'|\mathbf{y}(\nu-1)) = Q\left(\sqrt{d^2(\tilde{\mathbf{G}}, \tilde{\mathbf{E}})/(2\sigma_n^2)}\right), \tag{31}$$

where $d^2(\tilde{\mathbf{G}}, \tilde{\mathbf{E}})$ is the distance between the received signals corresponding to respective codewords $\tilde{\mathbf{G}}(\nu)$ and $\tilde{\mathbf{E}}(\nu)$ and is expressed as

$$d^2(\tilde{\mathbf{G}}, \tilde{\mathbf{E}}) = \mathbf{y}(\nu-1)\mathbf{A}\mathbf{y}^H(\nu-1), \tag{32}$$

$$\mathbf{A} = \left(\tilde{\mathbf{G}}(\nu) - \tilde{\mathbf{E}}(\nu)\right)\left(\tilde{\mathbf{G}}(\nu) - \tilde{\mathbf{E}}(\nu)\right)^H = \left(\mathbf{G}'(\nu) - \mathbf{E}'(\nu)\right)\Delta^{-2}\left(\mathbf{G}'(\nu) - \mathbf{E}'(\nu)\right)^H. \tag{33}$$

In calculating the distance of (32), we make the following approximation $\mathbf{y}(\nu) \approx \mathbf{h}(\nu)\mathbf{C}'(\nu)$ for moderate or high SNR scenarios. Then, (32) becomes

$$\begin{aligned} d^2(\tilde{\mathbf{G}}, \tilde{\mathbf{E}}) &= \mathbf{h}(\nu-1)\mathbf{C}'(\nu-1)\mathbf{A}\left(\mathbf{C}'(\nu-1)\right)^H \mathbf{h}^H(\nu-1) \\ &= \tilde{\mathbf{h}}(\nu)\Sigma_{\mathbf{h}}\mathbf{C}'(\nu-1)\mathbf{A}\left(\mathbf{C}'(\nu-1)\right)^H \Sigma_{\mathbf{h}}\tilde{\mathbf{h}}^H(\nu), \end{aligned} \tag{34}$$

where

$$\Sigma_{\mathbf{h}} = \text{diag}[\sigma_1, \sigma_2] = \text{diag}[\gamma_{10}, \gamma_{20}\tilde{g}_2], \tag{35}$$

and

$$\tilde{\mathbf{h}}(\nu) = \mathbf{h}(\nu)\Sigma_{\mathbf{h}}^{-1/2} = [h_{10}(\nu),\ h_{12}(\nu)h_{20}(\nu)] \tag{36}$$

is the normalized channel vector. For simplicity of the performance analysis, we assume the relay channel $h_{12}(\nu)$ is dominated by time-invariant component (e.g., the source terminal and the relay terminal have a clear line-of-sight and the scattering is relatively weak) and, therefore, can be approximated by a unit value. In addition, $h_{10}(\nu)$ and $h_{20}(\nu)$ are assumed to be uncorrelated complex Gaussian processes. In this case, $\tilde{\mathbf{h}}(\nu) = [h_{10}(\nu),\ h_{20}(\nu)] \sim \mathcal{CN}(0, \mathbf{I}_2)$.

In the underlying situation, the average power per symbol is $E_s = P/4$ (i.e., the total energy of a DSTC codeword is P). To clearly show the relationship between the pairwise CER and the input SNR, we rewrite (31) as

$$P(\mathbf{G}' \to \mathbf{E}'|\mathbf{y}(\nu-1)) = Q\left(\sqrt{\frac{d^2(\tilde{\mathbf{G}}, \tilde{\mathbf{E}})}{P}\frac{2E_s}{\sigma_n^2}}\right) \le \exp\left[\frac{-d^2(\tilde{\mathbf{G}}, \tilde{\mathbf{E}})}{P}\frac{E_s}{\sigma_n^2}\right], \tag{37}$$

where the last inequality is the Chernoff bound [2]. Because $\mathbf{y}(\nu)$ is approximated as a linear combination of i.i.d. channels $\tilde{\mathbf{h}}(\nu)$ and, therefore, constitute a set of dependent channel coefficients, averaging the above bound with respect to $\mathbf{y}(\nu-1)$ results in [2]

$$P(\mathbf{G}' \to \mathbf{E}') \leq \prod_{i=1}^{2} \left(1 + \frac{E_s}{\sigma_n^2}\frac{d_i}{P}\right)^{-1}, \tag{38}$$

where d_1 and d_2 are the eigenvalues of the following 2×2 matrix

$$\mathbf{K} = \mathbf{\Sigma_h} \mathbf{C}'(\nu-1) \mathbf{A} \left(\mathbf{C}'(\nu-1)\right)^H \mathbf{\Sigma_h}. \tag{39}$$

In the following, we consider two different cases. In the first case, matrix $\mathbf{K}$ is full rank, whereas in the second case, matrix $\mathbf{K}$ is rank one.

Case I: Full Rank Channel Environment

When $E_s d_i/(P\sigma_n^2) \gg 1$ for $i = 1, 2$, the CER can be approximated as

$$P(\mathbf{G}' \to \mathbf{E}') \leq \prod_{i=1}^{2} \left(1 + \frac{E_s}{\sigma_n^2}\frac{d_i}{P}\right)^{-1} \leq \left(\frac{E_s}{\sigma_n^2}\right)^{-2} \prod_{i=1}^{2} \left(\frac{d_i}{P}\right)^{-1} = \left(\frac{E_s}{4\sigma_n^2}\right)^{-2} \prod_{i=1}^{2} \left(\frac{4d_i}{P}\right)^{-1}. \tag{40}$$

The term $\left(\frac{E_s}{4\sigma_n^2}\right)^{-2}$ determines the diversity gain which indicates the slope at which the BER changes with the input SNR, whereas the term $\prod_{i=1}^{2}\left(\frac{4d_i}{P}\right)$ is a constant gain in controlling the BER and is referred to as the diversity product. In this case, the diversity gain of the system is two. Using the above results, it is seen that the diversity product is determined by the minimum product of $d_1 d_2$, i.e., the minimum determinant of $\mathbf{K}$. It can be shown that (refer to the Appendix)

$$\begin{aligned} \min \det(\mathbf{K}) &= \frac{1}{4(1+W)^2} \left|\det(\mathbf{\Sigma_h})\det(\mathbf{C}_2)\right|^2 \left(\min\left|\det(\mathbf{G}-\mathbf{E})\right|\right)^2 \\ &\quad + \frac{P_1 P_2 \gamma_{10}^2 \gamma_{20}^2 \tilde{g}_2^2}{4(1+W)} \left(\min \mathbf{c}_1 (\mathbf{G}-\mathbf{E})(\mathbf{G}-\mathbf{E})^H \mathbf{c}_1^H\right)^2 \\ &= \frac{\alpha^2 P_1 P_2 \gamma_{10}^2 \gamma_{20}^2 \tilde{g}_2^2}{4(1+W)^2} \left(\min\left|\det(\mathbf{G}-\mathbf{E})\right|\right)^2 \\ &\quad + \frac{P_1 P_2 \gamma_{10}^2 \gamma_{20}^2 \tilde{g}_2^2}{4(1+W)} \left(\min \mathbf{c}_1 (\mathbf{G}-\mathbf{E})(\mathbf{G}-\mathbf{E})^H \mathbf{c}_1^H\right)^2, \end{aligned} \tag{41}$$

where W is defined in (27), and

$$\mathbf{c}_1 = [c_{21}, c_{22}], \tag{42}$$

$$\mathbf{C}_2 = \begin{bmatrix} \alpha\sqrt{P_1} & 0 \\ 0 & \sqrt{P_2} \end{bmatrix} \begin{bmatrix} c_{11} & c_{12} \\ c_{21} & c_{22} \end{bmatrix} = \begin{bmatrix} \alpha\sqrt{P_1}c_{11} & \alpha\sqrt{P_1}c_{12} \\ \sqrt{P_2}c_{21} & \sqrt{P_2}c_{22} \end{bmatrix}. \quad (43)$$

The value of $\mathbf{c}_1(\mathbf{G}-\mathbf{E})(\mathbf{G}-\mathbf{E})^H\mathbf{c}_1^H$ is lower bounded by $\lambda_{\min}[(\mathbf{G}-\mathbf{E})(\mathbf{G}-\mathbf{E})^H]$, which is the minimum value of the smallest eigenvalues with respect to all the combinations of $\mathbf{G}$ and $\mathbf{E}$. That is,

$$\mathbf{c}_1(\mathbf{G}-\mathbf{E})(\mathbf{G}-\mathbf{E})^H\mathbf{c}_1^H \geq \lambda_{\min}[(\mathbf{G}-\mathbf{E})(\mathbf{G}-\mathbf{E})^H]. \quad (44)$$

Define

$$\beta = \frac{\lambda_{\min}[(\mathbf{G}-\mathbf{E})(\mathbf{G}-\mathbf{E})^H]}{\min|\det(\mathbf{G}-\mathbf{E})|} \quad (45)$$

as a factor determined by the used differential code. Then, the diversity product is lower bounded by

$$\min\det(\mathbf{K})\left(\frac{4}{P}\right)^2 \geq \frac{4P_1P_2\gamma_{10}^2\gamma_{20}^2\tilde{g}_2^2}{[(1+\alpha^2)P_1+P_2]^2}\frac{[\alpha^2+(1+W)\beta^2]}{(1+W)^2}\left(\min|\det[\mathbf{G}-\mathbf{E}]|\right)^2. \quad (46)$$

Now we consider the maximization of (46) in terms of the power allocations, leading to the optimal selection of P_1, P_2, and α. Because $(\min|\det[\mathbf{G}-\mathbf{E}]|)^2$ is independent of the power allocation, it suffices to consider only the following part of (46) for the purpose of optimization of the power allocation,

$$Q_1 = \frac{4P_1P_2\gamma_{10}^2\gamma_{20}^2\tilde{g}_2^2}{[(1+\alpha^2)P_1+P_2]^2}\frac{[\alpha^2+(1+W)\beta^2]}{(1+W)^2}. \quad (47)$$

By letting $\partial Q_1/\partial\alpha = 0$, we get

$$\alpha_{\text{opt}}^2 = \left[1-2(1+W)\beta^2+P_2/P_1\right]^+ = \left[1-2\left(1+\frac{P_2\gamma_{20}^2\sigma_{rn}^2}{\sigma_n^2(P_1\gamma_{12}^2+2\sigma_{rn}^2)}\right)\beta^2+\frac{P_2}{P_1}\right]^+, \quad (48)$$

where $[x]^+ = \max(0,x)$ (This operator is used to ensure that α^2 takes non-negative values). While the optimum power allocation between P_1 and P_2 can be obtained from the above expression, the analytic result is prohibitively complicated. However, the above results are helpful in determining the optimum power allocation. Specifically, when the interuser channel between the source and relay terminals has a good quality, i.e., γ_{12}^2 is large and σ_{rn}^2 is small, then $\tilde{g}^2 \approx 1$ and $W \approx 0$, and Q_1 becomes

$$Q_1' \approx \frac{4P_1P_2\gamma_{10}^2\gamma_{20}^2}{(1+\alpha^2)P_1+P_2}(\alpha^2+\beta^2). \quad (49)$$

Letting $\partial Q_1'/\partial P_1 = 0$ yields

$$(1+\alpha^2)P_1 = P_2. \tag{50}$$

Substituting this result back to (49), we obtain

$$Q'_{1,\text{opt}} \approx \frac{\gamma_{10}^2\gamma_{20}^2(\alpha^2+\beta^2)}{1+\alpha^2}. \tag{51}$$

In particular, when $\beta^2 = 1$, $Q'_{1,\text{opt}}$ is independent of α, providing that (50) is satisfied. On the other hand, α^2 assumes a large value when $\beta^2 < 1$, resulting in $P_1 \ll P_2$ and $\alpha^2 P_1 \approx P_2$.

Therefore, the optimum value of α depends on β. That is, given the same environment, different differential codes do not necessarily allocate the power in the same manner. When the relay noise is not negligible, the optimal value of Q_1' is compromised by the relay noise and in general β-dependent. Therefore, a differential code with higher $\min|\det(\mathbf{G}-\mathbf{E})|$ does not necessarily imply a high diversity product in the underlying cooperative diversity applications.

It is clear that, to optimize the power allocation, the channel attenuation characteristics have to be known. While in this paper we assume that the exact CSI is unavailable at the transmitters and receivers, we maintain that it is often practical to assume the channel quality at both transmitters and receivers because the attenuation characteristics vary with time in a much slower manner. It is emphasized that such large-scale channel attenuation characteristics are not required in employing the proposed differential distributed space-time coding scheme, but a good estimation of such information can be used to improve the system performance.

Case II: Rank 1 Channel Environment

When $E_s d_1/(P\sigma_n^2) \gg 1$ whereas $E_s d_2/(P\sigma_n^2) \ll 1$, (40) is no longer applicable. It happens, for example, when either the direct link or the relay link is highly impairing. In this case, (38) becomes

$$P(\tilde{\mathbf{G}} \to \tilde{\mathbf{E}}) \le \prod_{i=1}^{2}\left(1+\frac{E_s}{\sigma_n^2}\frac{d_i}{P}\right)^{-1} \le \left(\frac{E_s}{\sigma_n^2}\right)^{-1}\left(\frac{d_1}{P}\right)^{-1} = \left(\frac{E_s}{4\sigma_n^2}\right)^{-1}\left(\frac{4d_1}{P}\right)^{-1}. \tag{52}$$

When the relay channel is not reliable, that is, either γ_{20} or γ_{12} is very small, or the relay noise σ_{rn}^2 is very large, it is obvious that the relay should not be used and the system degenerates to the non-cooperative system.

On the other hand, when the direct channel between the source and the destination is unreliable, i.e., $\gamma_{10} \approx 0$, the system becomes a pure relay structure. In this case, α should be chosen as 0, and $\mathbf{K}$ defined in (39) becomes

$$\mathbf{K} = \mathrm{diag}\left[0,\ \frac{P_2\gamma_{20}^2\tilde{g}_2^2}{2(1+W)}\mathbf{c}_1(\mathbf{G}-\mathbf{E})(\mathbf{G}-\mathbf{E})^H\mathbf{c}_1^H\right]. \tag{53}$$

Using the results of (44) and (45), the minimum value of $4d_1/P$ in (52) is obtained as

$$\begin{aligned}\min\left(\frac{4d_1}{P}\right) &= \frac{1}{P}\frac{4P_2\gamma_{20}^2\tilde{g}_2^2}{2(1+W)}\min\left[\mathbf{c}_1\left(\mathbf{G}-\mathbf{E}\right)\left(\mathbf{G}-\mathbf{E}\right)^H\mathbf{c}_1^H\right] \\ &\geq \frac{2P_1P_2\gamma_{12}^2\gamma_{20}^2}{P_1+P_2}\frac{\sigma_n^2}{[\sigma_n^2(P_1\gamma_{12}^2+2\sigma_{rn}^2)+P_2\gamma_{20}^2\sigma_{rn}^2]}\beta\min|\det(\mathbf{G}-\mathbf{E})|.\end{aligned} \tag{54}$$

Because $\beta\min|\det(\mathbf{G}-\mathbf{E})|$ is independent of the power allocation, we only consider the following term for the optimization of the power allocation,

$$Q_2 = \frac{2P_1P_2\gamma_{12}^2\gamma_{20}^2}{P_1+P_2}\frac{\sigma_n^2}{[\sigma_n^2(P_1\gamma_{12}^2+2\sigma_{rn}^2)+P_2\gamma_{20}^2\sigma_{rn}^2]}. \tag{55}$$

Then, $\partial Q_2/\partial P_1 = 0$ results in

$$P_2 = \left[\sqrt{\sigma_n^2\sigma_{rn}^2+\gamma_{20}^2\gamma_{12}^2P_1^2}-\sigma_n\sigma_{rn}\right]\sigma_n/\left(\gamma_{20}^2\sigma_{rn}\right). \tag{56}$$

In particular, when we assume $P_1\gamma_{12} \gg 2\sigma_{rn}^2$, that is, the interuser channel has a high quality and the input SNR at the relay terminal is high, the above result becomes

$$P_2\gamma_{20}/\sigma_n = P_1\gamma_{12}/\sigma_{rn}. \tag{57}$$

Therefore, the power at different relay portions should be assigned proportional to the propagation gain and inversely proportional to the standard deviation of the noise generated in each relay portion.

VI. Numerical Results

In this section, we consider a simple situation where two users cooperate to transmit their respective information to the destination, as illustrated in Fig. 4. Two differential DSTC

codes are considered. In Scheme 1, the differential DSTC code is constructed based on Alamouti's space-time code, where each symbol uses a QPSK signal constellation, results in $N = 16$ codewords in the two time-slot space-time code. In Scheme 2, the differential DSTC is constructed based on the differential MIMO space-time code developed by Liang and Xia [27]. For the latter, the constellation size remains $N = 16$. Unless otherwise specified, the power is optimally allocated by adjusting P_1, P_2, and α to maximize Q_1 in (47), provided that the average power per symbol is unity.

A. Comparison with Co-located MIMO Systems

In the first set of simulations, we compare the CER performance of the proposed cooperative network with a MIMO system consisting of two co-located antennas. The two antennas in the MIMO system are assumed to have independent Rayleigh channels to the destination with unit variance. For the cooperative system, we assume $\gamma_{10} = \gamma_{20} = 1$ and $\gamma_{12} = \sqrt{125}$, which corresponds to the situation that the interuser distance between the source and relay terminals is one-fifth of the distance between the source terminal and the destination, and the power attenuation exponential is 3. In this case, the channels to the destination terminal, i.e., $h_{10}(\nu)$ and $h_{20}(\nu)$, are assumed Rayleigh faded, whereas the interuser channel is considered non-fading, i.e., $h_{12}(\nu) = 1$.

Fig. 5 compares the performance of the cooperative diversity system and the corresponding MIMO system. The SNR is defined as the reciprocal of the receiver noise power, as the transmit power is normalized to unity per symbol period. The relay receiver and the destination terminal receiver have the same noise power. It is seen that, the cooperative diversity system achieves the same diversity gain, and there is a performance degradation due to the relay noise in the cooperative diversity system. The performance degradation is very small when the channel quality between the source and relay is reasonably good.

We notice that, however, the spectrum efficiency of the cooperative network is half of the corresponding MIMO system because of the requirement of the broadcast phase.

B. Effect of Interuser Channel Fading

In the second set of simulations, we consider a scenario where $\gamma_{10} = 1$ and $\gamma_{12} = \gamma_{20} = \sqrt{8}$, which matches the situation that the relay terminal is in the mid-way between the source terminal and the destination. The power attenuation exponential remains to be 3. Channels $h_{10}(\nu)$ and $h_{20}(\nu)$ are assumed Rayleigh faded. Two different situations of interuser channel $h_{12}(\nu)$ are considered: Rayleigh faded and unfaded. Compared to the unfaded channel, the impact of channel fading in $h_{12}(\nu)$ is evidenced in Fig. 6 by a reduction in the diversity gain and a notable performance degradation.

It is noted that the CER results depicted in Fig. 6, even in the presence of the interuser channel fading, are generally better than those in Fig. 5. That is, by placing a relay terminal in a proper location, power savings can be achieved compared to a MIMO system.

C. Significance of Power Allocation

The third set of simulations uses similar parameters as in the second set, i.e., $\gamma_{10} = 1$, $\gamma_{20} = \gamma_{12} = \sqrt{8}$, and all the channels are considered Rayleigh faded. To examine the effect of power allocation, Fig. 7 compares the CER based on optimal power allocation and a fix power allocation with $P_1 = 1, P_2 = 2$, and $\alpha = 1$. Both cases have the same total energy of four over the four-symbol interval. It is seen that, compared to the optimal power allocation, the fixed power allocation yields an SNR loss of about 1.5 dB when the Alamouti code is used, and up to about 1 dB when the Liang-Xia code is used.

VII. Conclusions

A novel space-time cooperation protocol has been developed for effective cooperative diversity operation when the channel state information (CSI) is unavailable at the receivers. It has been shown that the proposed differential space-time cooperation scheme is effective, and the performance loss due to differential detection is limited to 3 dB of noise enhancement compared to coherent detection. We have analyzed the pairwise codeword error probability performance of the cooperative diversity system. Based on this result,

the optimization of the power allocation over the source and relay terminals are considered and the results provided useful guidelines in system designs.

Appendix: Derivation of Equation (41)

We first consider the minimum determinant of $\mathbf{C}'(\nu-1)\mathbf{A}\left(\mathbf{C}'(\nu-1)\right)^H$. For notation simplicity, we omit $(\nu-1)$ in the rest of this appendix. Partition matrix $\mathbf{C}'$ as

$$\mathbf{C}' = \begin{bmatrix} \sqrt{P_1}\mathbf{c}_1 & : \mathbf{C}_2 \\ \mathbf{0} & \end{bmatrix} \tag{A.1}$$

where $\mathbf{c}_1$ and $\mathbf{C}_2$ are defined in (43), and $\mathbf{0} = [0,0]$. Also denote $\mathbf{O}$ as the 2×2 zero matrix. Then we have

$$\begin{aligned}
\mathbf{C}'\mathbf{A}\left(\mathbf{C}'\right)^H &= \begin{bmatrix} \sqrt{P_1}\mathbf{c}_1 & : \mathbf{C}_2 \\ \mathbf{0} & \end{bmatrix} \begin{bmatrix} \mathbf{G}-\mathbf{E} & \mathbf{O} \\ \mathbf{O} & \mathbf{G}-\mathbf{E} \end{bmatrix} \begin{bmatrix} \mathbf{I}_2/2 & \mathbf{O} \\ \mathbf{O} & [2(1+W)]^{-1}\mathbf{I}_2 \end{bmatrix} \\
&\quad \cdot \begin{bmatrix} (\mathbf{G}-\mathbf{E})^H & \mathbf{O} \\ \mathbf{O} & (\mathbf{G}-\mathbf{E})^H \end{bmatrix} \begin{bmatrix} \sqrt{P_1}\mathbf{c}_1^H & \mathbf{0}^H \\ \mathbf{C}_2^H & \end{bmatrix} \\
&= \frac{1}{2}\begin{bmatrix} P_1\mathbf{c}_1(\mathbf{G}-\mathbf{E})(\mathbf{G}-\mathbf{E})^H\mathbf{c}_1^H & 0 \\ 0 & 0 \end{bmatrix} + \frac{1}{2(1+W)}\left[\mathbf{C}_2(\mathbf{G}-\mathbf{E})(\mathbf{G}-\mathbf{E})^H\mathbf{C}_2^H\right].
\end{aligned} \tag{A.2}$$

Because

$$\det\left(\begin{bmatrix} z_0 & 0 \\ 0 & 0 \end{bmatrix} + \begin{bmatrix} z_1 & z_2 \\ z_3 & z_4 \end{bmatrix}\right) = \det\begin{bmatrix} z_1+z_0 & z_2 \\ z_3 & z_4 \end{bmatrix} = \det\begin{bmatrix} z_1 & z_2 \\ z_3 & z_4 \end{bmatrix} + z_0 z_4, \tag{A.3}$$

and the last (right-bottom) element of $\mathbf{C}_2(\mathbf{G}-\mathbf{E})(\mathbf{G}-\mathbf{E})^H\mathbf{C}_2^H$ equals to $P_2\mathbf{c}_1(\mathbf{G}-\mathbf{E})(\mathbf{G}-\mathbf{E})^H\mathbf{c}_1^H$, then, we have

$$\begin{aligned}
\det\left(\mathbf{C}'\mathbf{A}\left(\mathbf{C}'\right)^H\right) &= \frac{1}{4(1+W)^2}\left|\det(\mathbf{C}_2)\det(\mathbf{G}-\mathbf{E})\right|^2 \\
&\quad + \frac{1}{4(1+W)}P_1P_2\left[\mathbf{c}_1(\mathbf{G}-\mathbf{E})(\mathbf{G}-\mathbf{E})^H\mathbf{c}_1^H\right]^2.
\end{aligned} \tag{A.4}$$

Noting the fact that

$$\left|\det(\mathbf{C}_2)\right|^2 = \det\left(\mathbf{C}_2\mathbf{C}_2^H\right) = \det\left\{\begin{bmatrix} \alpha\sqrt{P_1} & 0 \\ 0 & \sqrt{P_2} \end{bmatrix}\mathbf{C}\mathbf{C}^H\begin{bmatrix} \alpha\sqrt{P_1} & 0 \\ 0 & \sqrt{P_2} \end{bmatrix}\right\} = \alpha^2 P_1 P_2, \tag{A.5}$$

equation (41) follows straightforwardly from (A.4).

References

[1] G. J. Foschini and M. J. Gans, "On limits of wireless communications in a fading environment when using multiple antennas," *Wireless Personal Commun.*, vol. 6, no. 3, pp. 311–335, March 1998.

[2] V. Tarokh, H. Jafarkhani, and A. R. Calderbank, "Space-time block codes from orthogonal designs," *IEEE Trans. Inform. Theory*, vol. 45, no. 5, July 1999.

[3] S. M. Alamouti, "A simple transmitter diversity scheme for wireless communications," *IEEE J. Select. Areas Commun.*, vol. 16, pp. 1451–1458, Oct. 1998.

[4] A. F. Naguib, N. Seshadri, A. R. Calderbank, "Increasing data rate over wireless channels: space-time coding and signal processing for high data rate wireless communications," *IEEE Signal Proc. Mag.*, vol. 17, no. 3, pp. 76–92, May 2000.

[5] A. Sendonaris, E. Erkip, and B. Aazhang, "Increasing uplink capacity via user cooperation diversity," *Proc. IEEE Int. Symp. Info. Theory*, Cambridge, MA, p. 156, Aug. 1998.

[6] A. Sendonaris, E. Erkip, and B. Aazhang, "User cooperative diversity – Part I and Part II," *IEEE Trans. Commun.*, vol. 51, no. 11, pp. 1927–1948, Nov. 2003.

[7] J. N. Laneman, D. N. C. Tse, and G. W. Wornell, "Cooperative diversity in wireless networks: effective protocols and outrage behavior," *IEEE Trans. Inform. Theory*, accepted for publication.

[8] J. N. Laneman and G. W. Wornell, "Distributed space-time coded protocols for exploiting cooperative diversity in wireless networks", *IEEE Trans. Inform. Theory*, vol. 49, no. 10, pp. 2415–2425, Oct. 2003.

[9] A. F. Dana and B. Hassibi, "On the power effeciency of sensory and ad-hoc wireless networks," submitted to *IEEE Trans. Inform. Theory.*

[10] M. Dohler, E. Lefranc, H. Aghvami, "Space-time block codes for virtual antenna arrays," *IEEE Int. Symp. Personal, Indoor and Mobile Radio Communications*, pp. 414–417, Sept. 2002.

[11] P. A. Anghel, G. Leus, and M. Kaveh, "Multi-user space-time coding in a cooperative networks," *Proc. IEEE ICASSP*, Hong Kong, May 2003.

[12] Y. Hua, Y. Mei, and Y. Chang, "Parallel wireless mobile relays with space-time modulations," *Proc. IEEE Workshop on Statistical Signal Processing*, St. Louis, MO, Sept. 2003.

[13] A. Stefanov and E. Erkip, "On the performance analysis of cooperative space-time coded systems," *IEEE Wireless and Communications and Networking Conf.*, New Orleans, LO, March 2003.

[14] A. Stefanov and E. Erkip, "Cooperative space-time coding for wireless networks," *IEEE Information Theory Workshop*, Paris, France, March – April 2003.

[15] A. Stefanov and E. Erkip, "Cooperative coding for wireless networks," *IEEE Trans. Commun.*, vol. 52, no. 9, pp. 1470–1476, Sept. 2004.

[16] I. Hammerstroem, M. Kuhn, B. Rankov, A. Wittneben, "Space-time processing for cooperative relay networks," *IEEE Vehicular Technology Conf.*, Orlando, FL, Oct. 2003.

[17] R. U. Nabar and H. Bölcskei, "Space-time signal design for fading relay channels", *GLOBECOM*, San Francisco, CA, Dec. 2003.

[18] R. U. Nabar, F. W. Kneubühler, and H. Bölcskei, "Space-time signal design for fading relay channels", *GLOBECOM*, San Francisco, CA, Dec. 2003.

[19] M. Janani, A. Hedayat, T. E. Hunter, and A. Nosratinia, "Coded cooperation in wireless communi-

cations: space-time transmission and iterative decoding," *IEEE Trans. Signal Processing*, vol. 52, no. 2, pp. 362–371, Feb. 2004.

[20] Y. Jing and B. Hassibi, "Distributed space-time coding in wireless relay networks-Part I: basic diversity results," Submitted to *IEEE Trans. Wireless Communications.*

[21] Y. Jing and B. Hassibi, "Distributed space-time coding in wireless relay networks-Part II: tighter upper bounds and a more general case," Submitted to *IEEE Trans. Wireless Communications.*

[22] B. L. Hughes, "Differential space-time modulation," *IEEE Trans. Inform. Theory*, vol. 46, pp. 2567–2578, Nov. 2000.

[23] B. M. Hochwald and T. L. Marzetta, "Unitary space-time modulation for multiple-antenna communications in Rayleigh flat fading," *IEEE Trans. Inform. Theory*, vol. 46, pp. 543–564, March 2000.

[24] B. M. Hochwald and W. Sweldens, "Differential unitary space-time modulation," *IEEE Trans. Commun.*, vol. 48, pp. 2041–2052, Dec. 2000.

[25] V. Tarokh and H. Jafarkhani, "A differential detection scheme for transmit diversity," *IEEE J. Select. Areas Commun.*, vol. 18, pp. 1169–1174, July 2000.

[26] M. Berhler, and M. K. Varanasi, "Asymptotic error probability analysis of quadratic receivers in Rayleigh-fading channels with applications to unified analysis of coherent and noncoherent space-time receivers," *IEEE Trans. on Inform. Theory*, vol. 47, no. 6, pp. 2383–2399, Sept. 2001.

[27] X.-B. Liang and X.-G. Xia, "Unitary signal constellations for differential space-time modulation with two transmit antennas: parameteric codes, optimal designs, and bounds," *IEEE Trans. Inform. Theory*, vol. 48, no. 8, pp. 2291–2322, Aug. 2003.

[28] Z. Liu, G. B. Giannakis, and B. L. Hughes, "Double differential space-time block coding for time-varying fading channels," *IEEE Trans. Commun.*, vol. 49, pp. 1529–1539, Sept. 2001.

[29] A. Shokrollahi, B. Hassibi, B. M. Hochwald, and W. Sweldens, "Representation theory for high-rate multiple-antenna code design," *IEEE Trans. Inform. Theory*, vol. 47, pp. 2335–2367, Sept. 2001.

[30] H. Li and J. Li, "Differential and coherent decorrelating multiuser receivers for space-time-coded CDMA systems," *IEEE Trans. Signal Processing*, vol. 50, no. 10, pp. 2529–2537, Oct. 2002.

[31] E. Zimmermann, P. Herhold, and G. Fettweis, "On the performance of cooperative diversity protocols in practical wireless systems," *IEEE Vehi. Tech. Conf.*, pp. 2212-2216, Oct. 2003.

[32] Q. Zhao and H. Li, "Performance of differential modulation with wireless relays in Rayleigh fading channels," *IEEE Communications Letters*, to appear.

[33] P. Tarasak, H. Minn, V. K. Bhargava, "Differential modulation for two-user cooperative diversity systems", *Globecom*, Nov.-Dec. 2004.

[34] D. Chen and J. N. Laneman, "Modulation and demodulation for cooperative diversity in wireless systems," submitted to *IEEE Trans. Wireless Communications.*

[35] X. Li, "Space-time coded multi-transmission among distributed transmitters without perfect synchronization," *IEEE Signal Processing Letters*, vol. 11, no. 12, pp. 948–951, Dec. 2004.

[36] Y. Hua, A. Swami, and B. Daneshrad, "Combating synchronization errors in cooperative relays," *IEEE ICASSP*, Philadelphia, PA, March 2005.

[37] Y. Zhang, G. Wang, and M. G. Amin, "Imperfectly synchronized cooperative network using distributed space-frequency coding," *IEEE Vehicul. Tech. Conf.*, Dallas, TX, Sept. 2005.

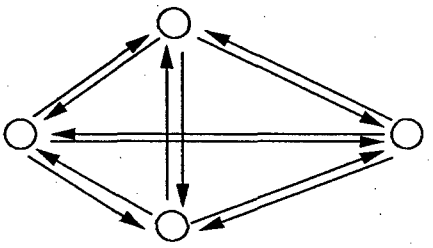

(a)

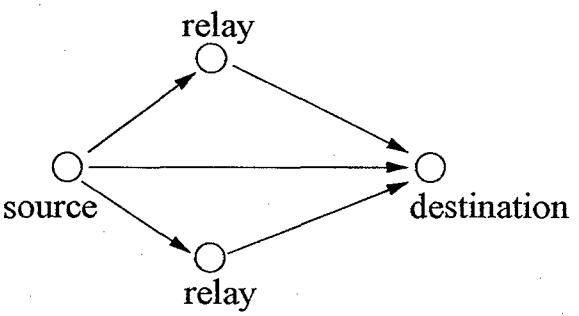

(b)

Fig. 1. System model.

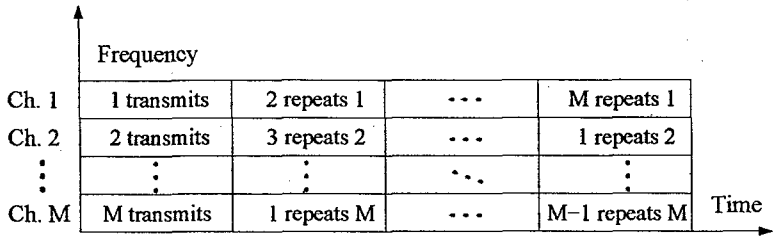

(a) repetition-based diversity scheme

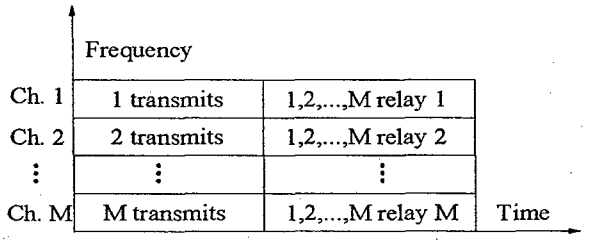

(b) space-time cooperation scheme I

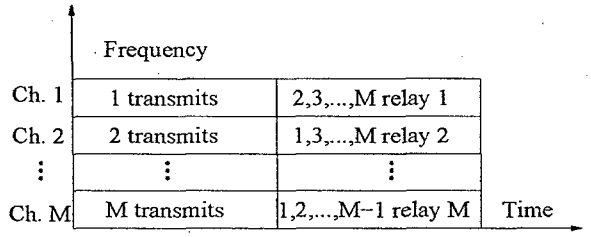

(c) space-time cooperation scheme II

Fig. 2. Cooperative diversity schemes.

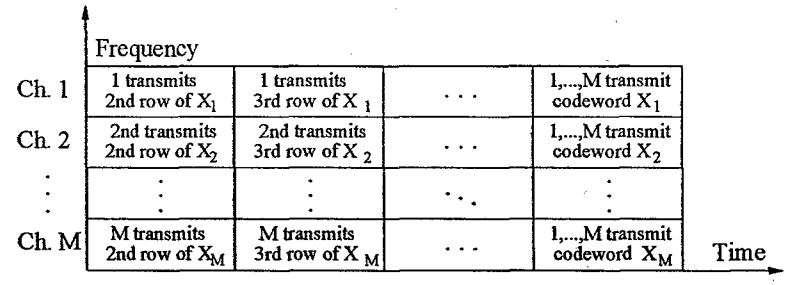

Fig. 3. The proposed space-time cooperation scheme.

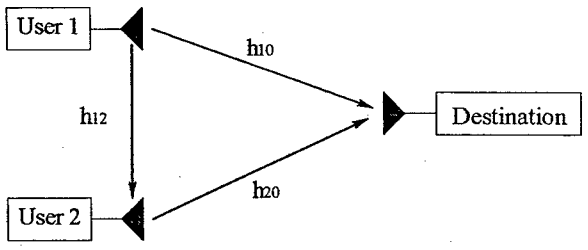

Fig. 4. Two-user system diagram.

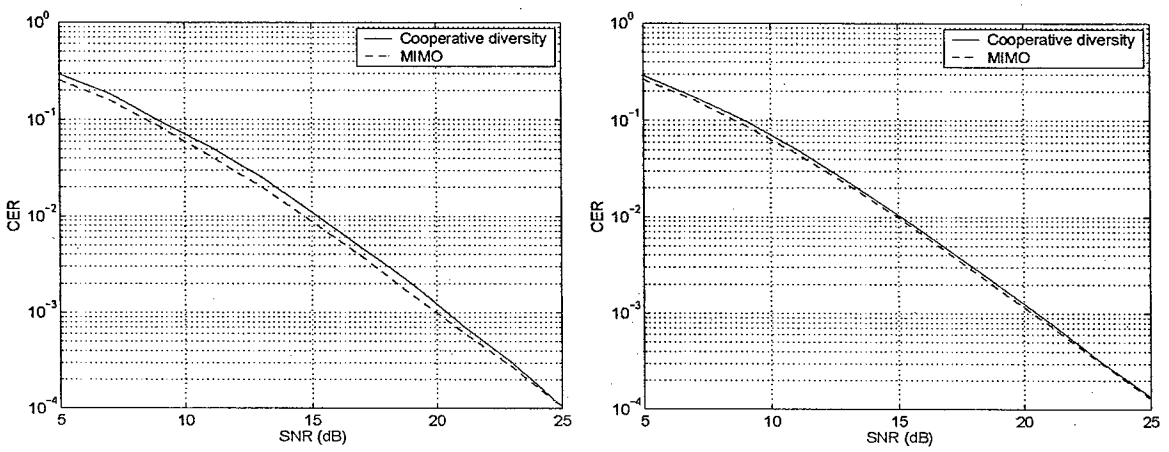

(a) Alamouti code (b) Liang-Xia code

Fig. 5. CER performance versus SNR for MIMO and cooperative diversity systems.

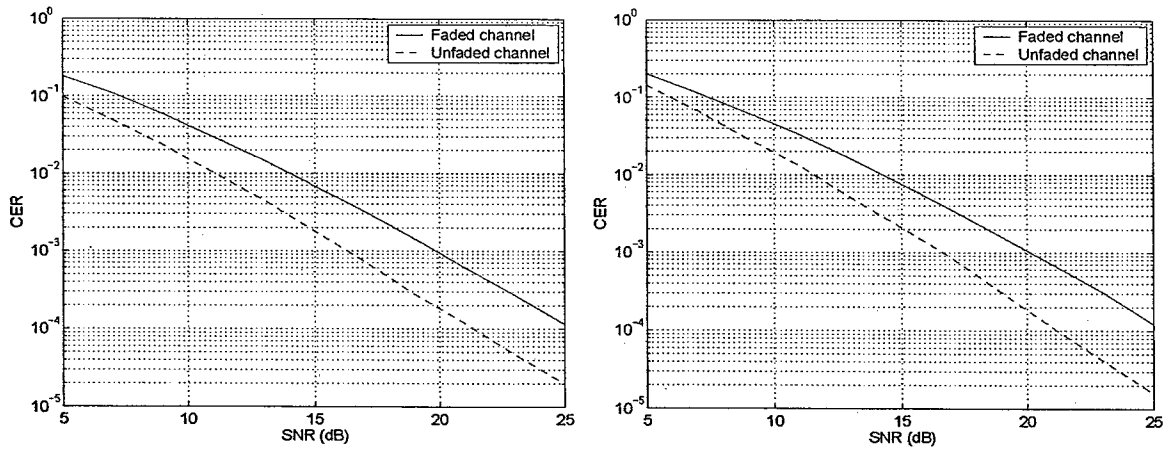

(a) Alamouti code (b) Liang-Xia code

Fig. 6. CER performance versus SNR with faded and unfaded channels between the source and relay terminals.

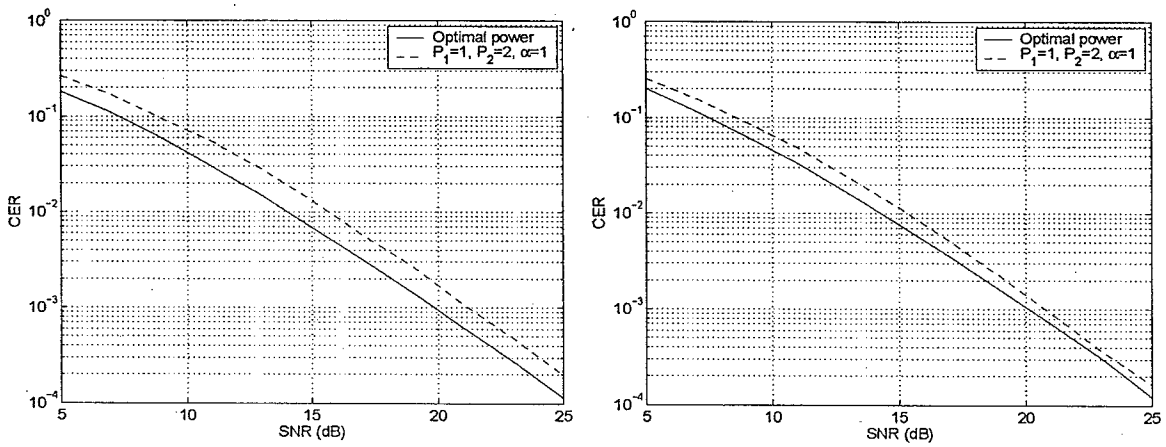

(a) Alamouti code (b) Liang-Xia code

Fig. 7. CER performance versus SNR for different power allocations.

Imperfectly Synchronized Cooperative Network Using Distributed Space-Frequency Coding

Yimin Zhang, Genyuan Wang, and Moeness G. Amin
Center for Advanced Communications
College of Engineering
Villanova University, Villanova, PA 19085
E-mail: {yimin.zhang,genyuan.wang,moeness.amin}@villanova.edu

Abstract

In distributed multiple-input-multiple-output (MIMO) systems, imperfect synchronization causes a unique problem in a coded cooperative diversity system. In the presence of a fractional-symbol delay between the signals transmitted from different relay nodes, the channels become highly dispersive even at a flat-fading environment. Existing methods solve such problem based on time-domain approaches where adaptive equalization is required at the receivers for combining the information transmitted from distributed sources. In this paper, we propose the use of OFDM-based approaches using distributed space-frequency codes. The proposed schemes are insensitive to fractional-symbol delays and lead to higher data rate transmission and simplified implementation. In addition, the proposed schemes permit the use of relatively simple amplify-and-forward algorithm in multi-hop wireless networks without delay accumulations. The proposed methods remove the time delay in each relaying hop by reconstructing the prefix and, as such, improve the spectral efficiency, while keeping a simplified relaying structure.

This work is supported in part by the ONR under Grant No. N00014-04-1-0617.

I. Introduction

In a wireless network, information transmission through relaying can be energy efficient. The use of multiple relaying nodes provides high diversity gain, improving robustness against channel impairments [1]. The concept of network cooperation or cooperative diversity has benefitted from the recent advances of space-time codes, transmit diversity, and multi-input-multi-output (MIMO) technologies. Recent research work has shown the feasibility of cooperative protocols and provided various capacity and performance analyses of cooperative diversity systems (see for example, [2]–[5] and references therein).

To achieve effective data transmission in a cooperative network surrounded by a flat-fading environment, several coded cooperation schemes have been developed. However, to adopt the detection schemes established for MIMO technologies, a fundamental assumption of all these schemes is that the relaying terminals are perfectly synchronized. Unlike the MIMO systems, however, perfect synchronization in diversity systems is highly unlikely in practice, because of the following reasons [6]: (a) An accurate synchronization between the relaying terminals with different locations, which are probably subject to continuous movements, is impractical. (b) Even for a network with fixed terminals (such as in a sensor network), changes in the parameters of electronic components may result in drifting and handshaking among transmitters is done infrequently so as to save energy and bandwidth. (c) Although nodes can synchronize the received signals as much as possible, low cost implementations may still make their timing and frequency slightly different, hence cause mismatch in the long run. (d) The major synchronization problem, however, lies in the delays of their signals when reaching at the receiving nodes in the next hop. Propagation delays may be unknown to them, while transmission times may be different. In fact, if the transmitting nodes try to synchronize toward one receiver, they may increase asynchronism toward other receivers because of different transmission distances. On the other hand, in most practical networks, nodes can (and are required) to maintain slot synchronization, which means that coarse slot synchronization is available. The difficulty lies in the fine transmission synchronization.

Most digital modulation signals guarantee no inter-symbol interference (ISI) only when the signals are accurately sampled at the symbol center. When the signal arrivals from

different relay terminals are not perfectly synchronized, the effect due to pulse tails resulted from sampling position error should be considered. This is particularly true when the receiver performs a symbol-based processing. To consider such effect, [6] proposed the use of a equivalent dispersive channel model, whether the channels are frequency-selective or frequency-nonselective. It also proposed a useful scheme which employs distributed space-time block code (STBC) in a time-reverse manner to achieve full diversity while tolerating imperfect synchronization. The difficulty of using this method, nevertheless, lies in the fact that it requires a channel equalizer at each receiver that makes the receiver very complicated and expensive.

In this paper, we propose the use of multi-carrier modulation exploiting distributed space-frequency coding schemes. The proposed schemes allow higher data rates and simplified implementation, as well as the distribution of the system complexity to transmitters and receivers. In addition, the feasibility of distributed space-frequency coding in a multi-hop relaying cooperative network is also considered. It is pointed out that the use of MIMO-OFDM methods allows the utilization of simple amplify-and-forward algorithm. While the time delay over different relay hops will be accumulated in the amplify-and-forward relaying process when space-time coding methods (e.g., time-reverse STBC, or TR-STBC [7]) are used, such delay accumulation problem can be easily avoided in the proposed method through the reconstruction of the cyclic prefix.

II. Channel Model

Consider a wireless network where a source node transmits a data packet to a destination node through a multi-hop wireless network. In each intermediate hop, the data packet is received by multiple nodes, e.g., nodes 1 to J in hop 1. These nodes can retransmit the data in the next hop in a cooperative manner with proper space-time (ST) encoding.

Without loss generality, the noise-free signals received at the kth node is expressed as

$$x_k(t) = \sum_{i=1}^{J} \int_{-\infty}^{\infty} \sqrt{P_i} h_{i,k}(t,\tau) s_i(t-\tau-\tau_{D,i,k}) d\tau, \tag{1}$$

where $s_i(t)$ is the signal waveform transmitted from node i, $h_{i,k}(t,\tau)$ and $\tau_{D,i,k}$ are the channel coefficients and the time delay between transmit node i and receive node k, respectively. It is assumed that channels $h_{i,k}(t,\tau)$ are time-invariant during the transmission

of a packet, but are randomly time-varying between packets. The channels are assumed spatially white, i.e., $h_{i,k}(t,\tau)$ are independent for different indices (i,k). In addition, $\sqrt{P_i}$ is the transmit power of node i. In a distributed MIMO system, the transmit power of different nodes may be different, depending on the a priori information of the large-scale attenuation characteristics at the transmitters [3], [12]. The total power is assumed to be a constant, i.e., $\sum_{i=1}^{J} P_i = P$.

Let $I_i(n)$ as the discrete information sequence transmitted from at the ith node, and $p(t)$ as the pulse shaping function. Then, (1) becomes

$$x_k(t) = \sum_{i=1}^{J} \sum_{m=-\infty}^{\infty} \sqrt{P_i} I_i(m) \int_{-\infty}^{\infty} h_{i,k}(t,\tau) p(t - \tau - \tau_{D,i,k} - mT_s) d\tau. \tag{2}$$

In general, the time delay consists of three factors: channel dispersion because of reflection and scattering ($\tau_{C,i,k}$), delay due to different locations of the relaying nodes ($\tau_{D,i,k}$), and the pulse shaping function spreading due to sampling position errors ($\tau_{W,i,k}$). Therefore, the significance of ISI depends not only on the channel length, but also on the node locations and the pulse shaping functions. Combining all these factors, we denote the upper bound of the effective channel length in terms of symbol period, as $L = [\max(\tau_{C,i,k}) + \max(\tau_{D,i,k}) + \max(\tau_{W,i,k})]/T_s$ with T_s denoting the symbol period. We use $L_C = \max(\tau_{C,i,k})/T_s$, $L_D = \max(\tau_{D,i,k})/T_s$, and $L_W = \max(\tau_{W,i,k})/T_s$ for notational simplicity, and $L = L_C + L_D + L_W$.

Sampling at $t = nT_s$, and taking the receiver noise into account, we have

$$x_k(n) = x_k(nT_s) = \sum_{i=1}^{J} \sum_{m=-\infty}^{\infty} \sqrt{P_i} I_i(m) \int_{-\infty}^{\infty} h_{i,k}(nT_s,\tau) p[(n-m)T_s - \tau - \tau_{D,i,k}] d\tau + v_k(n). \tag{3}$$

The noise is assumed to be of zero mean and unit variance, and is temporally and spatially white, i.e., $E[v_k(\tau) v_l^*(\nu)] = 0$ for $k \neq l$ or $\tau \neq \nu$, where * denotes complex conjugation.

III. Distributed MIMO-OFDM Schemes

A. MIMO-OFDM Transmission

We first review the MIMO-OFDM transmission using space-frequency (SF) codes in a transmitter with J co-located antennas. The following $J \times N$ SF codeword is formed in

the transmitter

$$\mathbf{C}_{\mathrm{SF}} = \begin{bmatrix} \mathbf{c}_1 \\ \mathbf{c}_2 \\ \vdots \\ \mathbf{c}_J \end{bmatrix} = \begin{bmatrix} c_1(0) & c_1(1) & \cdots & c_1(N-1) \\ c_2(0) & c_2(1) & \cdots & c_2(N-1) \\ \vdots & \vdots & \ddots & \vdots \\ c_J(0) & c_J(1) & \cdots & c_J(N-1) \end{bmatrix}, \tag{4}$$

where $c_i(n)$ denotes the channel symbol transmitted over the nth subcarrier by transmit antenna i, $i = 1, \cdots, J$, and $n = 0, \cdots, N-1$. The construction of space-frequency codes has been discussed in, for example, [8]–[10]. A detailed review of broadband MIMO-OFDM wireless communications is provided in [11].

The OFDM transformation of the source codeword applies an N-point IFFT to each row of the matrix $\mathbf{C}_{\mathrm{SF}}$. To eliminate the effect of ISI, cyclic prefix is inserted in the beginning of the transformed matrix. The OFDM symbol corresponding to the ith row of $\mathbf{C}_{\mathrm{SF}}$ is then transmitted using the ith transmit antenna.

At the receiver, after matched filtering, removing the cyclic prefix, and applying FFT to recover the transmitted SF codeword, information can be decoded, for example, using maximum likelihood detection.

B. Transmission of Distributed SF Codes

Now we extend the SF coded MIMO-OFDM approaches to the distributed wireless network. Similar to the protocol proposed in [3], [4] for constructing distributed ST codes, distributed SF codes can be constructed at the source terminal during the first hop. This paper only considers the intermediate hops where information is relayed from multiple distributed transmit nodes to multiple distributed receive nodes, forming a distributed MIMO structure. In particular, a relay node transmits a specific row of a SF codeword. The proposed method can be used for both flat and dispersive channels. In the latter, path diversity can be achieved [9], [10].

The OFDM transformation at the source codeword applies an N-point IFFT to each row of the matrix $\mathbf{C}_{\mathrm{SF}}$, resulting in

$$\mathbf{X}_{\mathrm{SF}} = \mathbf{C}_{\mathrm{SF}}\mathbf{F}, \tag{5}$$

where $\mathbf{F}$ is the $N \times N$ inverse Fourier transform matrix. After appending a cyclic prefix

of length C, the $J \times (N + C)$ matrix is obtained as

$$\mathbf{X}'_{\mathrm{SF}} = [\mathbf{x}_{\mathrm{SF}}(N - C), \cdots, \mathbf{x}_{\mathrm{SF}}(N - 1), \mathbf{X}_{\mathrm{SF}}], \tag{6}$$

where $\mathbf{x}_{\mathrm{SF}}(n)$ is the nth column of $\mathbf{X}_{SF}$. The frame length becomes $N + C$ symbol durations after the cyclic prefix is inserted. The OFDM symbol corresponding to the ith ($i = 1, \cdots, J$) column of $\mathbf{X}'_{\mathrm{SF}}$ is transmitted by the source node through the ith time frame.

C. Transmission Efficiency

In the single-carrier time-domain approaches, the minimum guard interval is $L_C + L_D + L_W$. In the proposed OFDM approach, the effective pulse tail L_W does not play a role. As a result, the guard interval is solely determined by the channel order, L_C, and the upper bound of the time delay between different transmit nodes, L_D. It could imply a significant reduction, particularly in flat or not heavily dispersive channels, since L_W may take a large value, depending on the synchronization strategy and the used pulse shaping function. By reducing the time delay effect from $L_C + L_W + L_D$ to $L_C + L_D$, the guard interval can be designed to be smaller than that in the single-carrier counterparts, resulting in improved data rates.

D. System Complexity

The proposed method requires transmitters and receivers to perform IFFT and FFT for OFDM modulations. It is usually a great reduction to the computational cost of an adaptive equalizer. It is noticed that the proposed approach requires IFFT or FFT operations in both transmit /receive sides, whereas the single-carrier time-domain approaches only require equalization performed at the receivers. Therefore, consider a multi-hop wireless network using the decode-and-forward algorithm, the proposed OFDM method provides significant advantages over the single-carrier approaches because the later demands high burden for equalizations in the decoding process. On the other hand, when we adopt the amplify-and-forward algorithm in the wireless network, single-carrier relaying approaches accumulate the channel delays over multiple hops, whereas the proposed method can easily remove such delay accumulation by reconstructing the cyclic prefix. The reconstruction

of the cyclic prefix is discussed in the following section.

IV. Cyclic Prefix Reconstruction in Multi-Hop Amplify-and-Forward Relaying

At the kth relaying node, the received signal corresponding to the nth subcarrier is given by

$$y_k(n) = \sum_{i=1}^{J} \sqrt{P_i}\hat{c}_i(n)H_{i,k}(n) + v_k(n), \tag{7}$$

where $\hat{c}_i(n)$ is the scaled and noisy replica of $c_i(n)$ contaminated in the previous hops, $H_{i,k}(n)$ is the Fourier transform of $h_{i,k}(t)$, and $v_k(n)$ denotes the additive complex Gaussian noise at the nth subcarrier.

In matrix format, for the nth subcarrier, the received signal at the J' relaying nodes, after the prefix is removed, is expressed as

$$\mathbf{y}(n) = \mathbf{H}(n)\mathbf{P}^{1/2}\hat{\mathbf{c}}(n) + \mathbf{v}(n), \tag{8}$$

where

$$\mathbf{y}(n) = [y_1(n), y_2(n), \cdots, y_J(n)]^T,$$

$$\hat{\mathbf{c}}(n) = [\hat{c}_1(n), \hat{c}_2(n), \cdots, \hat{c}_J(n)]^T,$$

$$\mathbf{v}(n) = [v_1(n), v_2(n), \cdots, v_J(n)]^T,$$

$$\mathbf{H}(n) = \begin{bmatrix} h_{1,1}(n), & h_{2,1}(n), & \cdots, & h_{J,1}(n) \\ h_{1,2}(n), & h_{2,2}(n), & \cdots, & h_{J,2}(n) \\ \vdots, & \vdots, & \ddots, & \vdots \\ h_{1,J'}(n), & h_{2,J'}(n), & \cdots, & h_{J,J'}(n) \end{bmatrix},$$

and

$$\mathbf{P} = \mathrm{diag}[P_1, P_2, \cdots, P_J].$$

The signal is retransmitted after the prefix is reconstructed from $\mathbf{y}(n)$. At the next hop, the received signal vector at the relaying nodes is expressed as

$$\begin{aligned} \mathbf{y}'(n) &= \mathbf{H}'(n)\left[\mathbf{H}(n)\mathbf{P}^{1/2}\hat{\mathbf{c}}(n) + \mathbf{v}(n)\right] + \mathbf{v}'(n) \\ &= \mathbf{H}'(n)\mathbf{H}(n)\mathbf{P}^{1/2}\hat{\mathbf{c}}(n) + \left[\mathbf{H}'(n)\mathbf{v}(n) + \mathbf{v}'(n)\right], \end{aligned} \tag{9}$$

where $\mathbf{H}'(n)$ is the channel matrix corresponding to the next hop. In general, when M hops are involved, the above process can be repeated. Denoting $\mathbf{H}_m(n)$ as the channel

matrix corresponding to the mth hop and the nth subcarrier, it is seen that the proposed amplify-and-forward scheme relays SF coded information with equivalent channel matrix $\prod_{m=1}^{M} \mathbf{H}_m(n)$, whereas the noise is accumulated. The information can be decoded using standard coherent detection methods if the combined channel state information (CSI) can be estimated at the destination, or using noncoherent detection methods that do not required CSI.

It is emphasized that, unlike the single-carrier amplify-and-forward process where the time delay over different hops will be accumulated, resulting in unrealistic implementations in multi-hop systems, the effect of the time delay in each hop is decoupled by the insertion and subtraction of the prefix, rendering to a manageable frame design and high spectral efficiency.

V. Numerical Results

A. Effect of Pulse Shaping Functions

To illustrate the effect of pulse shaping functions in an dispersive or imperfectly synchronized network using the single-carrier time-domain approaches, Fig. 1 depicts the impulse response of raised cosine filters with different sampling position errors of 0, $T_s/4$, and $T_s/2$, where the roll-off factor is 0.3. Denote $p(l)$ as the impulse response of the raised cosine filter sampled at the symbol rate, and define

$$\epsilon(n) = \frac{\sum\limits_{\text{all symbols}} |p(l)| - \sum\limits_{n \text{ dominant symbols}} |p(l)|}{\sum\limits_{\text{all symbols}} |p(l)|} \tag{10}$$

as the residual error of the impulse response after n dominant symbols are counted, the result is summarized in Table I. It is clear that, the impulse response spans roughly five to six symbols for both sampling position errors of $T_s/4$ and $T_s/2$. The long impulse response results in high equalizer complicity and, in a TR-STBC structure, a long guard interval.

The effect of sampling position errors can be reduced by using a large value of roll-off factor. Fig. 2 depicts the impulse response of raised cosine filters using roll-off factor of 1.0. While it implies a reduction in equalizer complexity and guard interval, the use of large roll-off factor results in a significant reduction of the spectral efficiency.

Unlike the time-domain approaches, the effect of pulse shaping in an OFDM system is

minimal. As a result, the effect of sampling position errors to the proposed MIMO-OFDM approach is negligible.

B. Effect of Cyclic Prefix Reconstruction

We consider a portion of a multi-hop relaying system as shown in Fig. 3. Two relaying hops (hop i and hop $i+1$) are included in this diagram to illustrate the capability of eliminating delay accumulation in the proposed scheme. Each relaying hop includes two transmit antennas ($M_t = 2$). Only one receiver is assumed at the receive end of the $(i+1)$th hop, because the performance of each node should be evaluated separately. While the relay nodes do not decode the signal, the bit error rate (BER) at the node is computed to measure the quality of the received signal.

The channels are considered to be independent random processes. It is assumed that the channels are fixed over a frame period, but vary randomly and assume complex Gaussian distribution over different frames. The channels are normalized such that they have a unit variance. In each hop, the total power is unity and is equally distributed over the two transmit antennas. The noise power is assumed to be the same over different relaying hops. The input signal-to-noise ratio (SNR) is defined as the reciprocal of the receiver noise power at each hop.

128 subcarriers are used for the OFDM signals, and the guard interval consists of six symbols, resulting in total 134 symbol periods over an OFDM frame. The distributed SF codewords are generated based on [10] where $\Gamma = 4$ and $P = 16$ are used. The source stream before SF coding is a binary sequence. Random permutation is applied in generating the SF codewords to achieve path diversity. 5000 frames are used to evaluate the BER performance.

The order of each channel is assumed to be five symbols. Therefore, without prefix reconstruction, the time delay over the two hops will be accumulated, resulting a total channel order of ten symbols. As a result, the six-symbol prefix does not provide enough protection against the channel dispersion, resulting in a BER floor if no equalization is applied (the solid line in Fig. 4). However, when the prefix is removed and reconstructed in each relay, the time delay can be eliminated in each relay. It is evident in Fig. 4 (the dashed line) that the BER in such case does not have a floor and a high diversity gain is

TABLE I

Residual Error of Impulse Response

n	1	2	3	4	5	6
$T_s/4$	0.440	0.261	0.163	0.101	0.0617	0.0364
$T_s/2$	0.658	0.315	0.219	0.123	0.0838	0.0442

achieved in the relay process.

VI. Conclusions

In a cooperative wireless network, channel dispersion exists as the result of several factors, e.g., channel length, pulse shaping function spreading, and spatial separations between the transmit nodes. We have considered the coded data transmission in a cooperative network with frequency-selective fading and proposed the distributed MIMO-OFDM schemes for effective multi-hop relaying. It is shown that, by reconstructing the cyclic prefix, the time delay effect in each relaying hop can be eliminated even using relatively simple amplify-and-forward algorithm. Therefore, the guard interval can be minimized and, thereby, high spectral efficiency is maintained.

References

[1] A. Sendonaris, E. Erkip, and B. Aazhang, "User cooperative diversity – Part I and Part II," *IEEE Trans. Commun.*, vol. 51, no. 11, pp. 1927–1948, Nov. 2003.

[2] J. N. Laneman and G. W. Wornell, "Distributed Space-Time Coded Protocols for Exploiting Cooperative Diversity in Wireless Networks", *IEEE Trans. Inform. Theory*, vol. 49, no. 10, pp. 2415–2425, Oct. 2003.

[3] G. Wang, Y. Zhang, and M. G. Amin, "Space-time cooperation diversity using high-rate codes," *Int. Symp. on Antennas and Propagation*, Sendai, Japan, Aug. 2004.

[4] G. Wang, Y. Zhang, and M. Amin, "Cooperation diversity using differential distributed space-time codes," *Joint Conf. of Asia-Pacific Conf. on Commun. and Int. Symp. on Multi-Dimensional Mobile Commun.*, Beijing, China, Aug. 2004.

[5] Y. Hua, Y. Mei, and Y. Chang, "Parallel wireless mobile relays with space-time modulations," *IEEE Workshop on Statistical Signal Processing*, St. Louis, MO, Sept. 2003.

[6] X. Li, "Space-time coded multi-transmission among distributed transmitters without perfect synchronization," *IEEE Signal Processing Letters*, vol. 11, no. 12, pp. 948–951, Dec. 2004.

[7] Z. Liu, G. B. Giannakis, B. Muquet, and S. Zhou, "Space-Time coding for broadband wireless communications," *Wireless Syst. Mobile Comput.*, vol. 1, no. 1, pp. 35– 53, Jan.–Mar. 2001.

[8] D. Agrawal, V. Tarokh, A. Naguib, and N. Seshadri, "Space-time coded OFDM for high data-rate wireless communication over wideband channels," in *Proc. IEEE Vehicular Technology Conf.*, vol. 3, pp. 2232-2236, 1998.

[9] W. Su, Z. Safar, M. Olfat, and K. J. R. Liu, "Obtaining full-diversity space-frequency codes from space-time codes via mapping," *IEEE Trans. Signal Processing*, vol. 51, no. 11, pp. 2905–2916, Nov. 2003.

[10] W. Su, Z. Safar, K. J. R. Liu, "Full-rate full-diversity space-frequency codes with optimum coding advantage," *IEEE Trans. Inform. Theory*, vol. 51, no. 1, pp. 229–249, Jan. 2005.

[11] G. L. Stüber, J. R. Barry, S. W. WcLaughlin, Y. (G.) Li, M. A. Ingram, and T. G. Pratt, "Broadband MIMO-OFDM wireless communications," *Proc. IEEE*, vol. 92, no. 2, pp. 271–294, Feb. 2004.

[12] Y. Zhang, "Differential modulation schemes for decode-and-forward cooperative diversity," *IEEE ICASSP*, Philadelphia, PA, March 2005.

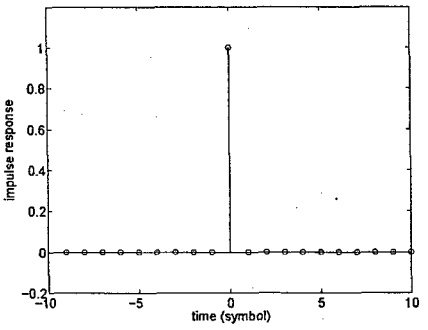

(a) no sampling position error

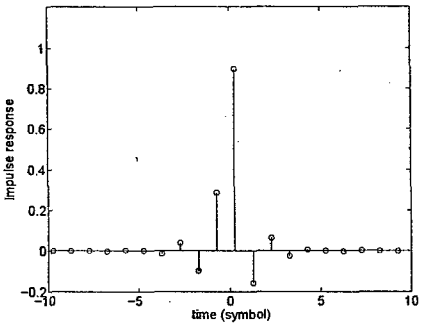

(b) sampling position error $= T_s/4$

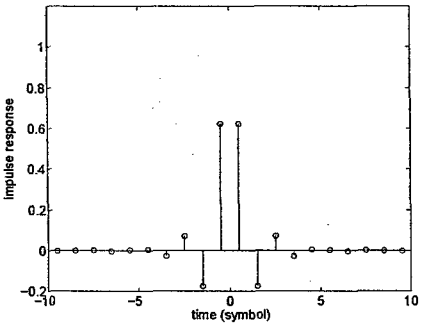

(c) sampling position error $= T_s/2$

Fig. 1. Impulse response of raised cosine filter with different sampling position errors (roll-off factor is 0.3).

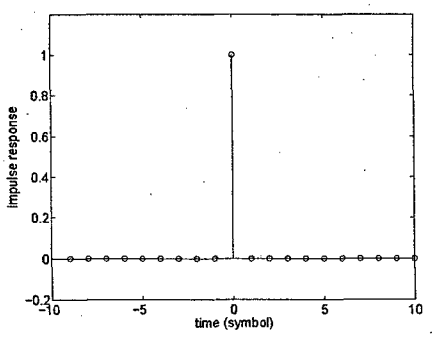

(a) no sampling position error

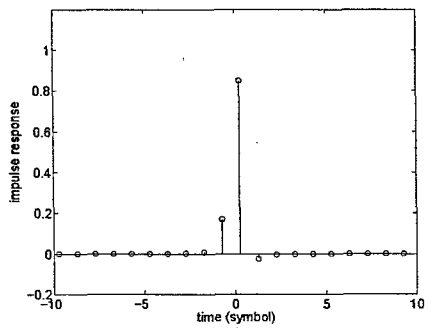

(b) sampling position error $= T_s/4$

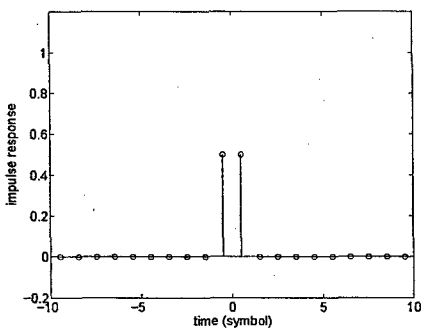

(c) sampling position error $= T_s/2$

Fig. 2. Impulse response of raised cosine filter with different sampling position errors (roll-off factor is 1.0).

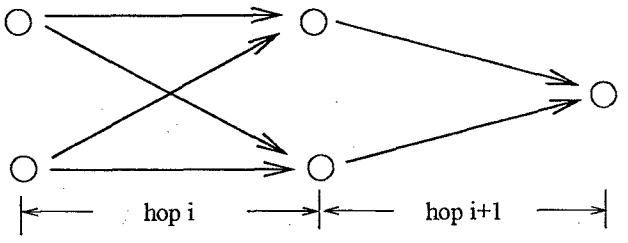

Fig. 3. Multi-hop relaying system under consideration.

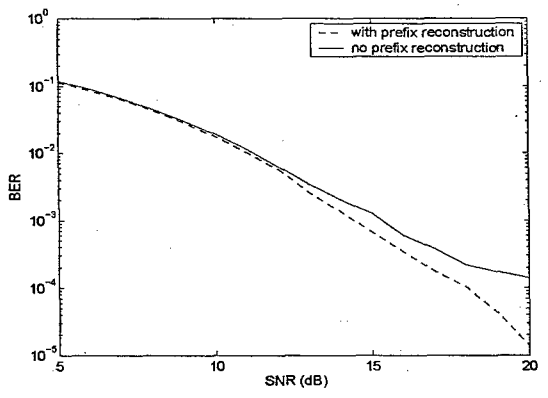

Fig. 4. BER with and without prefix reconstruction.

Space-Time Code Designs with Non-Vanishing Determinants Based on Cyclic Field Extension Families *

Genyuan Wang, Jian-Kang Zhang, Yimin Zhang, Moeness Amin, and Kon Max Wong

Abstract

The design of a linear space-time code with full rate, large diversity product, and non-vanishing minimum determinant of codewords continues to attract great attention. However, in most available no-vanishing determinant space-time codes for three, four and six transmit antennas, the average powers at each layer are different, which results in a high peak to average power ratio. In this paper, a new cyclic algebraic space-time design scheme is proposed and the optimal codes in this class are provided by using some specific cyclic field extensions. Our proposed codes not only include the available non-vanishing determinant cyclotomic space-time codes for three, four and six transmit antennas, but also have the desirable property that the optimal codes can be achieved with the same average power at each layer.

Keywords: Multi-layer space-time block codes, diversity product, full-rate, algebraic number theory, cyclotomic number rings, cyclic field extensions, lattices.

*The work of G. Wang, Y. Zhang and M. Amin is supported in part by ONR under grant No. N00014-04-1-0617 and NSF under grant No. EEC-0203459. G. Wang, Y. Zhang and M. Amin are with the Center for Advanced Communications, Villanova University, Villanova, PA 19085. Email: {genyuan.wang, yimin.zhang, moeness.amin}@villanova.edu. J.-K. Zhang and K. M. Wong are with the Department of Electrical and Computer Engineering, McMaster University, 1280 Main St. West, Hamilton, Ontario, Canada L8S 4K1. Email: {jkzhang,wongkm}@mail.ece.mcmaster.ca.

1 Introduction

Linear space-time block code designs based on algebraic field extensions have recently attracted great attention, see for example [1]-[12], due to the possibility of systematic constructions of full diversity and high data rate codes. Diagonal algebraic space-time block codes were first proposed in [3], where an n-dimensional diagonal space-time code $\mathrm{diag}([y_1, y_2, \cdots, y_n])$ was generated by $[y_1, \cdots, y_n]^T = G[x_1, \cdots, x_n]^T$, with matrix G and transmitted symbols $x_1, x_2, \cdots, x_n$ being properly chosen based on algebraic extension theory to achieve full diversity. The idea behind the diagonal algebraic space-time code can be tracked back to [1, 2], where the full diversity multi-dimensional signal constellation designs in both Rayleigh fading and additive Gaussian noise channel were considered. However, the symbol rate for the above diagonal space-time code design is one per channel use. In [6], a full diversity space-time code for two transmit antennas was proposed, where the symbol rate reached two per channel use. By employing algebraic number theory and threaded/multi-layer codes [14], more general full diversity and high symbol rate space-time code designs were proposed in [4, 6, 7, 11, 10]. Meanwhile, another type of full diversity and high rate space-time code was presented in [9] based on cyclic field extensions and division algebras .

In the early studies, the structure of code designs with high (full) rate and full diversity received more attention than the high diversity product. In most existing codes, the minimum determinant of non-zero codewords, which is the minimum determinant of any two different codewords, vanishes as the symbol constellation size increases.

Other space-time codes with a full symbol rate and high diversity product have been recently generated in [17, 18, 19, 21]. These codes not only have high diversity products, but also have the non-vanishing determinant property; i.e., the minimum determinant does not decrease as the symbol constellation size increases. Although the codes in [17, 19] for two transmit antennas have the same average powers at different layers, the cyclotomic space-time codes in [21] and [18] for three, four and six transmit antennas have different average powers at different layers, resulting a higher peak to average power ratio. In this paper, we propose a more general full diversity and full rate linear space-time code design with the non-vanishing determinant based on some specific cyclic field extensions, which is called a cyclic algebraic space-time code design. This class of cyclic

algebraic space-time codes includes all the cyclotomic space-time codes in [18] and [21] for three, four and six transmit antennas. In addition, the optimal cyclic algebraic space-time codes with largest diversity products were constructed with the same average power at each layer. [1]

This paper is organized as follows. In Section 2, the motivation and the problem description of this work are provided. In Section 3, the cyclic algebraic space-time code based on some specific cyclic field extension is introduced. The codewords with improved performance and the same average power at each layer are then given. Simulation results are presented in Section 4.

All lengthy proofs of the theorems are given in Appendix.

The following notation is used throughout this paper: capital English letters, such as, X and G, represent space-time codeword or matrix,

L_t: number of transmit antennas

$\mathbb{N}$: natural numbers

$\mathbb{Z}$: ring of integers

$\mathbb{Q}$: field of rational numbers

$\mathbb{C}$: field of complex numbers

$\phi(n)$: Euler function of positive integer n

$\zeta_m = \exp\left(j\frac{2\pi}{m}\right)$

$\mathbb{K}, \mathbb{F}$: general fields

$\mathbb{F}(\beta)$: field generated by β based on field $\mathbb{F}$

$(\mathbb{K}/\mathbb{F}, \beta, \sigma)$: cyclic field extension $\mathbb{K}/\mathbb{F}$ with $\mathbb{K} = \mathbb{F}(\beta)$, and σ of the generator of cyclic Galois group $Gal(\mathbb{K}/\mathbb{L})$

$X(\mathbb{K}/\mathbb{F}, \beta, \sigma, \rho)$: space-time code generated with cyclic field extension $(\mathbb{K}/\mathbb{F}, \beta, \sigma)$, $1, \rho, \cdots, \rho^{n-1}$ are the numbers used for adjusting at different layers of the code.

2 Motivation and Problem Description

Before providing the cyclic algebraic space-time code design, we first review cyclotomic space-time designs, based on which most of full rate non-vanishing determinant linear space-time codes are

[1] Before the submission of this paper, the authors learned that G. Rekaya, J. C. Belfiore and E. Viterbo recently also developed a non-vanishing determinant space-time code design for three, four and six transmit antennas with same average power at different layers [20].

developed.

2.1 Full Rate Cyclotomic Space-Time Codes Designs

In this subsection, we recall cyclotomic lattices, cyclotomic space-time codes and some of their fundamental properties obtained in [1, 2, 12]. For two positive integers m and n, let $N = mn$ and

$$L_t = \frac{\phi(N)}{\phi(m)}. \tag{1}$$

The variable L_t corresponds to the number of transmit antennas in a space-time code. There are totally L_t distinct integers l_i, $1 \leq i \leq L_t$, with $0 = l_1 < l_2 < \cdots < l_{L_t} \leq n-1$ such that $1 + l_i m$ and N are co-prime for any $1 \leq i \leq L_t$ (see for example p. 75 of [28]). With these L_t integers and $N = mn$, we define

$$G_{m,n} \triangleq \begin{bmatrix} \zeta_N & \zeta_N^2 & \cdots & \zeta_N^{L_t} \\ \zeta_N^{1+l_2 m} & \zeta_N^{2(1+l_2 m)} & \cdots & \zeta_N^{L_t(1+l_2 m)} \\ \vdots & \vdots & \ddots & \vdots \\ \zeta_N^{1+l_{L_t} m} & \zeta_N^{2(1+l_{L_t} m)} & \cdots & \zeta_N^{L_t(1+l_{L_t} m)} \end{bmatrix}_{L_t \times L_t}. \tag{2}$$

It can be verified that the above $G_{m,n}$ is unitary when $n = L_t$. We now define cyclotomic lattices.

Definition 1 *An L_t-dimensional cyclotomic lattice $\Gamma_{L_t}(G_{m,n})$ is a set of L_t-dimensional points $[y_1, \cdots, y_{L_t}]^T$ such that*

$$[y_1, \cdots, y_{L_t}]^T = G_{m,n}[x_1, \cdots, x_{L_t}]^T, \tag{3}$$

where $G_{m,n}$ is defined in (2) and $x_l \in \mathbb{Z}[\zeta_m]$.

Following the structure of threaded space-time codes in [14], a general multi-layer cyclotomic space-time code is defined as follows.

Definition 2 *Let L_t be the number of transmit antennas and $\Gamma_{L_t}(G_{m_l,n_l})$ be an L_t-dimensional cyclotomic lattice given in Definition 1, where G_{m_l,n_l} is defined in (2) for $l = 1, 2, \cdots, L_t$. Let $\rho_1, \cdots, \rho_{L_t}$ be L_t fixed complex numbers. Then, a multi-layer cyclotomic space-time code is defined*

as

$$\begin{bmatrix} \rho_1 y_1(1) & \rho_2 y_2(1) & \cdots & \rho_{L_t-1} y_{L_t-1}(1) & \rho_{L_t} y_{L_t}(1) \\ \rho_{L_t} y_{L_t}(2) & \rho_1 y_1(2) & \cdots & \rho_{L_t-2} y_{L_t-2}(2) & \rho_{L_t-1} y_{L_t-1}(2) \\ \vdots & \vdots & \vdots & \vdots & \vdots \\ \rho_2 y_2(L_t) & \rho_3 y_3(L_t) & \cdots & \rho_{L_t} y_{L_t}(L_t) & \rho_1 y_1(L_t) \end{bmatrix} =$$

$$\begin{bmatrix} \rho_1 x_1 & \rho_2 x_2 & \cdots & \rho_{L_t-1} x_{L_t-1} & \rho_{L_t} x_{L_t} \\ \rho_{L_t} \sigma_1(x_{L_t}) & \rho_1 \sigma_1(x_1) & \cdots & \rho_{L_t-2} \sigma_1(x_{L_t-2}) & \rho_{L_t-1} \sigma_1(x_{L_t-1}) \\ \vdots & \vdots & \vdots & \vdots & \vdots \\ \rho_2 \sigma_{L_t-1}(x_2) & \rho_3 \sigma_{L_t-1}(x_3) & \cdots & \rho_{L_t} \sigma_{L_t-1}(x_{L_t}) & \rho_1 \sigma_{L_t-1}(x_1) \end{bmatrix}, \quad (4)$$

where $[y_l(1), \cdots, y_l(L_t)]^T$ *is a point in cyclotomic lattice* $\Gamma_{L_t}(G_{m_l,n_l})$ *and* σ_l *are the* L_t *embeddings of* $\mathbb{Q}(\zeta_{mn})$ *to* $\mathbb{C}$ *that is fixed on* $\mathbb{Q}(\zeta_m)$ *for* $l = 1, \cdots, L_t$. *This multi-layer cyclotomic space-time code is denoted by* $X(\rho_1 G_{m_1,n_1}, \cdots, \rho_{L_t} G_{m_{L_t},n_{L_t}})$. *An L-layer cyclotomic space-time code with* $1 \leq L \leq L_t$ *is defined as a multi-layer cyclotomic space-time code* $X(\rho_1 G_{m_1,n_1}, \cdots, \rho_{L_t} G_{m_{L_t},n_{L_t}})$ *when* $\rho_l = 0$ *for* $l > L$ *and is denoted by* $X(\rho_1 G_{m_1,n_1}, \cdots, \rho_L G_{m_L,n_L})$.

2.2 Problem in the Cyclotomic Space-Time Code Designs

The key to designing a full rate cyclotomic space-time code is to find a proper cyclotomic field extension $\mathbb{Q}(\zeta_{mn})/\mathbb{Q}(\zeta_m)$ for given L_t and $\rho_l, l = 1, \cdots, L_t$, in (4) such that the resulting code achieves full diversity and a large diversity product. From the early studies on this topic, we know that there are infinite ways of determining the values of m, n, and ρ_l to generate full diversity full rate space-time codes. However, most of these codes do not have a large diversity product and the minimum determinant of codewords decrease to zero very rapidly when the constellation size of the codewords increases.

Recently, the generation of large diversity product space-time codes with a non-vanishing determinant has received much attention. The vital point to design this type of codes is to find a proper field extension $\mathbb{K}/\mathbb{F}$ and $\rho_l, l = 1, \cdots, L_t$, such that the determinant of every codeword belongs to the same lattice. The codewords provided in [17, 18, 19, 21] have the property that $\mathbb{F} = \mathbb{Q}(\zeta_4)$ or $\mathbb{Q}(\zeta_3) = \mathbb{Q}(\zeta_6)$, $\rho_l \in \mathbb{Z}[\zeta_4]$ or $\mathbb{Z}[\zeta_3] = \mathbb{Z}[\zeta_6]$, and the determinant of every codeword belongs to $\mathbb{Z}[\zeta_m]$. However, in the code design of [18, 21], $\rho_l = \rho^l, l = 1, \cdots, L_t$, with $|\rho| > 1$. Therefore, $|\rho_l|$ takes different values for different l; i.e., the average powers of the codewords at different layers are different. This results in a high peak to average power ratio. A close examination of the code design in [18, 21] reveals that the field extension $\mathbb{Q}(\zeta_{mn}/\mathbb{Q}(\zeta_m)$ based on minimal polynomial $x^n - \zeta_m$,

$m = 3, 4$, or 6, and ρ_l may not be a good choice. In this paper, we develop a code design using a more general field extension $\mathbb{K}/\mathbb{Q}(\zeta_m)$ with the minimal polynomial $x^n - \alpha$ for $\alpha \in \mathbb{Z}[\zeta_m]$ and ρ_l. The resulting new space-time codes have non-vanishing determinants with the same average power at each layer; i.e., $|\rho_l| = 1$, for three, four and six transmit antennas.

3 Full Rate Cyclic Algebraic Space-time Codes for Three, Four, and Six Transmit Antennas with Low Peak to Average Power Ratios

The existing cyclotomic code designs are obtained based on the cyclic field extension $(\mathbb{Q}(\zeta_{mn})/\mathbb{Q}(\zeta_n), \zeta_{mn})$ with the minimal polynomial $x^n - \zeta_m$, $m = 6$ or $m = 3$. In this section, we generalize the cyclic field extension to the $(\mathbb{Q}(\zeta_{mn})/\mathbb{Q}(\zeta_n), \beta)$ with a minimal polynomial $x^n - \alpha$, and $\beta^n = \alpha \in \mathbb{Z}[\zeta_m]$. We find optimal full rate space-time codes for three, four, and six transmit antenna in this class. The results show that optimal full rate space-time codes can be achieved with $|\rho| = 1$, which means that the average powers at different layers of the codewords are identical; i.e., a lower peak to average power ratio than that achieved by the cyclotomic space-time codes. Before providing the optimal codes, we introduce some concepts and results.

Definition 3 *[28] A Galois extension $\mathbb{K}/\mathbb{F}$ is called cyclic if the Galois group $Gal(\mathbb{K}/\mathbb{F})$ is a cyclic group.*

By the cyclic extension theory we have the following proposition.

Proposition 1 *[28] Let $\mathbb{F}$ be a field containing a primitive nth root of unity, and let $\mathbb{K} = \mathbb{F}(\sqrt[n]{\alpha})$ for some $\alpha \in \mathbb{F}$. Then $\mathbb{K}/\mathbb{F}$ is a cyclic Galois extension. Moreover, $m = [\mathbb{K} : \mathbb{F}]$ is equal to the order of the coset $\alpha\mathbb{F}^{*n}$ in the group $\mathbb{F}^*/\mathbb{F}^{*n}$, and $\min(\mathbb{F}, \sqrt[n]{\alpha}) = x^m - d$ for some $d \in \mathbb{F}$.*

From Proposition 1, we know that for a field $\mathbb{F}$ containing a primitive nth root of unity and its extension $\mathbb{F}[\sqrt[n]{\alpha}]$ with a minimal polynomial $x^n - \alpha$ over $\mathbb{F}$, $\mathbb{K}/\mathbb{F}$ is a cyclic Galois extension of dimension n. Therefore, there are a number of n embeddings $\sigma_l = \sigma^l$ of $\mathbb{K}$ to $\mathbb{C}$ such that $\sigma(x) = x$ for $x \in \mathbb{F}$ and $\sigma(\sqrt[n]{\alpha}) = \omega\sqrt[n]{\alpha} = \zeta_n\sqrt[n]{\alpha}$.

Definition 4 *An n-dimensional cyclic algebraic space-time code $X(\mathbb{K}/\mathbb{F}, \beta, \sigma, \rho)$ based on a cyclic field extension $\mathbb{K}/\mathbb{F}$ with $\beta = \sqrt[n]{\alpha}$ is a set of $n \times n$ matrices with the form of*

$$X = \begin{bmatrix} x_1 & \rho x_2 & \cdots & \rho^{n-2}x_{n-1} & \rho^{n-1}x_n \\ \rho^{n-1}\sigma(x_n) & \sigma(x_1) & \cdots & \rho^{n-3}\sigma(x_{n-2}) & \rho^{n-2}\sigma(x_{n-1}) \\ \vdots & \vdots & \ddots & \vdots & \vdots \\ \rho\sigma^{n-1}(x_2) & \rho^2\sigma^{n-1}(x_3) & \cdots & \rho^{n-1}\sigma^{n-1}(x_n) & \sigma^{n-1}(x_1) \end{bmatrix}, \tag{5}$$

where $x_l, l = 1, \cdots, n$ are determined by $x_l = \sum_{k=1}^{n} x_{k,l}\beta^{k-1}$ with $x_{k,l}$ being algebraic integers in $\mathbb{F}$. While ρ in (5) can be any complex number, in this paper, it is chosen from algebraic integers in field $\mathbb{F}$.

Notice that the codes in [9] and [18] are generated with the following form

$$X = \begin{bmatrix} x_1 & x_2 & \cdots & x_{n-1} & x_n \\ \widetilde{\rho}\sigma(x_n) & \sigma(x_1) & \cdots & \sigma(x_{n-2}) & \sigma(x_{n-1}) \\ \vdots & \vdots & \ddots & \vdots & \vdots \\ \widetilde{\rho}\sigma^{n-1}(x_2) & \widetilde{\rho}\sigma^{n-1}(x_3) & \cdots & \widetilde{\rho}\sigma^{n-1}(x_n) & \sigma^{n-1}(x_1) \end{bmatrix}. \tag{6}$$

Although the codewords in (6) and (5) differ in forms, it does not affect the criterion for finding a desirable code. The choice (5) saves the average transmit energy when $|\rho| > 1$, as is the case for many good codes.

Similar to (4), the cyclic algebraic space-time code defined in (5) can be rewritten as points of a complex lattice as follows,

$$\begin{bmatrix} y_1(1) & \rho y_2(1) & \cdots & \rho^{n-2}y_{n-1}(1) & \rho^{n-1}y_n(1) \\ \rho^{n-1}y_n(2) & y_1(2) & \cdots & \rho^{n-3}y_{n-2}(2) & \rho^{n-2}y_{n-1}(2) \\ \vdots & \vdots & \vdots & \vdots & \vdots \\ \rho y_2(n) & \rho^2 y_3(n) & \cdots & \rho^{n-1}y_n(n) & y_1(n) \end{bmatrix}, \tag{7}$$

where $[y_l(1), \cdots, y_l(n)]^T$ is a point in complex lattice $\Gamma_n(G_{n,\beta})$ with a generating matrix $G_{n,\beta}$ over $\mathbb{Z}[\zeta_n]$ for $l = 1, \cdots, n$,

$$G_{n,\beta} \triangleq \begin{bmatrix} 1 & 1 & \cdots & 1 \\ \zeta_n & \zeta_n^2 & \cdots & \zeta_n^n \\ \vdots & \vdots & \ddots & \vdots \\ \zeta_n^{n-1} & \zeta_n^{2(n-1)} & \cdots & \zeta_n^{n(n-1)} \end{bmatrix} \begin{bmatrix} 1 & 0 & \cdots & o \\ 0 & \beta & 0 & 0 \\ \vdots & \vdots & \ddots & \vdots \\ 0 & 0 & \cdots & \beta^{n-1} \end{bmatrix}. \tag{8}$$

Therefore, $[y_1(1), y_1(2), \cdots, y_1(n), \rho y_2(1), \rho y_2(2), \cdots, \rho y_2(n), \cdots, \rho^{n-1}y_n(1), \rho^{n-1}y_n(2), \cdots, \rho^{n-1}y_n(n)]$ can be considered as a point of larger complex lattice $\Gamma_{nn}(G_{n,\beta}, \rho G_{n,\beta}, \cdots, \rho^{n-1}G_{n,\beta})$, with a gen-

erating matrix $\mathcal{G}(G_{n,\beta}, \rho G_{n,\beta}, \cdots, \rho^{n-1}G_{n,\beta})$ over $\underbrace{\mathbb{Z}[\zeta_n] \times \mathbb{Z}[\zeta_n] \times \cdots \mathbb{Z}[\zeta_n]}_{n}$,

$$\mathcal{G}(G_{n,\beta}, \rho G_{n,\beta}, \cdots, \rho^{n-1}G_{n,\beta}) = \begin{bmatrix} G_{n,\beta} & 0 & \cdots & 0 \\ 0 & \rho G_{n,\beta} & \cdots & 0 \\ \vdots & \vdots & \ddots & \vdots \\ 0 & 0 & \cdots & \rho^{n-1}G_{n,\beta} \end{bmatrix}. \tag{9}$$

The absolute value of the determinant $|\det(\mathcal{G}(G_{n,\beta}, \rho G_{n,\beta}, \cdots, \rho^{n-1}G_{n,\beta}))|$ of the generating matrix $\mathcal{G}(G_{n,\beta}, \rho G_{n,\beta}, \cdots, \rho^{n-1}G_{n,\beta})$ is

$$|\det(\mathcal{G}(G_{n,\beta}, \rho G_{n,\beta}, \cdots, \rho^{n-1}G_{n,\beta}))| = |\det(G_n)|^n \rho^{n^2(n-1)/2} \beta^{n^2(n-1)/2}. \tag{10}$$

As a result, for a given integer n, we can compare two n-dimensional cyclic algebraic space-time codes $X(\mathbb{K}_1/\mathbb{F}_1, \beta_1, \sigma_1, \rho_1)$ and $X(\mathbb{K}_2/\mathbb{F}_2, \beta_2, \sigma_2, \rho_2)$ with the following criterion by using the results in [21].

Lemma 1 *For any two n-dimensional cyclic algebraic space-time codes $X(\mathbb{K}_1/\mathbb{F}_1, \beta_1, \sigma_1, \rho_1)$ and $X(\mathbb{K}_2/\mathbb{F}_2, \beta_2, \sigma_2, \rho_2)$, the former is better than the latter if $d_{min}(\mathbb{K}_2/\mathbb{F}_2, \beta_2, \sigma_2, \rho_2) = d_{min}(\mathbb{K}_1/\mathbb{F}_1, \beta_1, \sigma_1, \rho_1)$ and $|\beta_1\rho_1| \leq |\beta_2\rho_2|$, where*

$$d_{min}(\mathbb{K}/\mathbb{F}, \beta, \sigma, \rho) = \min_{X \neq 0, X \in X(\mathbb{K}/\mathbb{F}, \beta, \sigma, \rho)} |\det(X)| \tag{11}$$

is called the minimal determinant of code $X(\mathbb{K}/\mathbb{F}, \beta, \sigma, \rho)$.

In a special case where $\mathbb{F} = \mathbb{Q}(\zeta_n)$ and $\alpha = \zeta_n$, the cyclotomic space-time code is a cyclic algebraic space-time code. In all the cyclotomic space-time codes with non-vanishing determinants, $\mathbb{F} = \mathbb{Q}(\zeta_3) = \mathbb{Q}(\zeta_6)$, or $\mathbb{F} = \mathbb{Q}(\zeta_4)$. In this paper, we only consider the special case where $\mathbb{F} = \mathbb{Q}(\zeta_3) = \mathbb{Q}(\zeta_6)$, or $\mathbb{F} = \mathbb{Q}(\zeta_4)$. In the following, we will design optimal cyclic algebraic space-time codes for three, four, and six transmit antennas over $\mathbb{F} = \mathbb{Q}(\zeta_3) = \mathbb{Q}(\zeta_6)$, or $\mathbb{F} = \mathbb{Q}(\zeta_4)$ under the diversity product criterion.

Definition 5 *[18] Let $\mathbb{K}$ be a field and $\mathbb{F}$ a cyclic extension of degree d of $\mathbb{F}$, σ be the generator of Galois cyclic Galois group $Gal(\mathbb{K}/\mathbb{F})$. Take $\gamma \in \mathbb{F}^*$. The algebra $A = (\mathbb{K}/\mathbb{F}, \sigma, \gamma)$ generated by $\mathbb{K}$ and an element e is called a cyclic algebra, where $e^d = \gamma$, and $e \cdot \bar{x} = \bar{x} \cdot \sigma(e)$, for any $\bar{x} \in K$. This algebra $A = (\mathbb{K}/\mathbb{F}, \sigma, \gamma)$ can be written as*

$$A = (\mathbb{K}/\mathbb{F}, \sigma, \gamma) \doteq \mathbb{K} \oplus e \cdot \mathbb{K} \oplus \cdots \oplus e^{d-1} \cdot \mathbb{K}. \tag{12}$$

This algebra can be constructed as a subalgebra of $M_d(\mathbb{K})$, the d-dimensional matrix algebra over $\mathbb{K}$, by setting

$$e = \begin{bmatrix} 0 & 1 & \cdots & 0 \\ \vdots & \vdots & \ddots & \vdots \\ 0 & 0 & \ddots & 1 \\ \gamma & 0 & \cdots & 0 \end{bmatrix}, \qquad \bar{x} = diag(\sigma^l(x)), \qquad l = 0, \cdots, d-1, \tag{13}$$

From the definitions of cyclic algebra and cyclic algebraic space-time code, we know that a n-dimensional cyclic algebraic space-time code $X(\mathbb{K}/\mathbb{F}, \beta, \sigma, \rho)$ is a degree n cyclic algebra $(\mathbb{K}/\mathbb{F}, \sigma, \rho^n)$. In the design and proof of the optimality of a cyclic algebraic space-time code, we need to introduce the following lemma.

Lemma 2 *[18],[26] A cyclic algebra in the definition 5 is a division algebra if and only if $\gamma, \gamma^2, \cdots, \gamma^{d-1}$ are not algebraic norms of elements in $\mathbb{K}(\gamma, \gamma^2, \cdots, \gamma^{d-1})$.*

3.1 Optimal Cyclic Algebraic Space-time Code for Three Transmit Antennas

In this subsection, we assume that $\mathbb{F} = \mathbb{Q}(\zeta_3)$ and $\mathbb{K} = \mathbb{F}(\beta)$ is a cyclic field extension of degree 3 for some β with $\beta^3 = \alpha \in \mathbb{Z}[\zeta_3]$.

Now let us consider field extension towers $\mathbb{Q} \subset \mathbb{Q}(\zeta_3) \subset \mathbb{Q}(\zeta_3, \beta)$. Then, any $z \in \mathbb{Z}[\zeta_3, \beta]$ can be written as $z = z_1 + z_2\beta + z_3\beta^2 \in \mathbb{Q}(\zeta_3, \beta) = \mathbb{F}(\beta)$, where $z_k \in \mathbb{Z}[\zeta_3], k = 1, 2, 3$. Notice that $\mathbb{N}_{\mathbb{Q}(\zeta_3,\beta)/\mathbb{Q}(\zeta_3)}(z) = \prod_{k=1}^{3} \sigma_k(z)$, where $\sigma_k, k = 1, 2, 3$ are the three embedding of $\mathbb{Q}(\zeta_3, \beta)$ to $\mathbb{C}$ that is fixed over $\mathbb{Q}(\zeta_3)$ with $\sigma_k(\beta) = \zeta_3^{k-1}\beta$. Hence, from the definition of the relative algebraic norm we have

$$\begin{aligned} \mathbb{N}_{\mathbb{Q}(\zeta_{\zeta_3},\beta)/\mathbb{Q}(\zeta_3)}(z) &= z_1^3 + \beta^3 z_2^3 + \beta^6 z_3^3 + 3\beta^3(\zeta_3 + \zeta_3^2) z_1 z_2 z_3 \\ &= z_1^3 + \beta^3 z_2^3 + \beta^6 z_3^3 - 3\beta^3 z_1 z_2 z_3. \end{aligned} \tag{14}$$

If we let $\beta = 2^{1/3}$, then, we know from the algebraic number theory that $\mathbb{Q}(\zeta_3, 2^{1/3})/\mathbb{Q}(\zeta_3)$ is a cyclic field extension of degree 3. In the following we will prove that ζ_3 and ζ_6 are not the algebraic norm of some integer of $\mathbb{Q}(\zeta_3, 2^{1/3})$ over $\mathbb{Q}(\zeta_3)$.

Theorem 1 *For any $x, y \in \mathbb{Z}[\zeta_3, 2^{1/3}]$, if $\mathbb{N}_{\mathbb{Q}(\zeta_3,2^{1/3})/\mathbb{Q}(\zeta_3)}(x) = \zeta_6 \mathbb{N}_{\mathbb{Q}(\zeta_3,2^{1/3})/\mathbb{Q}(\zeta_3)}(y)$, $\mathbb{N}_{\mathbb{Q}(\zeta_3,2^{1/3})/\mathbb{Q}(\zeta_3)}(x) = \zeta_3 \mathbb{N}_{\mathbb{Q}(\zeta_3,2^{1/3})/\mathbb{Q}(\zeta_3)}(y)$, or $\mathbb{N}_{\mathbb{Q}(\zeta_3,2^{1/3})/\mathbb{Q}(\zeta_3)}(x) = \zeta_3^2 \mathbb{N}_{\mathbb{Q}(\zeta_3,2^{1/3})/\mathbb{Q}(\zeta_3)}(y)$ then, $x = y = 0$.*

The proof of Theorem 1 is given in Appendix.

Similarly, we can prove that 2 is not the algebraic norm of some integer of $\mathbb{Q}(\zeta_3, \zeta_6) = \mathbb{Q}(\zeta_{18})$ over $\mathbb{Q}(\zeta_3)$.

Theorem 2 *For any* $x, y \in \mathbb{Z}[\zeta_{18}]$ $(x, y \in \mathbb{Z}[\zeta_9])$, *if* $\mathbb{N}_{\mathbb{Q}(\zeta_{18})/\mathbb{Q}(\zeta_6)}(x) = 2\mathbb{N}_{\mathbb{Q}(\zeta_{18})/\mathbb{Q}(\zeta_6)}(y)$ $(\mathbb{N}_{\mathbb{Q}(\zeta_9)/\mathbb{Q}(\zeta_3)}(x) = 2\mathbb{N}_{\mathbb{Q}(\zeta_9)/\mathbb{Q}(\zeta_3)}(y))$, *then,* $x = y = 0$.

For any cyclic algebraic space-time codeword $X \in X(\mathbb{Q}(\zeta_3, \beta)/\mathbb{Q}(\zeta_3), \beta, \sigma, \rho)$ with the following form

$$X = \begin{bmatrix} x & \rho y & \rho^2 z \\ \rho^2\sigma(z) & \sigma(x) & \rho\sigma(y) \\ \rho\sigma^2(y) & \rho^2\sigma^2(z) & \sigma^2(x) \end{bmatrix}, \tag{15}$$

where $x = \sum_{l=1}^{3} x_l\beta^{l-1}$, $y = \sum_{l=1}^{3} y_l\beta^{l-1}$, $z = \sum_{l=1}^{3} z_l\beta^{l-1}$, with $x_l, y_l, z_l \in \mathbb{Z}[\zeta_3], \beta^3 \in \mathbb{Z}[\zeta_3], \rho^3 \in \mathbb{Z}[\zeta_3]$, we can prove that its determinant belongs to $\mathbb{Z}[\zeta_3]$; i.e.,

Theorem 3 *The determinant* $\det(X)$ *of matrix* X *with the form of (15) belongs to* $\mathbb{Z}[\zeta_3]$, *i.e.,*

$$\det(X) \in \mathbb{Z}[\zeta_3]. \tag{16}$$

The proof of Theorem 3 is provided in Appendix.

The following theorem guarantees that cyclic algebraic space-time codes $X(\mathbb{Q}(\zeta_3, 2^{1/3})/\mathbb{Q}(\zeta_3), 2^{1/3}, \sigma, \zeta_9)$, $X(\mathbb{Q}(\zeta_3, 2^{1/3})/\mathbb{Q}(\zeta_3), 2^{1/3}, \sigma, \zeta_{18})$, $X(\mathbb{Q}(\zeta_9)/\mathbb{Q}(\zeta_3), \zeta_9, \sigma, 2^{1/3})$, and $X(\mathbb{Q}(\zeta_{18})/\mathbb{Q}(\zeta_6), \zeta_{18}, \sigma, 2^{1/3})$ for three transmit antennas provide full rate full diversity with non-vanishing determinants.

Theorem 4 *The cyclic algebraic space-time code* $X(\mathbb{Q}(\zeta_3, 2^{1/3})/\mathbb{Q}(\zeta_3), 2^{1/3}, \sigma, \zeta_9)$, $X(\mathbb{Q}(\zeta_3, 2^{1/3})/\mathbb{Q}(\zeta_3), 2^{1/3}, \sigma, \zeta_{18})$, $X(\mathbb{Q}(\zeta_9)/\mathbb{Q}(\zeta_3), \zeta_9, \sigma, 2^{1/3})$, *and* $X(\mathbb{Q}(\zeta_{18})/\mathbb{Q}(\zeta_6), \zeta_{18}, \sigma, 2^{1/3})$, *are full diversity space-time code with the minimum determinant 1.*

Proof of Theorem 4: From Theorem 3 we know that the minimal determinants of these cyclic algebraic space-time codes are either 1 or 0. Therefore, we only need to prove that these cyclic algebraic space-time codes enable full diversity, i.e., if $\det(X) = 0$, then, $X = 0$, since they are linear. In addition, from Theorem 1, Theorem 2 and Lemma 2, we know that any non-zero codeword X in the algebraic space-time codes of Theorem 4 does not have a zero-divisor, i.e., if $\det(X) = 0$, then, $X = 0$.

Q.E.D.

Furthermore, we can prove that the resulting cyclic algebraic space-time codes for three transmit anetnnas in Theorem 4 is optimal based on the criterion given in Lemma 1.

Theorem 5 *Under the diversity product criterion,* $X(\mathbb{Q}(\zeta_3, 2^{1/3})/\mathbb{Q}(\zeta_3), 2^{1/3}, \sigma, \zeta_9)$, $X(\mathbb{Q}(\zeta_3, 2^{1/3})/\mathbb{Q}(\zeta_3), 2^{1/3}, \sigma, \zeta_{18})$, $X(\mathbb{Q}(\zeta_9)/\mathbb{Q}(\zeta_3), \zeta_9, \sigma, 2^{1/3})$ *and* $X(\mathbb{Q}(\zeta_{18})/\mathbb{Q}(\zeta_6), \zeta_{18}, \sigma, 2^{1/3})$ *are the optimal cyclic space-time codes for three transmit antennas with the minimal determinant 1.*

The proof of Theorem 5 is given in Appendix. From Lemma 1 we know that diversity product of a cyclic algebraic space-time code is determined by $|\beta\rho|$, the absolute value of product β and ρ. Therefore, the main idea to prove the optimality of these codes is to prove $\beta^3 = 2$ and $\rho^3 = \zeta_3$ are integers in $\mathbb{Z}[\zeta_3]$ with the minimum product $|\beta\rho|$ such that ρ, ρ^2 are not relative algebraic norm of any elements of $\mathbb{Q}(\zeta_3, \beta)$ over $\mathbb{Q}(\zeta_3)$.

Remarks: The cyclic algebraic code $X(\mathbb{Q}(\zeta_9)/\mathbb{Q}(\zeta_3), \zeta_9, \sigma, 2^{1/3})$ is a cyclotomic space-time code, but $X(\mathbb{Q}(\zeta_3, 2^{1/3})/\mathbb{Q}(\zeta_3), 2^{1/3}, \sigma, \zeta_9)$ is not. Although they have the same diversity product, i.e., the same performance under the diversity product criterion, the former with $\rho = 2^{1/3} > 1$ has different average power at each layer and the latter with $|\rho| = |\zeta_9| = 1$ has the same average power at each layer. Therefore, the latter has a lower peak to average power ratio.

3.2 Cyclic Algebraic Space-Time Code for Four and Six Transmit Antennas

In this subsection, we will generate cyclic algebraic codes for four and six transmit antennas.

Let $\alpha = \beta^4 \in \mathbb{Z}[\zeta_4]$, $\beta, \beta^2, \beta^3 \notin \mathbb{Q}(\zeta_4)$, $\mathbb{Q}(\zeta_4, \beta)/\mathbb{Q}(\zeta_4)$ be a 4-dimensional cyclic field extension; i.e., $[\mathbb{Q}(\zeta_4, \beta) : \mathbb{Q}(\zeta_4)] = 4$ and $1, \beta, \beta^2, \beta^3$ is a base of $\mathbb{Q}(\zeta_4, \beta)$ over $\mathbb{Q}(\zeta_4)$. Let σ be the generator of the Galois group of a field extension $\mathbb{Q}(\zeta_4, \beta)/\mathbb{Q}(\zeta_4)$ with $\sigma^k(\beta) = \zeta_4^{k-1}\beta, k = 1, 2, 3, 4$. For any element $x = x_1 + x_2\beta + x_3\beta^2 + x_4\beta^3$ with $x_k \in \mathbb{Z}[\zeta_4]$, its relative algebraic norm $\mathbb{N}_{\mathbb{Q}(\zeta_4,\beta)/\mathbb{Q}(\zeta_4)}(x)$

can be expressed as

$$\begin{aligned}
\mathbb{N}_{\mathbb{Q}(\zeta_4,\beta)/\mathbb{Q}(\zeta_4)}(x) &= \prod_{k=1}^{4}\sigma^{k-1}(x) \\
&= -x_1^4+\beta^4(x_2^4+2x_1^2x_3^2+4x_1^2x_2x_4-4x_1x_2^2x_3) \\
&+ \beta^8(4x_2x_3^2x_4-4x_1x_3x_4^2-2x_2^2x_4^2-x_3^4)+\beta^{12}x_4^4 \\
&= -x^4+\alpha(x_2^4+2x_1^2x_3^2+4x_1^2x_2x_4-4x_1x_2^2x_3) \\
&+ \alpha^2(4x_2x_3^2x_4-4x_1x_3x_4^2-2x_2^2x_4^2-x_3^4)+\alpha^3x_4^4 \\
&= -x_1^4+\alpha f(x_1,x_2,x_3,x_4,\alpha)\in\mathbb{Z}[\zeta_4], \qquad (17)
\end{aligned}$$

where

$$\begin{aligned}
f(x_1,x_2,x_3,x_4,\alpha) &= (x_2^4+2x_1^2x_3^2+4x_1^2x_2x_4-4x_1x_2^2x_3) \\
&+ \alpha(4x_2x_3^2x_4-4x_1x_3x_4^2-2x_2^2x_4^2-x_3^4)+\alpha^2x_4^4\in\mathbb{Z}[\zeta_4]. \qquad (18)
\end{aligned}$$

Similar to Theorem 4 for the three transmit antennas case, we have the following non-vanishing determinant theorem for four transmit antennas.

Theorem 6 *$X(\mathbb{Q}(\zeta_4,\beta)/\mathbb{Q}(\zeta_4),\beta,\sigma,\zeta_{16})$ where $\beta=(2\pm j)^{1/4}$ is a full rate, full diversity non-vanishing determinant code with the minimum determinant 1 and its average power at each layer is the same.*

The proof of Theorem 6 consists of two parts. In the first part, we first prove that j, $-j$, and -1 can not be a algebraic norm of any element of $\mathbb{Q}(\zeta_4,\beta)$ over $\mathbb{Q}(\zeta_4)$. Then, by Lemma 2, we know that $X(\mathbb{Q}(\zeta_4,\beta)/\mathbb{Q}(\zeta_4),\beta,\sigma,\zeta_{16})$ is a full diversity space-time code. This part constitutes Lemma 3 in the Appendix. In the second part, we prove that, for any codeword $X\in X(\mathbb{Q}(\zeta_4,\beta)/\mathbb{Q}(\zeta_4),\beta,\sigma,\zeta_{16})$, its determinant $\det(X)\in\mathbb{Z}[\zeta_4]$, which forms Lemma 4 in Appendix.

Finally, combining Lemma 3 and Lemma 4, we prove that $X(\mathbb{Q}(\zeta_4,\beta)/\mathbb{Q}(\zeta_4),\beta,\sigma,\zeta_{16})$ is a full diversity space-time code with the minimal determinant 1. Since $|\rho|=|\zeta_{16}|=1$, the average power of this code at every layer is the same. The detail of the proof is given in Appendix.

Analogously, we obtain the following theorem.

Theorem 7 *$X(\mathbb{Q}(\zeta_4,\beta)/\mathbb{Q}(\zeta_4),\beta,\sigma,\zeta_{16})$ with $\beta=(2+j)^{1/4}$ is an optimal cyclic algebraic space-time code with the same average power at each layer.*

The proof of Theorem 7 is similar to that of Theorem 5. Here we only give the outline of its proof. In order to prove this theorem, it suffices to verify that $\beta^4 = 2+j$ and $\rho^4 = j$ are the integers in $\mathbb{Z}[\zeta_4]$ with the minimal value $|\beta\rho|$ such that ρ, ρ^2, ρ^3 are not the relative norm of any elements of $\mathbb{Q}(\zeta_4, \beta)$ over $\mathbb{Q}(\zeta_4)$.

Similarly, we have the following two theorems for six transmit antennas.

Theorem 8 *The cyclic algebraic code* $X(\mathbb{Q}(\zeta_6, \beta)/\mathbb{Q}(\zeta_6), (2+\zeta_6)^{1/6}, \sigma, \zeta_{36})$ *is a full diversity, full rate, determinant non-vanishing code with the minimal determinant 1 and the average power at each layer is the same.*

Theorem 9 $X(\mathbb{Q}(\zeta_6, \beta)/\mathbb{Q}(\zeta_6), \beta, \sigma, \zeta_{36})$ *with* $\beta = (2+\zeta_6)^{1/6}$ *is an optimal cyclic algebraic space-time code with the same average power at each layer. .*

4 Simulation Results

In this section we consider a MIMO system with three transmit antennas and two receive antennas. We compare the error performance of the space-time code $X(\mathbb{Q}(\zeta_9)/\mathbb{Q}(\zeta_3), \zeta_9, \sigma, (3+\exp(j\pi/3))^{1/3})$ proposed in [18] with our proposed code $X(\mathbb{Q}(\zeta_3, 2^{1/3})/\mathbb{Q}(\zeta_3), 2^{1/3}, \sigma, \zeta_9)$. While both have non-vanishing determinants, the latter has a lower peak to average power ratio than the former, since $|\rho| = |(3+\exp(j\pi/3))^{1/3}| > 1$ in the former whereas $|\rho| = |\zeta_9| = 1$ in the latter code. Moreover, according to the diversity product criterion, the proposed code also has better codeword error performance. Our simulation results depicted in Fig. 1 show that our new code achieveds about 2dB gains over the one proposed in [18].

5 Conclusion

A systemic non-vanishing determinant space-time code design has been proposed using some cyclic field extensions. Based on the diversity product criterion, the optimal space-time codes for three, four and six transmit antennas have been obtained. We have proved that these optimal codes have the same average power at each layer and, subsequently a low peak to average power ratio.

References

[1] X. Giraud, E. Boutillon, and J.-C. Belfiore, "Algebraic tools to build modulation schemes for fading channels," *IEEE Trans. Inform. Theory*, vol. 43, pp. 938-952, May 1997.

[2] J. Boutros and E. Viterbo, "Signal space diversity: a power- and bandwidth-efficient diversity technique for the Rayleigh fading channel," *IEEE Trans. Inform. Theory*, vol. 44, pp. 1453-1467, July 1998.

[3] M. O. Damen, K. A. Meraim, and J.-C. Belfiore, "Diagonal algebraic space-time block codes," *IEEE Trans. Inform. Theory*, vol. 48, pp. 628-636, March 2002.

[4] M. O. Damen, A. Tewfik, and J.-C. Belfiore, "A construction of a space-time code based on number theory," *IEEE Trans. Inform. Theory,* vol.48, pp. 753-760, March 2002.

[5] B. A. Sethuraman, B. S. Rajan, and V. Shashidhar, "Full-diversity, high rate space-time block codes from division algebras," Partially presented in ICC'2002 and ISIT'2002. *IEEE Trans. Inform. Theory*, vol. 49, pp. 2596-2616, Oct. 2003.

[6] M. O. Damen and N. C. Beaulieu, "On two high-rate algebraic space-time codes," *IEEE Trans. Inform. Theory,* vol. 49, pp. 1059-1063, April 2003.

[7] H. El Gamal and M. O. Damen, "Universal space-time coding," *IEEE Trans. Inform. Theory,* vol. 49, pp. 1097-1119, May 2003.

[8] M. O. Damen, H. El Gamal, and N. C. Beaulieu "Systematic construction of full diversity algebraic constellations," *IEEE Trans. Inform. Theory*, 2003, to appear.

[9] S. Galliou and J. C. Belfiore, "A new family of full rate, fully diversity space-time codes based on Galois theory," *Proc. ISIT'02,* Lausanne, Switzerland, June 30-July 5, 2002.

[10] M. O. Damen, H. El Gamal, and N. C. Beaulieu, "Linear threaded algebraic space-time constellations," *IEEE Trans. Inform. Theory*, vol.49, pp. 2372-2388, Oct. 2003.

[11] X. Ma and G. B. Giannakis, "Full-diversity full rate complex-field space-time coding," *IEEE Trans. Signal Processing,* vol. 51, pp. 2917-2930, Nov. 2003.

[12] G. Wang, H. Liao, H. Wang, and X.-G. Xia, "Systematic and optimal cyclotomic space-time code designs based on high dimensional lattices," *Proc. Globecom'03*, San Francisco, Dec. 1-Dec. 5, 2003. Also, submitted to *IEEE Trans. Inform. Theory*, Feb. 2003.

[13] G. J. Foschini, "Layered space-time architecture for wireless communication in a fading environment when using multiple antennas," *AT&T Bell Labs. Tech. J.*, vol. 1, no. 2, pp. 41-59, 1996.

[14] H. El Gamal and A. R. Hammons Jr., "A new approach to layered space-time code and signal processing," *IEEE Trans. Inform. Theory*, vol. 47, pp. 2335-2367, Sept. 2001.

[15] B. Hassibi and B. M. Hochwald, "High-rate codes that are linear in space and time," *IEEE Trans. Inform. Theory*, vol. 48, pp. 1473-1484, June 2002.

[16] R. W. Heath and A. J. Paulraj, "Linear dispersion codes for MIMO systems based on frame theory," *IEEE Trans. Signal Processing*, vol. 50, pp. 2429-2441, Oct. 2002.

[17] H. Yao and G. W. Wornell, "Achieveing the full MIMO diversity-multiplexing frontier with rotatio-based space-time codes," in *Proceedings Allerton Conf. Commun., Cont., and Computing,*(Illinois), October 2003.

[18] J. C. Belfiore and G. Rekaya, "Quaternionic Lattices for space-time coding," in *Proceedings of ITW2003,* Paris, France, March 2003.

[19] J. C. Belfiore, G. Pekaya, and E. Viterbo, "The Golden Coden: A 2×2 full rate space-time code with non vanishing determinants," in *Proceedings of ISIT2004*, June 2004.

[20] G. Rekayay, J. C. Belfiorey and E. Viterbo " Algebraic 3×3, 4×4 and 6×6 Space-Time Codes with non-vanishing Determinants," to appear at *ISITA2004,* Parma, Italy, October, 2004

[21] G. Wang, and X-G. Xia, "On optimal multi-layer cyclotomic space-time code designs," in *Proceedings of ISIT2004*, June 2004.

[22] J.-C. Guey, M. P. Fitz, M. R. Bell, and W.-Y. Kuo, "Signal design for transmitter diversity wireless communication systems over Rayleigh fading channels," *Proc. IEEE VTC'96*, pp.136-140. Also in *IEEE Trans. Commun.*, vol. 47, pp. 527-537, Apr. 1999.

[23] V. Tarokh, N. Seshadri, and A. R. Calderbank, "Space-time codes for high data rate wireless communication: Performance criterion and code construction," *IEEE Trans. Inform. Theory*, vol. 44, no. 2, pp. 744-765, 1998.

[24] S. Alamouti, "A simple transmit diversity technique for wireless communications," *IEEE J. Select. Areas Commun.*, vol. 16, no. 8, pp. 1451-1458, 1998.

[25] E. Viterbo and J. Boutros, "A universal lattice code decoder for fading channel," *IEEE Trans. Inform. Theory*, vol. 45, pp. 1639-1642, July 1999.

[26] A. A. Albert, *Structure of Algebras,* AMS Colloqium Pub. XXIV,1961.

[27] S. Lang, *Algebraic Number Fields*, Springer-Verlag, New York, 1986.

[28] P. Morandi, *Field and Galois Theory*, Springer-Verlag, New York, 1996.

[29] I. Stewart and D. Tall, *Algebraic Number Theory and Fermat's Last Theorem*, 3rd Ed., A K Peters, Natick, Massachusetts, 2002.

[30] R. A. Mollin, *Algebraic Number Theory*, Chapman & Hall/CRC, 1999.

[31] J. H. Conway and N. J. A. Sloane, *Sphere Packings, Lattices and Groups*, 3rd Ed., Springer-Verlag, New York, 1998.

Appendix

Proof of Theorem 1

Here we only prove the first part of Theorem 1. The second part can be proved in the similar way. Let $x = x_1 + \beta x_2 + \beta^2 x_3, y = y_1 + \beta y_2 + \beta^2 y_3$, with $\beta = 2^{1/3}$, $x_k, y_k \in \mathbb{Z}[\zeta_3], k = 1, 2, 3$. Since $2\mathbb{Z}([\zeta_3]$ is a ideal of ring $\mathbb{Z}[\zeta_3]$, for any given x and y,i.e., $x_k, y_k \in \mathbb{Z}[\zeta_3]$, x and y can be written as follows with some integer l_0

$$x_k = \sum_{l=1}^{l_0} 2^{l-1} x_{k,l}, \qquad y_k = \sum_{l=1}^{l_0} 2^{l-1} y_{k,l}, \tag{19}$$

where $x_{k,l}, y_{k,l} \in \{0, \exp(j2p\pi/6), \sqrt{3}\exp(j\pi/6)\exp(j2p\pi/6), p = 1, \cdots, 6\}$ for $k = 1, 2, 3$ and $l = 1, \cdots, l_0$. If $\mathbb{N}_{\mathbb{Q}(\zeta_{\zeta_3,\alpha})/\mathbb{Q}(\zeta_3)}(x) = \zeta_6 \mathbb{N}_{\mathbb{Q}(\zeta_{\zeta_3,\alpha})/\mathbb{Q}(\zeta_3)}(y)$, then, from (14) we have the following equation

$$y_1^3 - \zeta_6 x_1^3 = 2\left\{\left(x_2^3 + 2x_3^3 - 3x_1x_2x_3\right) - \zeta_6\left(y_2^3 + 2y_3^3 - 3y_1y_2y_3\right)\right\}, \tag{20}$$

that is

$$\begin{aligned} y_{1,1}^3 - \zeta_6 x_{1,1}^3 &= 2\left\{\left(x_2^3 + 2x_3^3 - 3x_1x_2x_3\right) - \zeta_6\left(y_2^3 + 2y_3^3 - 3y_1y_2y_3\right)\right\} \\ &+ 2\left\{\left(3x_{1,1}^2\widetilde{x}_{1,1} + 6x_{1,1}\widetilde{x}_{1,1}^2 + 4\widetilde{x}_{1,1}^3\right) - \zeta_6\left(3y_{1,1}^2\widetilde{y}_{1,1} + 6y_{1,1}y_{1,1}^2 + 4y_{1,1}^3\right)\right\}, \end{aligned} \tag{21}$$

where $\widetilde{x}_{1,1} = \sum_{p=2}^{l_0} 2^{p-2}x_{l,p}, \widetilde{y}_{1,1} = \sum_{p=2}^{l_0} 2^{p-2}y_{l,p}$. The term on the right hand side of (21) belongs to $2\mathbb{Z}[\zeta_3]$, so does the term on the left side hand side of (21); i.e.,

$$x_{1,1}^3 - \zeta_6 y_{1,1}^3 \in 2\mathbb{Z}[\zeta_3]. \tag{22}$$

Checking (22) with

$$x_{1,1}, y_{1,1} \in \{0, \exp(j2p\pi/6), \sqrt{3}\exp(j\pi/6)\exp(j2p\pi/6), p = 1, ..., 6\}, \tag{23}$$

we can find that it is true only when $x_{1,1} = y_{1,1} = 0$. In this case, equation (21) becomes

$$y_2^3 - \zeta_6 x_2^3 = 2\left\{\left(x_3^3 + 2\widetilde{x}_{1,1}^3 - 3\widetilde{x}_{1,1}x_2x_3\right) - \zeta_6\left(y_3^3 + 2\widetilde{y}_{1,1}^3 - 3\widetilde{y}_{1,1}y_2y_3\right)\right\}, \tag{24}$$

that is

$$\begin{aligned} y_{2,1}^3 - \zeta_6 x_{2,1}^3 &= 2\left\{\left(x_3^3 + 2\widetilde{x}_{1,1}^3 - 3\widetilde{x}_{1,1}x_2x_3\right) - \zeta_6\left(y_3^3 + 2\widetilde{y}_{1,1}^3 - 3\widetilde{y}_{1,1}y_2y_3\right)\right\} \\ &+ 2\left\{\left(3x_{2,1}^2\widetilde{x}_{2,1} + 6x_{2,1}\widetilde{x}_{2,1}^2 + 4\widetilde{x}_{2,1}^3\right) - \zeta_6\left(3y_{2,1}^2\widetilde{y}_{2,1} + 6y_{2,1}\widetilde{y}_{2,1}^2 + 4\widetilde{y}_{2,1}^3\right)\right\}, \end{aligned} \tag{25}$$

where $\widetilde{x}_{2,1} = \sum_{p=2}^{l_0} 2^{p-2}x_{2,p}, \widetilde{y}_{2,1} = \sum_{p=2}^{l_0} 2^{p-2}y_{2,p}$. The term on the right hand side of (25) belongs to $2\mathbb{Z}[\zeta_3]$, so does the term on the left hand side of (25), i.e.,

$$y_{2,1}^3 - \zeta_6 x_{2,1}^3 \in 2\mathbb{Z}[\zeta_3]. \tag{26}$$

Similar to the proof for $x_{1,1} = 0$ and $y_{1,1} = 0$, we can obtain that

$$x_{2,1} = y_{2,1} = 0. \tag{27}$$

and furthermore, $x_{1,2} = y_{1,2} = x_{3,1} = y_{3,1} = 0$. Finally, we have $x = y = 0$.

Q.E.D.

Proof of Theorem 3

It can be directly verified by computation that

$$\begin{aligned}\det(X) &= \sigma(x)\sigma^2(x)\sigma^3(x) + \rho^3\sigma(y)\sigma^2(y)\sigma^3(y) + \rho^6\sigma(z)\sigma^2(z)\sigma^3(z) \\ &- \rho^3\left(\sigma(x)\sigma^2(y)\sigma^3(z) + \sigma(y)\sigma^2(z)\sigma^3(x) + \sigma(z)\sigma^2(x)\sigma^3(y)\right). \qquad (28)\end{aligned}$$

Since $\sigma(x)\sigma^2(x)\sigma^3(x) = \mathrm{N}_{\mathbb{Q}(\zeta_3,\beta)/\mathbb{Q}(\zeta_3)}(x) \in \mathbb{Z}[\zeta_3]$, $\sigma(y)\sigma^2(y)\sigma^3(y) = \mathrm{N}_{\mathbb{Q}(\zeta_3,\beta)/\mathbb{Q}(\zeta_3)}(y) \in \mathbb{Z}[\zeta_3]$, $\sigma(z)\sigma^2(z)\sigma^3(z) = \mathrm{N}_{\mathbb{Q}(\zeta_3,\beta)/\mathbb{Q}(\zeta_3)}(z) \in \mathbb{Z}[\zeta_3]$ and $\rho^3, \rho^6 \in \mathbb{Z}[\zeta_3]$, the first three terms of (28) belong to $\mathbb{Z}[\zeta_3]$. Now we only need to prove that the coefficient of ρ^3 in (28) also belongs $\mathbb{Z}[\zeta_3]$, i.e.,$\sigma(x)\sigma^2(y)\sigma^3(z) + \sigma(y)\sigma^2(z)\sigma^3(x) + \sigma(z)\sigma^2(x)\sigma^3(y) \in \mathbb{Z}[\zeta_3]$. Notice that $\sigma(x)\sigma^2(y)\sigma^3(z) + \sigma(y)\sigma^2(z)\sigma^3(x) + \sigma(z)\sigma^2(x)\sigma^3(y)$ in (28) can be rewritten as

$$\begin{aligned}&\sigma(x)\sigma^2(y)\sigma^3(z) + \sigma(y)\sigma^2(z)\sigma^3(x) + \sigma(z)\sigma^2(x)\sigma^3(y) \\ =& \sum_{l_1,l_2,l_3\in\{1,2,3\}} \beta^{l_1+l_2+l_3-3}x_{l_1}y_{l_2}z_{l_3}\left(\zeta_3^{l_2+2l_3} + \zeta_3^{l_3+2l_1} + \zeta_3^{l_1+2l_2}\right). \qquad (29)\end{aligned}$$

If $l_1 + l_2 + l_3$ is divided by 3, then, $\beta^{l_1+l_2+l_3-3}x_{l_1}y_{l_2}z_{l_3}\left(\zeta_3^{l_2+2l_3} + \zeta_3^{l_3+2l_1} + \zeta_3^{l_1+2l_2}\right) \in \mathbb{Z}[\zeta_3]$. If $l_1 + l_2 + l_3$ is not divided by 3, then, $l_1 + 2l_3, l_3 + 2l_1$ and $l_1 + 2l_2$ are not congruent to each other under modulo 3. Therefore, they run through a complete residue system of 3. As a result, $\zeta_3^{l_2+2l_3} + \zeta_3^{l_3+2l_1} + \zeta_3^{l_1+2l_2} = 1 + \zeta_3 + \zeta_3^2 = 0$. Therefore, $\sigma(x)\sigma^2(y)\sigma^3(z) + \sigma(y)\sigma^2(z)\sigma^3(x) + \sigma(z)\sigma^2(x)\sigma^3(y)$ and hence, $\det(X)$ belongs to $\mathbb{Z}[\zeta_3]$.

Q.E.D.

Proof of Theorem 5

First we prove that $X(\mathbb{Q}(\zeta_3, 2^{1/3})/\mathbb{Q}(\zeta_3), 2^{1/3}, \sigma, \zeta_9)$, $X(\mathbb{Q}(\zeta_3, 2^{1/3})/\mathbb{Q}(\zeta_3), 2^{1/3}, \sigma, \zeta_{18})$ and $X(\mathbb{Q}(\zeta_{18})/\mathbb{Q}(\zeta_6), \zeta_{18}, \sigma, 2^{1/3})$ have the same average powers. Since

$$P_{X(\mathbb{Q}(\zeta_3,2^{1/3})/\mathbb{Q}(\zeta_3),2^{1/3},\sigma,\zeta_9)} = P_{X(\mathbb{Q}(\zeta_3,2^{1/3})/\mathbb{Q}(\zeta_3),2^{1/3},\sigma,\zeta_{18})} = |2\det(G_{3,3})|^3 = 2^3|\det(G_{3,3})|^3, \qquad (30)$$

$$P_{X(\mathbb{Q}(\zeta_{18})/\mathbb{Q}(\zeta_6),\zeta_{18},\sigma,2^{1/3})} = 2 \times 2^2|\det(G_{3,3})|^3 = 2^3|\det(G_{3,3})|^3, \qquad (31)$$

and the minimum determinants of cyclic algebraic space-time codes $X(\mathbb{Q}(\zeta_3, 2^{1/3})/\mathbb{Q}(\zeta_3), 2^{1/3}, \sigma, \zeta_9)$, $X(\mathbb{Q}(\zeta_3, 2^{1/3})/\mathbb{Q}(\zeta_3), 2^{1/3}, \sigma, \zeta_{18})$ and $X(\mathbb{Q}(\zeta_{18})/\mathbb{Q}(\zeta_6), \zeta_{18}, \sigma, 2^{1/3})$ are 1, therefore, they have the same performance based on the diversity product criterion.

In the following, we will prove that any other cyclic algebraic space-time code over $\mathbb{Q}(\zeta_3)$ defined in this paper has a less diversity product than $X(\mathbb{Q}(\zeta_3, 2^{1/3})/\mathbb{Q}(\zeta_3), 2^{1/3}, \sigma, \zeta_9)$ and $X(\mathbb{Q}(\zeta_{18})/\mathbb{Q}(\zeta_6), \zeta_{18}, \sigma, 2^{1/3})$ have. From the definition of cyclic algebraic space-time codes, we know that $\beta^3 \in \mathbb{Z}[\zeta_6] = \mathbb{Z}[\zeta_3]$. Now we consider the following four cases according to the different values of β:

1. $\beta^3 \in \{\exp(j2p\pi/6), p = 1, \cdots, 6\}$.
2. $\beta^3 \in \{\sqrt{3}\zeta_{12}\exp(j2p\pi/6), p = 1, \cdots, 6\}$.
3. $\beta^3 \in \{2\exp(j2p\pi/6), p = 1, \cdots, 6\}$.
4. $|\beta^3| > 2$.

Case 1: $\beta^3 \in \{\exp(j2p\pi/6), p = 1, \cdots, 6\}$. If $\beta^3 = 1$, or $\beta^3 = -1$, then, $\beta \in \mathbb{Z}[\zeta_6)] \subset \mathbb{Q}(\zeta_6)$. So $\mathbb{Q}(\beta, \zeta_6) = \mathbb{Q}(\zeta_6)$,. In this case, β can not be used for the cyclic space-time code design. If $\beta_0^3 = \zeta_6, \zeta_6^2, \zeta_6^4$ or ζ_6^5, then, for any $|\rho^3| < 2$ with $\rho^3 \in \mathbb{Z}[\zeta_3]$, $X(\mathbb{Q}(\zeta_3, \beta_0)/\mathbb{Q}(\zeta_3), \beta, \sigma, \rho)$ can not generate any full rate full diversity space-time code. It is not difficulty to find that every element in the set $\mathcal{S} = \{\exp(j2p\pi/6), \sqrt{3}\exp(j\pi/6)\exp(j2p\pi/6), p = 1, \cdots, 6\}$ is an algebraic norm of some elements in $\mathbb{Q}(\zeta_6, \beta_0)$ over $\mathbb{Q}(\zeta_6)$. From Lemma 2, we know that $X(\mathbb{Q}(\zeta_3, \beta_0/\mathbb{Q}(\zeta_3), \beta, \sigma, \rho)$ cannot generate any full rate space-time code for $\rho^3 \in \mathcal{S}$. If choose ρ such that $|\rho|^3 \geq 2$, the average power of $X(\mathbb{Q}(\zeta_3, \beta_0)/\mathbb{Q}(\zeta_3), \beta, \sigma, \rho)$ satisfies

$$P_{X(\mathbb{Q}(\zeta_3,\beta_0)/\mathbb{Q}(\zeta_3),\beta,\sigma,\rho)} = |\rho|^9 |\det(G_{3,3})|^3 \geq 2^3 |\det(G_{3,3})|^3 = P_{X(\mathbb{Q}(\zeta_3,2^{1/3})/\mathbb{Q}(\zeta_3),2^{1/3},\sigma,\zeta_9)}. \quad (32)$$

Case 2: $\beta^3 \in \{\sqrt{3}\zeta_{12}\exp(j2p\pi/6), p = 1, \cdots, 6\}$. In this case, it is not hard to find that $\exp(j2p\pi/6), p = 1, \cdots, 6$ are algebraic norms of some elements in $\mathbb{Q}(\zeta_6, \beta)$ over $\mathbb{Q}(\zeta_6)$. To generate a full rate cyclic algebraic space-time code $X(\mathbb{Q}(\zeta_3, \beta)/\mathbb{Q}(\zeta_3), \beta, \sigma, \rho)$, ρ can not be chosen from set $\exp(j2p\pi/6), p = 1, \cdots, 6$. If choose ρ with $|\rho|^3 \geq \sqrt{3}$, the average power of $X(\mathbb{Q}(\zeta_3, \beta)/\mathbb{Q}(\zeta_3), \beta, \sigma, \rho)$ satisfies

$$\begin{aligned} P_{X(\mathbb{Q}(\zeta_3,\beta)/\mathbb{Q}(\zeta_3),\beta,\sigma,\rho)} &= |\rho|^9 |\beta|^9 |\det(G_{3,3})|^3 \geq \sqrt{3}^3 \sqrt{3}^3 |\det(G_{3,3})|^3 \\ &> 2^3 |\det(G_{3,3})|^3 = P_{X(\mathbb{Q}(\zeta_9)/\mathbb{Q}(\zeta_3),\zeta_9,\sigma,2^{1/3})}. \end{aligned} \quad (33)$$

So it can not achieve optimal cyclic algebraic space-time code in this case.

Case 3: $\beta^3 \in \{2\exp(j2p\pi/6), p = 1, \cdots, 6\}$. In this case, by Theorem 1, ζ_6, ζ_3 and ζ_3^2 are not the algebraic norms of any element of $\mathbb{Q}(\zeta_3, \beta)$ over $\mathbb{Q}(\zeta_3)$. Therefore, $X(\mathbb{Q}(\zeta_3, 2^{1/3})/\mathbb{Q}(\zeta_3), 2^{1/3}, \sigma, \rho)$ is a full diversity space-time code with diversity product 1 with $\rho^3 = \zeta_3$ or $\rho^3 = \zeta_6$. Therefore, these ρ are the numbers with smallest absolute value that make $\mathbb{Q}(\zeta_3, \beta)$ over $\mathbb{Q}(\zeta_3)$. $X(\mathbb{Q}(\zeta_3, 2^{1/3})/\mathbb{Q}(\zeta_3), 2^{1/3}, \sigma, \rho)$ has minimum determinate 1.

Case 4: $|\beta^3| > 2$. In this case, for any $\rho > 0$ with $\rho^3 \in \mathbb{Z}[\zeta_3]$, $|\rho| \geq 1$.

$$P_{X(\mathbb{Q}(\zeta_3,\beta)/\mathbb{Q}(\zeta_3),\beta,\sigma,\rho)} = |\beta|^9|\rho|^9|\det(G_{3,3})|^3 > 2^3|\det(G_{3,3})|^3 = P_{X(\mathbb{Q}(\zeta_3,2^{1/3})/\mathbb{Q}(\zeta_3),2^{1/3},\sigma,\zeta_9)}. \quad (34)$$

So the optimal cyclic algebraic space-time code can not be obtained in this case. This completes the proof of Theorem.

Q.E.D.

Proof of Theorem 6

In order to prove Theorem 6, we first establish the following Lemma 3 and Lemma 4.

Lemma 3 *For any two algebraic integers x and y of $\mathbb{Q}(\zeta_4, \beta)$, if $\mathbb{N}_{\mathbb{Q}(\zeta_4,\beta)/\mathbb{Q}(\zeta_4)}(x) = \zeta_4^k \mathbb{N}_{\mathbb{Q}(\zeta_4,\beta)/\mathbb{Q}(\zeta_4)}(y)$, for $k = 1, 2$ or 3, then $x = y = 0$, i.e., j, $-j$, and -1 can not be a algebraic norm of any element of $\mathbb{Q}(\zeta_4, \beta)$ over $\mathbb{Q}(\zeta_4)$, where $\beta = (2 \pm j)^{1/4}$.*

Proof. Here we only give the proof in the case where $\beta = \alpha^{1/4} = (2 + j)^{1/4}$ and $k = 2$. The other cases can be proved in a similar way.

For any given x, y with $x = x_1 + x_2\beta + x_3\beta^2 + x_4\beta^3$, $y = y_1 + y_2\beta + y_3\beta^2 + y_4\beta^3$, $x_m, y_m \in \mathbb{Z}[\zeta_4], m = 1, 2, 3, 4$, because $(2 + i)\mathbb{Z}[\zeta_4]$ is a ideal of ring $\mathbb{Z}[\zeta_4]$, there is an integer l_0 such that

$$\begin{aligned} x &= \sum_{l=1}^{l_0} x_{1,l}\alpha^{l-1} + \beta\sum_{l=1}^{l_0} x_{2,l}\alpha^{l-1} + \beta^2\sum_{l=1}^{l_0} x_{3,l}\alpha^{l-1} + \beta^3\sum_{l=1}^{l_0} x_{4,l}\alpha^{l-1}, \\ y &= \sum_{l=1}^{l_0} y_{1,l}\alpha^{l-1} + \beta\sum_{l=1}^{l_0} y_{2,l}\alpha^{l-1} + \beta^2\sum_{l=1}^{l_0} y_{3,l}\alpha^{l-1} + \beta^3\sum_{l=1}^{l_0} y_{4,l}\alpha^{l-1}, \end{aligned} \quad (35)$$

where $x_{m,l}, y_{m,l} \in \mathcal{S} = \{0, 1, -1, j, -j, 1+j, 1-j, -1+j, -1-j, 2, -2, 2j, -2j\}$. If $\mathbb{N}_{\mathbb{Q}(\zeta_4,\beta)/\mathbb{Q}(\zeta_4)}(x) = -\mathbb{N}_{\mathbb{Q}(\zeta_4,\beta)/\mathbb{Q}(\zeta_4)}(y)$, by (17) and (18), we have

$$x_1^4 + y_1^4 = -\alpha(f(x_1, x_2, x_3, x_4, \alpha) + f(y_1, y_2, y_3, y_4, \alpha)). \quad (36)$$

Substituting (35) into (36) yields

$$x_{1,1}^4 + y_{1,1}^4 = -\alpha(f(x_1, x_2, x_3, x_4, \alpha) + f(y_1, y_2, y_3, y_4, \alpha)) + \alpha(g(x_1, x_{1,1}) + g(y_1, y_{1,1})), \quad (37)$$

where

$$g(x_1, x_{1,1}) = \alpha^{-1}(x_1^4 - x_{1,1}^4) \in \mathbb{Z}[\zeta_4], \quad (38)$$

$$g(y_1, y_{1,1}) = \alpha^{-1}(y_1^4 - y_{1,1}^4) \in \mathbb{Z}[\zeta_4]. \quad (39)$$

Then the term on the right hand side of equation (37) belongs to $\alpha\mathbb{Z}[\zeta_4]$, so does the term on the left hand side of equation (37), i.e.,

$$x_{1,1}^4 + y_{1,1}^4 \in \alpha\mathbb{Z}[\zeta_4]. \quad (40)$$

Checking (40) for $x_{1,1}, y_{1,1} \in \mathcal{S}$, we can find that (40) is true only when $x_{1,1} = y_{1,1} = 0$. In this case,

$$\begin{aligned} x &= \beta\left(\sum_{l=1}^{l_0} x_{2,l}\alpha^{l-1} + \beta\sum_{l=1}^{l_0} x_{3,l}\alpha^{l-1} + \beta^2\sum_{l=1}^{l_0} x_{4,l}\alpha^{l-1} + \beta^3\sum_{l=2}^{l_0} x_{1,l}\alpha^{l-1}\right) = \beta\bar{x}, \\ y &= \beta\left(\sum_{l=1}^{l_0} y_{2,l}\alpha^{l-1} + \beta\sum_{l=1}^{l_0} y_{3,l}\alpha^{l-1} + \beta^2\sum_{l=1}^{l_0} y_{4,l}\alpha^{l-1} + \beta^3\sum_{l=2}^{l_0} y_{1,l}\alpha^{l-1}\right) = \beta\bar{y}, \end{aligned} \quad (41)$$

and

$$\begin{aligned} \mathbb{N}_{\mathbb{Q}(\zeta_4,\beta)/\mathbb{Q}(\zeta_4)}(x) &= \beta^4\mathbb{N}_{\mathbb{Q}(\zeta_4,\beta)/\mathbb{Q}(\zeta_4)}(\bar{x}) = \alpha\mathbb{N}_{\mathbb{Q}(\zeta_4,\beta)/\mathbb{Q}(\zeta_4)}(\bar{x}) = \alpha(x_2^4 + f(x_2, x_3, x_4, \bar{x}_1), \alpha), \\ \mathbb{N}_{\mathbb{Q}(\zeta_4,\beta)/\mathbb{Q}(\zeta_4)}(y) &= \beta^4\mathbb{N}_{\mathbb{Q}(\zeta_4,\beta)/\mathbb{Q}(\zeta_4)}(\bar{y}) = \alpha\mathbb{N}_{\mathbb{Q}(\zeta_4,\beta)/\mathbb{Q}(\zeta_4)}(\bar{y}) = \alpha(y_2^4 + f(y_2, y_3, y_4, \bar{y}_1), \alpha), \end{aligned} \quad (42)$$

where

$$\begin{aligned} \bar{x}_1 &= \sum_{l=2}^{l_0} x_{1,l}\beta^{l-2}, \qquad \bar{y}_1 = \sum_{l=2}^{l_0} y_{1,l}\beta^{l-2}, \\ \bar{x} &= \sum_{l=1}^{l_0} x_{2,l}\alpha^{l-1} + \beta\sum_{l=1}^{l_0} x_{3,l}\alpha^{l-1} + \beta^2\sum_{l=1}^{l_0} x_{4,l}\alpha^{l-1} + \beta^3\sum_{l=2}^{l_0} x_{1,l}\alpha^{l-1}, \\ \bar{y} &= \sum_{l=1}^{l_0} y_{2,l}\alpha^{l-1} + \beta\sum_{l=1}^{l_0} y_{3,l}\alpha^{l-1} + \beta^2\sum_{l=1}^{l_0} y_{4,l}\alpha^{l-1} + \beta^3\sum_{l=2}^{l_0} y_{1,l}\alpha^{l-1}. \end{aligned} \quad (43)$$

With the above notation, equation (37) becomes

$$x_{2,1}^4 + y_{2,1}^4 = -\alpha(f(x_2, x_3, x_4, \bar{x}_1, \alpha) + f(y_2, y_3, y_4, \bar{y}_1, \alpha)) + \alpha(g(x_2, x_{2,1}) + g(y_{12}, y_{2,1})). \quad (44)$$

The term on the right hand side of the equation (44) belongs to $\alpha\mathbb{Z}[\zeta_4]$, so does the term on the left hand side of equation (44), i.e.,

$$x_{2,1}^4 + y_{2,1}^4 \in \alpha\mathbb{Z}[\zeta_4]. \tag{45}$$

Following a similar step to prove $x_{1,1} = y_{1,1} = 0$ in equation (40), we can get $x_{2,1} = y_{2,1} = 0$, and furthermore, $x_{3,1} = y_{3,1} = 0$, $x_{4,1} = y_{4,1} = 0$, $x_{1,2} = y_{1,2} = 0, \cdots, x_{m,l_0} = y_{m,l_0} = 0$. Hence, we get $x = y = 0$.

Q.E.D.

Lemma 4 *For any codeword* $X \in X(\mathbb{Q}(\zeta_4, \beta)/\mathbb{Q}(\zeta_4), \beta, \sigma, \zeta_{16})$, $\det(X) \in \mathbb{Z}[\zeta_4]$.

Proof. For 4×4 matrix

$$X_1 = \begin{bmatrix} a_1 & b_1 & c_1 & d_1 \\ d_2 & a_2 & b_2 & c_2 \\ c_3 & d_3 & a_3 & b_3 \\ b_4 & c_4 & d_4 & a_4 \end{bmatrix}, \tag{46}$$

its determinant $\det(X_1)$ is

$$\begin{aligned} \det(X_1) &= a_1a_2a_3a_4 - b_1b_2b_3b_4 + c_1c_2c_3c_4 - d_1d_2d_3d_4 \\ &- (a_1a_2b_3d_4 + a_1b_2d_3a_4 + b_1d_2a_3a_4 + d_1a_2a_3b_4) \\ &+ (a_1b_2b_3c_4 + b_1c_2a_3b_4 + c_1a_2b_3b_4 + b_1b_2c_3a_4) \\ &+ (c_1d_2d_3a_4 + d_1d_2a_3c_4 + d_1a_2c_3d_4 + a_1c_2d_3w_4) \\ &- (c_1d_2b_3c_4 + c_1c_2d_3b_4 + b_1c_2c_3d_4 + d_1b_2c_3c_4) \\ &+ (b_1d_2b_3d_4 + d_1b_2d_3b_4) - (a_1c_2a_3c_4 + c_1a_2c_3a_4). \end{aligned} \tag{47}$$

So, for a codeword $X \in X(\mathbb{Q}(\zeta_4, \beta)/\mathbb{Q}(\zeta), \beta, \sigma, \rho)$ with the form of

$$X = \begin{bmatrix} x & \rho y & \rho^2 z & \rho^3 w \\ \rho^3\sigma(w) & \sigma(x) & \rho\sigma(y) & \rho^2\sigma(z) \\ \rho^2\sigma^2(z) & \rho^3\sigma^2(w) & \sigma^2(x) & \rho\sigma^2(y) \\ \rho\sigma^3(y) & \rho^2\sigma^3(z) & \rho^3\sigma^3(w) & \sigma^3(w) \end{bmatrix} \tag{48}$$

we have

$$\begin{aligned}
\det(X) &= x\sigma(x)\sigma^2(x)\sigma^3(x) - \rho^4 y\sigma(y)\sigma^2(y)\sigma^3(y) + \rho^8 z\sigma(z)\sigma^2(z)\sigma^3(z) - \rho^{12} w\sigma(w)\sigma^2(w)\sigma^3(w) \\
&- \rho^4(x\sigma(x)\sigma^2(y)\sigma^3(w) + x\sigma(y)\sigma^2(w)\sigma^3(x) + y\sigma(w)\sigma^2(x)\sigma^3(x) + w\sigma(x)\sigma^2(x)\sigma^3(y)) \\
&+ \rho^4(x\sigma(y)\sigma^2(y)\sigma^3(z) + y\sigma(y)\sigma^2(z)\sigma^3(x) + y\sigma(z)\sigma^2(x)\sigma^3(y) + z\sigma(x)\sigma^2(y)\sigma^3(y)) \\
&+ \rho^8(z\sigma(w)\sigma^2(w)\sigma^3(x) + w\sigma(w)\sigma^2(x)\sigma^3(z) + w\sigma(x)\sigma^2(z)\sigma^3(w) + x\sigma(z)\sigma^2(w)\sigma^3(w)) \\
&- \rho^8(z\sigma(w)\sigma^2(y)\sigma^3(z) + w\sigma(y)\sigma^2(z)\sigma^3(z) + y\sigma(z)\sigma^2(z)\sigma^3(w)) \\
&+ \rho^8(y\sigma(w)\sigma^2(y)\sigma^3(w) + w\sigma(y)\sigma^2(w)\sigma^3(y)) \\
&- \rho^4(x\sigma(z)\sigma^2(x)\sigma^3(z) + z\sigma(x)\sigma^2(z)\sigma^3(x)). \qquad (49)
\end{aligned}$$

Since the symmetry of the elements in (49), and $x\sigma(x)\sigma^2(x)\sigma^3(x) = \mathbb{N}_{\mathbb{Q}(\zeta_4,\beta)}(x) \in \mathbb{Z}[\zeta_4]$, $\rho^4 \in \mathbb{Z}[\zeta_4]$, we only need to prove that

$$x\sigma(x)\sigma^2(y)\sigma^3(w) + x\sigma(y)\sigma^2(w)\sigma^3(x) + y\sigma(w)\sigma^2(x)\sigma^3(x) + w\sigma(x)\sigma^2(x)\sigma^3(y) \in \mathbb{Z}[\zeta_4]$$

and

$$x\sigma(z)\sigma^2(x)\sigma^3(z) + z\sigma(x)\sigma^2(z)\sigma^3(x) \in \mathbb{Z}[\zeta_4].$$

Let $x = \sum_{m=1}^{4} x_m\beta^{m-1}$, $y = \sum_{m=1}^{4} y_m\beta^{m-1}$, $z = \sum_{m=1}^{4} z_m\beta^{m-1}$, $w = \sum_{m=1}^{4} w_m\beta^{m-1}$.

$$\begin{aligned}
& x\sigma(x)\sigma^2(y)\sigma^3(w) + x\sigma(y)\sigma^2(w)\sigma^3(x) + y\sigma(w)\sigma^2(x)\sigma^3(x) + w\sigma(x)\sigma^2(x)\sigma^3(y) \\
= & \sum_{m_1,m_2,m_3,m_4} x_{m_1}x_{m_2}y_{m_3}z_{m_4}\{\beta^{m_1}\sigma(\beta^{m_2})\sigma^2(\beta^{m_3})\sigma^3(\beta^{m_4}) + \beta^{m_2}\sigma(\beta^{m_3})\sigma^2(\beta^{m_4})\sigma^3(\beta^{m_1}) \\
& \qquad +\beta^{m_3}\sigma(\beta^{m_4})\sigma^2(\beta^{m_1})\sigma^3(\beta^{m_2}) + \beta^{m_4}\sigma(\beta^{m_1})\sigma^2(\beta^{m_2})\sigma^3(\beta^{m_3})\} \\
= & \sum_{m_1,m_2,m_3,m_4} x_{m_1}x_{m_2}y_{m_3}z_{m_4}\{\beta^{m_1+m_2+m_3+m_4-4}(j^{m_2+2m_3+3m_4} + j^{m_3+2m_4+3m_1} \\
& \qquad +j^{m_4+2m_1+3m_2} + j^{m_1+2m_2+3m_3})\}, \qquad (50)
\end{aligned}$$

where, $1 \le m_1, m_2, m_3, m_4 \le 4$. It is easy to verify that $j^{m_2+2m_3+3m_4} + j^{m_3+2m_4+3m_1} + j^{m_4+2m_1+3m_2} + j^{m_1+2m_2+3m_3} = 0$ if $m_1 + m_2 + m_3 + m_4$ is not divided by 4. Therefore, $\sigma(x)\sigma^2(y)\sigma^3(w) + x\sigma(y)\sigma^2(w)\sigma^3(x) + y\sigma(w)\sigma^2(x)\sigma^3(x) + w\sigma(x)\sigma^2(x)\sigma^3(y) \in \mathbb{Z}[\zeta_4]$ and as a result, $\det(X) \in \mathbb{Z}[\zeta_4]$.

Q.E.D.

Proof of Theorem 8

The proof of Theorem 8 can be done by establishing the following Lemma 5 and Lemma 6 and using Lemma 2 with $|\zeta_{36}| = 1$.

Lemma 5 *For any two algebraic integers x and y of $\mathbb{Q}(\zeta_6, \beta)$, if $\mathbb{N}_{\mathbb{Q}(\zeta_6,\beta)/\mathbb{Q}(\zeta_6)}(x) = \zeta_6^k \mathbb{N}_{\mathbb{Q}(\zeta_6,\beta)/\mathbb{Q}(\zeta_4)}(y)$, for $k = 1, 2, 3, 4,$ or 5, then $x = y = 0$, i.e., ζ_6^k can not be a algebraic norm of any element of $\mathbb{Q}(\zeta_6, \beta)$ over $\mathbb{Q}(\zeta_6)$, where $\beta = (2 + \zeta_6)^{1/6}$.*

Proof. Similar to the proof of lemma 3 for four transmitter antennas and using the fact that $x = y = 0$, if $x^6 - \zeta_6^k y^6 \in (2 + \zeta_6)\mathbb{Z}(\zeta_6)$, for $x, y \in \{0, \zeta_6^p, \sqrt{3}\zeta_{12}\zeta_6^p, 2\zeta_6^p, p = 1, \cdots, 6\}$.

Q.E.D.

Lemma 6 *For any codeword $X \in X(\mathbb{Q}(\zeta_6, \beta)/\mathbb{Q}(\zeta_6), (2 + \zeta_6)^{1/6}, \sigma, \zeta_{36})$, then* $\det(X) \in \mathbb{Z}[\zeta_6]$.

Proof. Similarly, the proof of this lemma can be done by using the fact that $f_1 + f_2 = 0$ if $m_1 + m_2 + m_3 + m_4 + m_5 + m_6$ is not divided by 6, where

$$f1 = \zeta_6^{m_2+2m_3+3m_4+4m_5+5m_6} + \zeta_6^{m_3+2m_4+3m_5+4m_6+5m_1} + \zeta_6^{m_4+2m_5+3m_6+4m_1+5m_2},$$

$$f2 = \zeta_6^{m_5+2m_6+3m_1+4m_2+5m_3} + \zeta_6^{m_6+2m_1+3m_2+4m_3+5m_4} + \zeta_6^{m_1+2m_2+3m_3+4m_4+5m_5}.$$

Q.E.D.

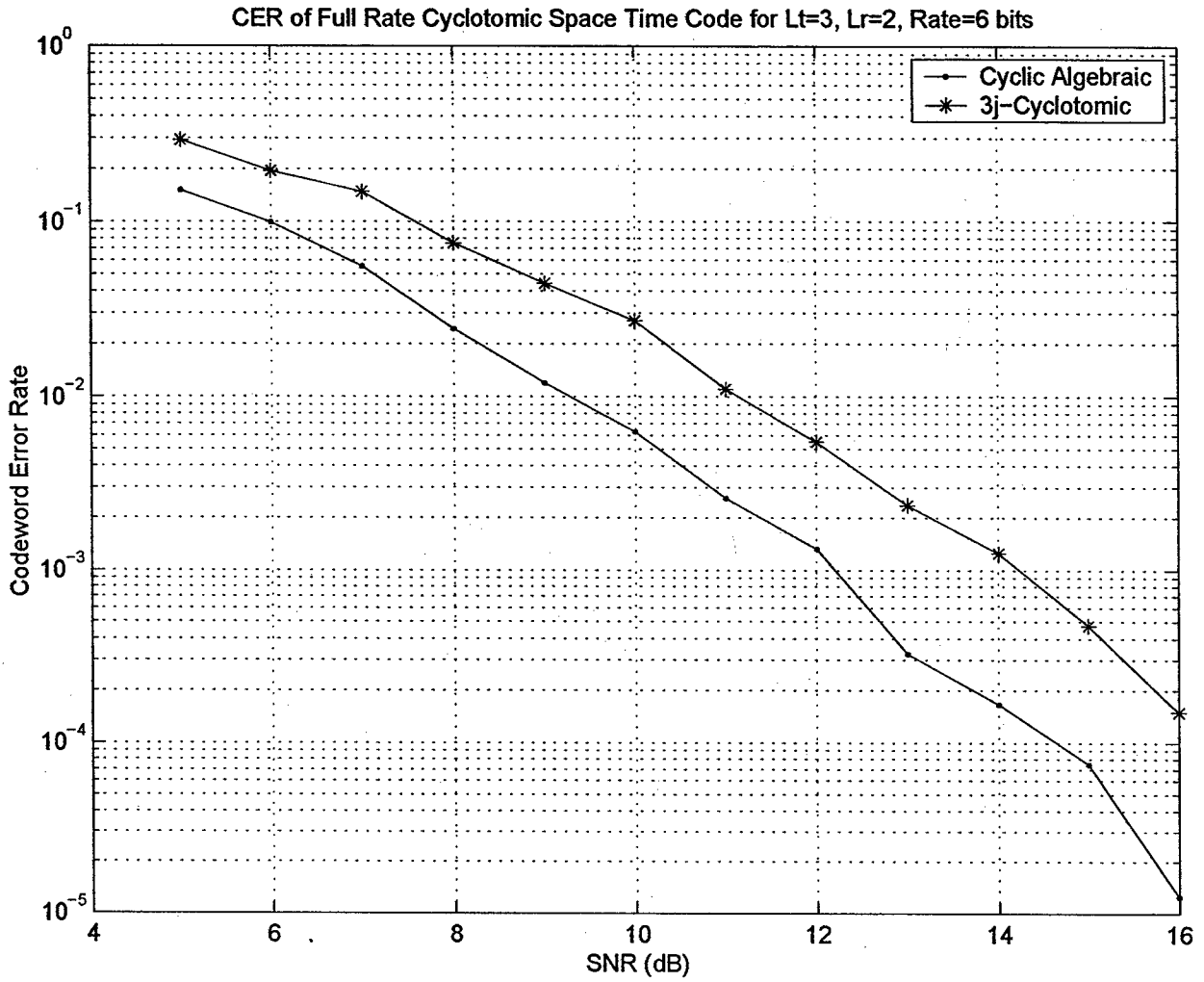

Figure 1: Codeword Error Probabilities of Cyclic Algebraic Space-Time Code and Cyclotomic Space-Time Code with Three Transmit and Two Receive Antennas.

Multi-Sensor Communications in Unmanned Surface Vehicle Networks*

Gjergji Kurti†, Yimin Zhang†, Morgan Watson‡, and Moeness Amin†

† Center for Advanced Communications
Villanova University, Villanova, PA, 19085

‡ Naval Surface Wardare Center
Philadelphia, PA 19112

Abstract

Unmanned surface vehicles (USVs) are envisioned to be a multi-mission, rapidly configurable, long endurance unmanned platform providing offboard sensor and weapon capability to perform critical missions like intelligence, surveillance, reconnaissance, anti-submarine warfare, mine countermeasures, communications, and navigation. In this paper, we consider the propagation environment and the related technology of multi-sensor communications in unmanned surface vehicle networks located in a rough sea environment. We first investigate the statistical model of the propagation environment, where we provide the analytical expressions of the wave height, the probability of having line-of-sight between two USVs in terms of the weather condition and antenna height, and the spatial correlation of the propagation channels related to different antennas. We then investigate the fading reduction capability of a multiple-input-multiple-output (MIMO) system and the performance in general Ricean channels with different channel correlations is examined. The results are important to the understanding of the communication environment where USV communications take place.

*This work was supported in part by the ONR under Grant No. N00014-04-1-0617.

1 INTRODUCTION

Unmanned surface vehicles (USVs) are envisioned to be a multi-mission, rapidly configurable, long endurance unmanned platform providing offboard sensor and weapon capability to perform critical missions like intelligence, surveillance, reconnaissance, anti-submarine Warfare, mine countermeasures, communications, and navigation. The main technical challenges during these USV missions are to provide optimal performance while being subjected to adverse motions, multi-vehicle control issues, data fusion challenges and obstacle avoidance maneuvering. Most importantly, in an autonomous environment, vehicle communications are likely subjected to fading, jamming and interference, thus subjecting the vehicle to robust and reliable communication challenges.

In this paper, we consider the propagation environment and technology of multi-sensor communications in unmanned surface vehicle networks located in a rough sea environment. We first investigate the statistical model of the propagation environment, where we provide the analytical expressions of the wave height, the probability of having line-of-sight (LOS) between two USVs in terms of the weather condition and antenna height, and the spatial correlation of the propagation channels related to different antennas. We then investigate the fading reduction capability of a multiple-input-multiple-output (MIMO) system and the performance in general Ricean channels with different channel correlations is examined. The results are important to the understanding of the communication environment where USV communications take place.

The offerings and design architectures of multi-sensor communication methodologies are then discussed. In combating channel impairment problem caused from multipath fading, diversity and array processing methods have been effectively used for many years. These methods improve the communication quality and enhance the communication quality without increasing the total transmit power or consuming additional bandwidth resources. While traditional array processing and diversity techniques use multiple antennas at the receiver and a single antenna at the transmitter (referred to as single-input-multiple-output, or SIMO, system), the development of space-time coding techniques also permits the use of multiple transmit antennas as well, resulting in more effective MIMO systems. We pointed out that, depending on the communication

characteristics, particularly the statistical distribution and spatial correlation characteristics, different multi-sensor techniques may be preferred in different fading environments to achieve robust and reliable USV networking connectivity. Analytical as well as numerical results will be provided to demonstrate the effectiveness of the multi-sensor techniques for various communication scenarios.

This paper is organized as follows. Section 2 discusses the wave height and period distributions, and their relationship to the weather status is examined. Section 3 considers the probability of sea status. The probability of having LOS is investigated in Section 4. Section 5 examines the space-time correlation coefficients between propagation channels related to different antennas. Section 6 considers the structure and advantages of MIMO systems in combating multipath fading and the bit error rate (BER) performance is examined numerically.

2 WAVE HEIGHT AND PERIOD DISTRIBUTIONS

In this section, we review the wave height and period distributions in a sea surface. Wave height and wave period are highly correlated random variables [Och98]. Therefore, in order to study the wave distribution we need to consider the joint probability of the wave height and the wave period. The simplest case is when there is a fully developed sea, which is described by the Pierson-Moskowitz (P-M) spectrum [PM64]. In this case, there is only one crest and one trough for each half-cycle of the wave. Therefore, the wave spectrum is generally considered to be narrowband. In order to simplify the problem, we introduce the following assumptions:

a. Waves are considered to be a steady-state ergodic random process;

b. Waves are a Gaussian random process with zero mean and a variance representing the sea severity;

c. The wave spectral density function is narrowband;

d. Wave peaks and troughs are statistically independent.

2.1 Wave Spectrum

The P-M spectrum is defined as [PM64]

$$S(w) = \frac{ag^2}{w^5} \exp\ \left\{-b\left(\frac{g/U}{w}\right)^4\right\}, \tag{1}$$

where w is the wave frequency, $g = 9.81\ m/s^2$ is the gravitational acceleration, U is the wind speed measured at 19.5 m above the sea surface, and $a = 8.10 \times 10^{-3}$ and $b = 0.74$ are constants. The modal frequency $\bar{w}$ and, consequently, the wave period $\bar{T}$ and the wave length $\bar{L}$, are given by a function of wind speed as

$$\bar{w} = 0.87(g/U) \tag{2}$$

$$\bar{T} = \frac{2\pi}{\bar{w}} = \frac{2\pi U}{0.87g} \tag{3}$$

$$\bar{L} = \frac{2\pi g}{\bar{w}^2}. \tag{4}$$

It is evident from Eqs. (1)–(4) that the P-M spectrum depends only on the wind speed U.

Usually, the wave spectrum and the sea state are described in terms of significant wave height H_s, instead of the wind speed U. The significant wave height H_s is defined as the average height of 1/3 of the highest waves and is computed through the following procedure: Measure the wave height for a few minutes and select 90 wave crests and record their heights; Then choose 30 highest waves and calculate the average height. A more useful definition of H_s, however, is given by the integration of the spectral density function given in Eq. (1), yielding,

$$\int_0^\infty S(w)dw = \frac{a}{4b}\frac{U^4}{g^2}. \tag{5}$$

Moreover, by assuming that the wave spectrum is narrowband, the area under the spectral density function is equal to [Och98]

$$\int_0^\infty S(w)dw = (H_s/4)^2. \tag{6}$$

Combining Eqs. (5) and (6), the following relationship can be derived between the wind speed U and the significant wave height H_s,

$$H_s = 2\sqrt{a/b}(U^2/g) = 0.21U^2/g. \tag{7}$$

Using Eqs. (1) and (7), the P-M spectrum can be expressed in terms of the significant height as

$$S(w) = 8.10 \times 10^{-3} \frac{g^2}{w^5} \exp\left\{ -\frac{0.032(g/H_s)^2}{w^4} \right\}. \tag{8}$$

Fig. 1 depicts the significant wave height H_s and the average period $\bar{T}$ versus the wind speed U for the P-M spectrum as given by Eqs. (3) and (7).

2.2 Wave Height and Wave Length

While the wave spectrum gives a general result of the sea state, it does not fully describe it. As we mentioned earlier, the wave dispersion, period and height are not statistically independent. For example, the higher the waves the longer the period. Therefore, we need to consider the joint probability density function between these variables.

Consider fully developed seas, which are assumed by the P-M spectrum, and we assume that waves are narrowband Gaussian random processes whose spectrum is highly concentrated in the vicinity of the modal frequency $\bar{w}$. To examine the bandwidth of the wave spectrum, we define a spectrum width parameter v as [LH83]

$$v = \left(\frac{m_0 m_2}{m_1^2} - 1 \right)^{1/2} = \sqrt{\frac{\mu_2}{\mu_0}} \frac{1}{\bar{w}}, \tag{9}$$

where

$$m_j = \int_0^\infty w^j S(w) dw \tag{10}$$

is the jth moment of the spectrum, and μ_0 and μ_2 are expressed as

$$\mu_0 = \int_0^\infty S(w) dw = m_0, \tag{11}$$

$$\mu_2 = \int_0^\infty (w - \bar{w})^2 S(w) dw = (m_0 m_2 - m_1^2)/m_0, \tag{12}$$

respectively.

For a general wave spectrum defined as

$$S(w) = \frac{A}{w^5} \exp\left(-B/w^4\right), \tag{13}$$

the moments can be expressed in terms of A and B as [Och98]

$$m_0 = \frac{A}{4B}, \tag{14}$$

$$m_1 = 0.306\frac{A}{B^{3/4}}, \tag{15}$$

$$m_2 = \frac{\sqrt{\pi}}{4}\frac{A}{\sqrt{B}}, \tag{16}$$

$$m_4 = \infty. \tag{17}$$

Note that the P-M spectrum is a special case of the model depicted in Eq. (13) where $A = ag^2$ and $B = b(g/U)^4$. By substituting Eqs. (14)–(16) into Eq. (9), the width of the wave spectrum defined by Eq. (13) is found to be

$$v = \left(\frac{\frac{A}{4B}\frac{\sqrt{\pi}}{4}\frac{A}{\sqrt{B}}}{(0.306)^2\frac{A^2}{B^{3/2}}} - 1\right)^{1/2} = \left(\frac{\sqrt{\pi}}{16(0.306)^2} - 1\right)^{1/2} \simeq 0.43. \tag{18}$$

Eq. (18) shows that the parameter v is a constant in this case, which is in agreement with the normalized P-M spectrum, where the frequency axis is normalized by its modal frequency $\bar{w}$ [Och98, p. 34]. Moreover, since $v < 0.6$ the narrowband assumption remains valid [LM83].

2.3 Joint Probability Function

Define

$$\zeta = \frac{H}{2\sqrt{m_0}} \tag{19}$$

as the dimensionless wave height, and

$$\eta = \frac{T}{\bar{T}} \tag{20}$$

as the dimensionless period, and let $\bar{T}$ represent the mean (average) wave period. The joint probability density function (pdf) of wave height and period in dimensionless form is given by [Och98]

$$f(\zeta,\eta) = \frac{1}{v\sqrt{2\pi}}\left(1+\frac{v^2}{4}\right)\frac{\zeta^2}{\eta^2}\exp\left\{-\frac{\zeta^2}{2}\left[1+\left(1-\frac{1}{\eta}\right)^2\frac{1}{v^2}\right]\right\}, \quad 0<\zeta<\infty, 0<\eta<\infty. \tag{21}$$

Since the P-M spectrum has a constant wave bandwidth as given by v in Eq. (18), $f(\zeta,\eta)$ is independent of the wind speed. Fig. 2 depicts the value of $f(\zeta,\eta)$ versus the dimensionless

wave height and dimensionless wave period. Moreover, the marginal pdf of wave height can be obtained from Eq. (21) as

$$f(\zeta) = \int_0^\infty f(\zeta, \eta) d\eta = \zeta \exp(-\zeta^2/2)\left(1 + \frac{v^2}{4}\right)\Phi(\zeta/v), \quad 0 < \zeta < \infty, \tag{22}$$

where

$$\Phi(u) = \frac{1}{\sqrt{2\pi}} \int_{-\infty}^{u} \exp(-u^2/2) du. \tag{23}$$

Note that, for narrowband wave spectrum, i.e., $v < 0.6$, the value of $(1 + (v^2/4))\Phi(\zeta/v)$ in Eq. (22) is very close to unity.

The most probable wave height and wave period are found, respectively, from $\partial f(\zeta, \eta)/\partial \zeta = 0$ and $\partial f(\zeta, \eta)/\partial \eta = 0$, and are expressed as

$$\zeta = \sqrt{\frac{2}{1 + v^2}} \tag{24}$$

and

$$\eta = \frac{1}{1 + v^2}. \tag{25}$$

The wave period T can be expressed in terms of the wave frequency by

$$T = 2\pi/w. \tag{26}$$

Therefore, the dimensionless wave period can be expressed in terms of the wave frequency as

$$\eta = \frac{T}{\bar{T}} = \frac{2\pi/w}{2\pi/\bar{w}} = \frac{\bar{w}}{w}. \tag{27}$$

Moreover, using the direct relationship between the wave frequency and the associated wave length expressed in Eq. (4), the dimensionless wave period can be expressed as

$$\eta = \frac{\bar{w}}{w} = \frac{\sqrt{2\pi g/\bar{L}}}{\sqrt{2\pi g/L}} = \sqrt{\frac{L}{\bar{L}}}. \tag{28}$$

3 PROBABILITY OF SEA CONDITIONS

In the previous section, we have discussed the joint pdf of the wave height and wave length which provides a general view of the probability that a certain scale of wave occurs in a given sea state. In order to fully describe the situation in a probabilistic sense, we introduce in this section the probability of the sea states that a USV is subjected to [Och98].

In general, the sea severity is a function of the frequency of occurrence of storms, water depth, wind direction, etc. Thus, there is no scientific basis for selecting a specific probability distribution function to represent the statistical properties of the sea state (or the significant wave heights). Nevertheless, data collected over the years has yielded many different distributions. It is generally accepted that a great part of the significant wave height data is well represented by the log-normal probability distribution [Och78]. However, the Weibull probability distribution is accepted when waves are high [BS86, MB90]. The generalized gamma distribution is introduced by [Och98] which has the advantage of representing both the log-normal and Weibull distributions. The pdf $f(x)$ and the cumulative distribution function $F(x)$ of the generalized gamma distribution are given by

$$f(x) = \frac{c}{\Gamma(m)} \lambda^{cm} x^{cm-1} \exp[-(\lambda x)^c], \tag{29}$$

$$F(x) = \Gamma\{m, (\lambda x)^c\}/\Gamma(m), \tag{30}$$

where $0 < x < \infty$,

$$\Gamma(m) = \int_0^\infty x^{m-1} e^{-x} dx, \tag{31}$$

$$\Gamma(m, x) = \int_0^x x^{m-1} e^{-x} dx \tag{32}$$

are gamma functions, and m, c, and λ are constants dependent to the actual sea environment.

Table 1 shows the data collected in the North Sea over a period of three years [Bou78]. For this set of data, the parameters for the generalized gamma distribution are estimated as $m = 1.60$, $c = 0.98$ and $\lambda = 1.37$. Both $f(x)$ and $F(x)$ are plotted in Fig. 3. In this case, there is a 5% probability that the significant wave height is larger than 3 m ($H_s \geq 3$ m).

4 PROBABILITY OF HAVING LOS

In this section, we consider the problem whether two USVs that are in a rough sea environment will have an LOS communication. The existence or absence of the LOS is a key factor that affects the propagation channel characteristics.

Depending on the location of the two USVs, we can classify the communication scenario into two categories: long-distance and short-distance communications. Refer to Fig. 4, the former

Table 1: Significant wave heights [Bou78].

Significant wave height (m)	No. of observations
0–0.5	1280
0.5–1.0	1549
1.0–1.5	1088
1.5–2.0	628
2.0–2.5	402
2.5–3.0	192
3.0–3.5	115
3.5–4.0	63
4.0–4.5	38
4.5–5.0	18
5.0–5.5	21
5.5–6.0	7
6.0–6.5	8
6.5–7.0	2
7.0–7.5	1
	Total 5412 in 3 years

occurs when the distance between the two USVs, L_a, is much larger than the most probable wave length, L. The latter occurs when the USVs are closer and their distance is comparable to the most probable wave length. In this paper, we only consider long-distance scenarios.

4.1 Single-Wave Scenario

We first consider a scenario where only one significant wave is present between the two USVs. Denote H_e as the height of the wave where a USV is located, and H_w as the height of the significant wave. The pdf of both H_e and H_w can be expressed by the following formula

$$f(H) = \frac{2H}{H_s} \exp\left\{-2\left(\frac{H}{H_s}\right)^2\right\}, H > 0, \tag{33}$$

where H_s is the significant wave height. Assume that the heights H_e and H_w are independent, then their joint pdf is expressed by

$$f(H_e, H_w) = \frac{2H_e}{H_s} \exp\left\{-2\left(\frac{H_e}{H_s}\right)^2\right\} \frac{2H_w}{H_s} \exp\left\{-2\left(\frac{H_w}{H_s}\right)^2\right\}, \quad H_e > 0, H_w > 0. \tag{34}$$

Denote H_a as the antenna height relative to the wave level, then the height of the antenna is $H_a + H_e$. For simplicity of analysis, we consider that the probability of having LOS between the

two USVs equals to the probability that the antennas of both USVs are higher than the peak of the significant wave. The probability that an antenna is higher than the significant wave is given by

$$\begin{aligned} P(H_a + H_e > H_w) &= \int_0^{\infty} \int_0^{H_a+H_e} f(H_e, H_w) dH_w dH_e \\ &= \int_0^{\infty} \int_0^{H_a+H_e} \frac{2H_e}{H_s} \exp\left\{ -2\left(\frac{H_e}{H_s}\right)^2 \right\} \frac{2H_w}{H_s} \exp\left\{ -2\left(\frac{H_w}{H_s}\right)^2 \right\} dH_w dH_e. \end{aligned} \tag{35}$$

Therefore, the probability of having LOS between the two USVs is a function of the antenna height H_a and the significant wave height H_s, and is expressed as

$$P[LOS] = \{P(H_a + H_e > H_w)\}^2, \tag{36}$$

where the square operation emphasizes the fact that the antennas of both USVs have to be higher than the significant wave. The results for two different sea states represented by $H_s = 2$ m and $H_s = 3$ m are depicted in Fig. 5. It is evident that the probability of having LOS is very sensitive to the antenna height H_a as well as the significant wave height H_s.

4.2 Multi-Wave Scenario

Now we consider the situation where multiple significant waves are present between the two USVs. Since the significant waves constitute of only one-third (1/3) of the waves, the number of significant waves between the two USVs is determined from the ratio between the distance between the boats, L_a, and the most probable wave length, L, as

$$N = \frac{L_a}{3L}, \tag{37}$$

where the most probable wave length L is given by Eq. (24). By using $v = 0.43$ as derived in (18), we have

$$\begin{aligned} \eta &= \sqrt{\frac{L}{\bar{L}}} = \frac{1}{1+0.43^2} = 0.844, \\ \bar{L} &= \frac{2\pi g}{0.4^2 g/H_s} = \frac{2\pi H_s}{0.4^2}. \end{aligned}$$

From these equation, we can express L in terms of H_s as

$$L = 0.844^2 \bar{L} = \frac{0.844^2 2\pi H_s}{0.4^2}. \tag{38}$$

Assume that the N significant waves are statistically independent, we can express the probability of having LOS as

$$P[LOS] = \{P(H_a + H_e > H_w)\}^{2N}. \tag{39}$$

Fig. 6 shows the $P[LOS]$ for different distances between the two boats defined by the parameter N and different sea states defined by $H_s = 2$ m and $H_s = 3$ m, respectively. The probability of having LOS decreases as the number of significant waves increases.

5 SPATIAL CORRELATION

In this section, we consider the spatial correlation between the propagation channels related to two spatially separated antennas. We first review the general concept of spatial correlation developed in a wideband Nakagami-Rice fading environment. Denote Δx as the distance between two receive antennas, denoted as Rx1 and Rx2 in Fig. 7, and B as the bandwidth of the signal. Then the wideband spatial correlation function is given by [KI00]

$$\rho_{\delta P}(\Delta x) = \frac{\int_{-\frac{B}{2}}^{\frac{B}{2}} \int_{-\frac{B}{2}-f}^{\frac{B}{2}-f} \{|\rho_{a,fx}(\Delta f, \Delta x; f)|^2\} d\Delta f df}{\int_{-\frac{B}{2}}^{\frac{B}{2}} \int_{-\frac{B}{2}-f}^{\frac{B}{2}-f} \{|\rho_{a,fx}(\Delta f, 0; f)|^2\} d\Delta f df}, \tag{40}$$

where $\rho_{a,fx}(\Delta f, \Delta x; f)$ is the space-frequency correlation coefficient between the two receive antennas with a frequency difference Δf. When the time delay and the angle-of-arrival (AOA) of a particular wave are statistically independent, $\rho_{a,fx}(\Delta f, \Delta x; f)$ can be decoupled into the frequency correlation coefficient $\rho_{a,f}(\Delta f)$ and the spatial correlation coefficient $\rho_{a,x}(\Delta x; f)$, i.e.,

$$\rho_{a,fx}(\Delta f, \Delta x; f) \approx \rho_{a,f}(\Delta f) \rho_{a,x}(\Delta x; f). \tag{41}$$

Substituting Eq. (41) into Eq. (40) simplifies the double integral into two single integrals.

Denote $p_s(\tau)$ as the normalized power delay profile. Then, $\rho_{a,f}(\Delta f)$ is given by [Cla68]

$$\rho_{a,f}(\Delta f) = \int_{-\infty}^{\infty} p_s(\tau) \exp(-j2\pi \Delta f \tau) d\tau. \tag{42}$$

Similarly, the spatial correlation coefficient $\rho_{a,x}(\Delta x; f)$ can be obtained as [KI00]

$$\rho_{a,x}(\Delta x; f) = \int_0^{2\pi} \Omega(\theta) \exp\left(\frac{j2\pi f \Delta x \cos(\theta - \theta_b)}{C}\right) d\theta, \tag{43}$$

where $\Omega(\theta)$ is the normalized angular power profile, and C is the velocity of light.

5.1 Proposed Model

We now propose a model to evaluate the value of $\rho_{a,x}(\Delta x; f)$, whose general expression is given in (43). In a rough sea, the sea surface can be described as a combination of a large number of small waves and a small number of high waves. We consider the case that a high wave with height h obstructs the LOS between the two communicating USVs, whereas a number of random smaller waves surrounding both USVs are modeled using the ring scattering model. Therefore, the propagation from a transmit antenna to a receive antenna experiences scattering as well as diffraction.

In considering the diffraction effect, the diffration edge in the top of a high wave is assumed to have an angular power profile $\Omega(\theta)$ which is composed of two components: (i) the diffraction component which is assumed to be uniformly distributed about a mean angle θ_b with a diffraction width β, and (ii) the scattering component which is assumed to be uniformly distributed over $[0, 2\pi]$. We define S as the strength between the scattered and diffracted components of the received signals. The composite angular profile for multipath waves is then given by

$$\Omega(\theta) = \begin{cases} \dfrac{1}{\beta(1+S)} + \dfrac{S}{2\pi(1+S)}, & \text{if } |\theta| \leq \dfrac{\beta}{2}, \\ \dfrac{S}{2\pi(1+S)}, & \text{otherwise.} \end{cases} \tag{44}$$

Therefore, the new spatial correlation coefficient is obtained by combining Eqs. (43) and (44), i.e.,

$$\begin{aligned} \rho_{a,x}(\Delta x; f) &= \int_0^{2\pi} \frac{S}{2\pi(1+S)} \exp\left[jk\Delta x \cos(\theta - \theta_b)\right] d\theta \\ &\quad + \int_{\theta_b - \beta/2}^{\theta_b + \beta/2} \frac{1}{\beta(1+S)} \exp\left[jk\Delta x \cos(\theta)\right] d\theta, \end{aligned} \tag{45}$$

where $k = 2\pi f/C$. The first integral in Eq. (45) is independent of θ_b and is the 0th order

first-kind Bessel function $J_0(k\Delta x)$. Therefore,

$$\rho_{a,x}(\Delta x; f) = \frac{S}{1+S} J_0(k\Delta x) + \int_{\theta_b - \frac{\beta}{2}}^{\theta_b + \frac{\beta}{2}} \frac{\exp(jk\Delta x \cos(\theta))}{\beta(1+S)} d\theta. \tag{46}$$

The second term of Eq. (46) can be analytically solved only for certain θ_b and small β. Specifically, when $\theta_b = 0$, by using the evenness of the cosine function and a Taylor series expansion, the integration reduces to

$$\int_0^{\frac{\beta}{2}} \frac{2\exp[jk\Delta x(1-\theta^2/2)]}{\beta(1+S)} d\theta = \frac{2\exp(jk\Delta x)}{\beta(1+S)} \int_0^{\frac{\beta}{2}} \exp\left[-jk\Delta x \frac{\theta^2}{2}\right] d\theta. \tag{47}$$

The expression $\int_0^{\beta/2} \exp(-jk\Delta x\theta^2/2) d\theta$ can be identified as the Fresnel integral, $F(u)$, in complex form, where $u = \sqrt{\beta^2 k\Delta x/2}$. For the special case that $S = 0$, i.e., there is no scattering component, the spatial correlation coefficient is simplified to

$$\rho_{a,x}(\Delta x; f) = \frac{|F(u)|^2}{u^2} = 1. \tag{48}$$

6 MIMO Communications

In this section, we consider MIMO communications in rough sea environment. The Ricean channel model is first described, and the MIMO performance is then investigated. Cooperative diversity is also an alternative technology in rough sea environment [ZWW04].

6.1 Ricean Channel Model

It is well known that the general model of the envelope (magnitude) of a communication channel is well represented by the Ricean distribution [UJ00, Rap02]. The Ricean distribution of an envelope is the result of a complex Gaussian channel with non-zero mean. The mean value usually corresponds to the determinant component due to direct path propagation in the presence of LOS, whereas the random component is due to multipath scattering.

The Ricean distribution of the envelope x is given by

$$p(x) = \begin{cases} \frac{x}{\sigma_0^2} \exp\left\{-\frac{x^2+A^2}{2\sigma_0^2}\right\} I_0\left(\frac{xA}{\sigma_0^2}\right), & x \geq 0, \\ 0, & x < 0, \end{cases} \tag{49}$$

where A is the peak amplitude of the determinant component and $I_0(\cdot)$ is the modified Bessel function of the first kind and zero-order. The Ricean distribution is often described in terms of

a parameter K which is defined as the ratio between the determinant component power and the variance of the random components, i.e.,

$$K = \frac{A^2}{2\sigma_0^2}. \tag{50}$$

Note that, the total power of a Ricean distributed envelope is

$$P = A^2 + 2\sigma_0^2. \tag{51}$$

In particular, when $A = 0$, i.e., there is no determinant component, the Ricean distribution reduces to Rayleigh fading.

6.2 MIMO Performance

MIMO technology has ignited a new revolution in information communications. By using multiple antennas at the two ends of a communication link, a high diversity gain is achieved, and the channel capacity between a transmitter and a receiver in a fading, scattering environment grows linearly with the number of antennas [Fos96, Tel99, FG98, TSC98].

In this paper, we consider a simple setting where each USV is equipped with two antennas. The channels between the two transmit and two receive antennas can be denoted using the following matrix

$$\mathbf{H} = \begin{bmatrix} h_{11} & h_{12} \\ h_{21} & h_{22} \end{bmatrix}, \tag{52}$$

where $h_{i,k}$ is the complex coefficient of the channel connecting the ith transmit antenna and the kth receive antenna, $i, k = 1, 2$.

As we discussed earlier, the channels are in general Ricean distributed and have correlation between them. In a Ricean channel, as the value of K increases, the random component becomes less significant and, therefore, the correlation between the channels becomes less significant. Note that the determinant components are time-invariant and, therefore, are coherent.

The performance of the MIMO system is evaluated for different sea scenarios. The Alamouti space-time code [Ala98] with quadrature phase shift keying (QPSK) modulation is used in transmitting the MIMO signals. Fig. 9 shows the bit error rate (BER) performance for different values of $K = 0, 1$, and 5, whereas for each plot, the spatial correlation coefficient ρ between the

two antennas takes values of 0, 0.5, 0.7, and 1. When $\rho = 0$ the channel are uncorrelated and when $\rho = 1$ the channels are fully correlated (coherent). The results clearly show the advantage of the MIMO system compared to the corresponding single-antenna system, particularly in low spatial correlation scenarios. When the channels are coherent, the MIMO only achieves 3 dB array gain compared to the single antenna case (Note that Alamouti code assumes no channel state information at the transmitter and, therefore, no beamforming gain is achieved at the transmitter). Therefore, it becomes clear that higher diversity gain is achieved with lower spatial correlation, which underscores the importance of having low channel correlation in a fading environment.

7 CONCLUSIONS

In this paper, we have considered the application of multiple-input-multiple-output (MIMO) technology in networked communications between unmanned surface vehicles (USVs) in a rough sea environment. Specifically, we have taken a detailed investigation in the channel modeling, which includes the wave height, period, and length. The probability of having line-of-sight between two USVs is derived, and its relationship to the antenna height and significant wave height is revealed. We then developed the spatial correlation between the propagation channels associated to two antennas in a rough sea environment. Finally, the MIMO technology is examined in such an environment, and the advantages of using MIMO technology is demonstrated. The results presented in this paper are important to the understanding of the communication environment where USV communications take place.

REFERENCES

[Ala98] Alamouti, S. M., "A simple transmit diversity technique for wireless communications," *IEEE J. Sel. Areas in Comm.*, vol. 16, no. 8, pp. 1451–1458, Oct. 1998.

[Bou78] Bouws, E., "Wind and wave climate in the Netherlands sectors of the North Sea between 53° and 54° north latitude," Scientific Report W. R. Koninklijk Netherlands Meterologisch Inst. 78–9, 1978.

[BS86] Burrows, R. and Salih, B. A., "Statistical modelling of long-term wave climates," *Proc. 20th Int. Conf. Coastal Engng.*, Taipei, vol. 1, pp. 42–56, 1986.

[Cla68] Clarke, R. H., "A statistical theory of mobile-radio reception," *Bell System Tech. J.*, pp. 957–1000, July/Aug. 1968.

[FG98] Foschini, G. J. and Gans, M. J., "On limits of wireless communications in a fading environment when using multiple antennas," *Wireless Personal Communications*, vol. 6, no. 3, pp. 311–335, March 1998.

[Fos96] Foschini, G. J., "Layered space-time architecture for wireless communications in a fading environment when using multi-element antennas," *Bell Labs Tech. J.*, pp. 41–59, 1996.

[KC97] Kalkan, M., and Clarke, R. H., "Prediction of the space-frequency correlation function for base station diversity reception," *IEEE Trans. Vehi. Tech.*, vol. 46, no. 1, pp. 176–184, 1997.

[KI00] Karasawa Y. and Iwai H., "Formulation of spatial correlation statistics in Nakagami-Rice fading environments," IEEE Trans. Antennas Propagat., vol. 48, no. 1, pp. 12–18, 2000.

[LM83] Longuet-Higgins, M. S., "On the joint distribution of wave periods and amplitudes in a random wave field," *Proc. Roy. Soc.*, London, Ser. A, 289, pp. 241–58, 1983.

[MB90] Mathiesen, J. and Bitner-Gregersen, E., "Joint distribution for significant wave height and zero-crossing period," *Appl. Ocean Res.*, vol. 12, no. 2, pp. 93–103, 1990.

[Och78] Ochi, M. K., "On long-term statistics for ocean and coastal waves," *Proc. 16th conf. Coastal Engng.*, Hamburg, vol. 1, pp. 59–75, 1978.

[Och92] Ochi, M. K., "New approach for estimating the severest sea state from statistical data," *Proc. 23rd Int. Conf. Coastal Engng.*, Venice, vol. 1, pp, 512–25, 1992.

[Och98] Ochi, M. K., *Ocean Waves: The Stochastic Approach*, Cambrige, 1998.

[PM64] Pierson, W. J. and Moskowitz, L., "A proposed spectral form for fully developed wind

seas based on the similarity theory of S. A. Kitaigorodskii," *J. Geophys. Res.*, vol. 69, no. 24, pp. 5181–80, 1964.

[Rap02] Rappaport, T. S., *Wireless Communications: Principles and Practice*, Second Edition, Prentice-Hall, 2002.

[Tel99] Telatar, I. E., "Capacity of multi-antenna Gaussian channels," *European Transactions on Telecommunications*, vol. 10, no. 6, pp. 585–595, Nov.-Dec. 1999.

[TSC98] Tarokh, V., Seshadri, N., and Calderbank, A. R., "Space-time codes for high data rate wireless communication: Performance criterion and code construction," *IEEE Trans. Inform. Theory*, vol. 44, pp. 744–765, 1998.

[UJ00] Ungan B. U. and Johnson J. T. "Time statistics of propagation over the ocean surface: A numerical study," *IEEE Trans. Geoscience and Remote Sensing*, vol. 38, no. 4, pp. 1626–1634, 2000.

[ZWW04] Zhang, Y., Wang, G., Watson, M., and Amin, M., "Cooperative wireless network for unmanned surface vehicles," *AUVSI Unmanned Systems*, Anaheim, CA, Aug. 2004.

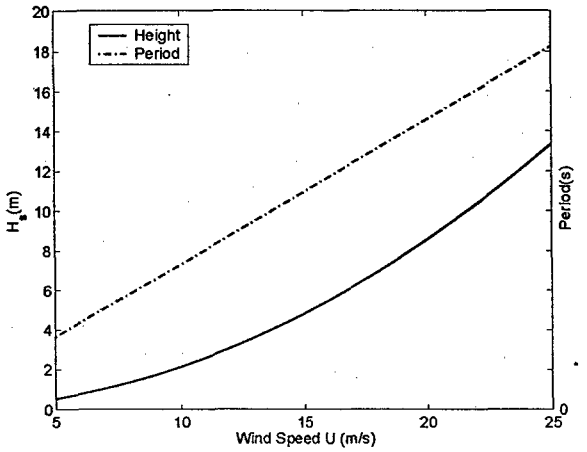

Figure 1: Significant wave height versus wind speed.

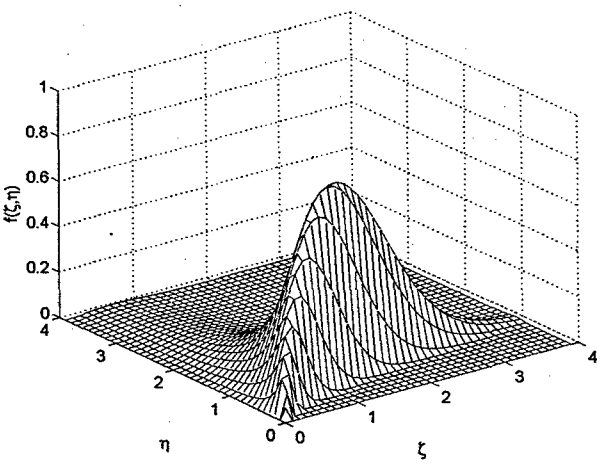

Figure 2: Significant wave height versus dimensionless wave height and dimensionless wave period.

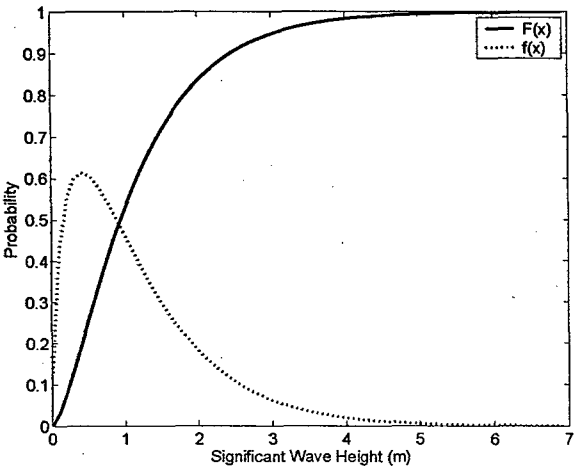

Figure 3: Cumulative distribution function of significant wave height.

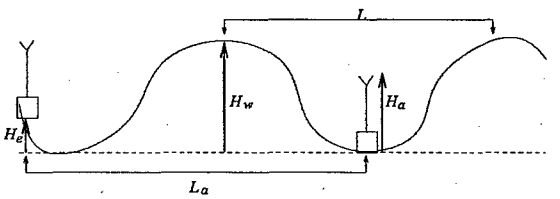

Figure 4: Model of LOS.

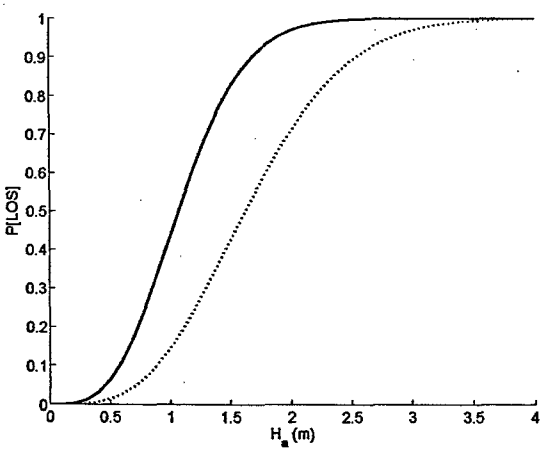

Figure 5: Probability of having $P[LOS]$ for a single significant wave.

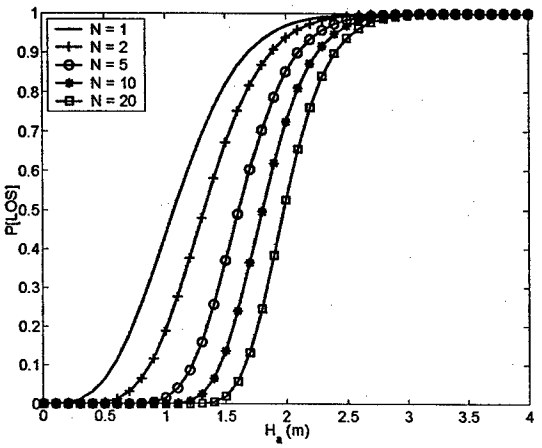

(a) $H_s = 2$ m

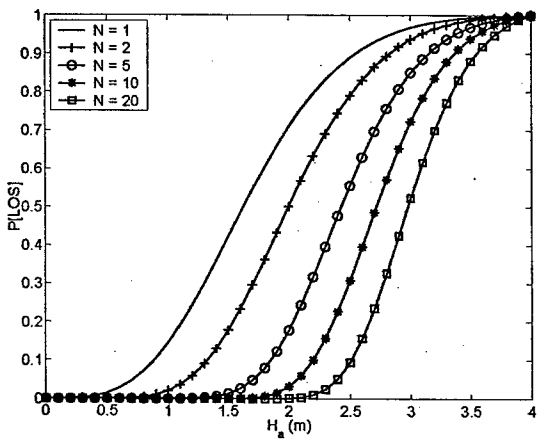

(b) $H_s = 3$ m

Figure 6: Probability of having LOS $P[LOS]$ for multiple significant waves.

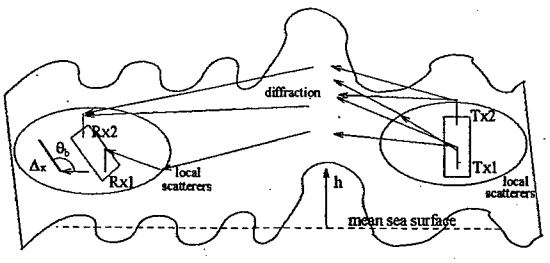

Figure 7: Illustration of the communication environment.

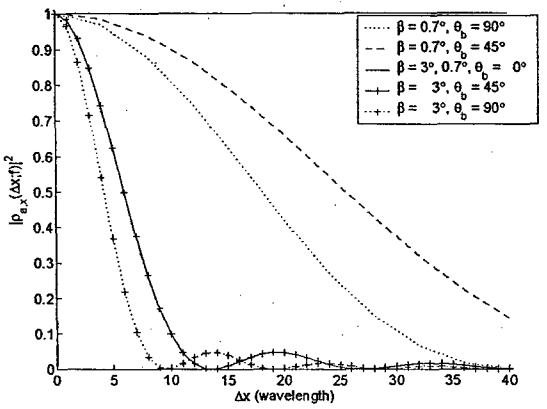

(a) S = 0

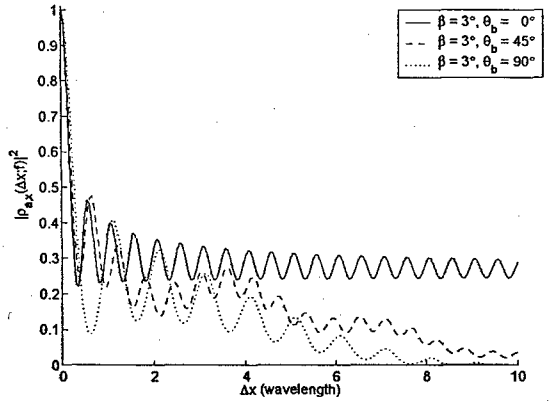

(b) S = 1

Figure 8: Spatial correlation coefficient versus Δx.

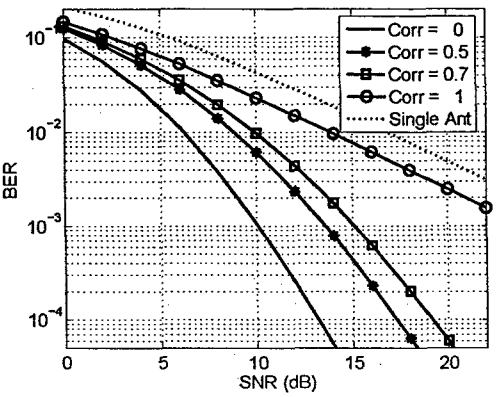

(a) $K = 0$

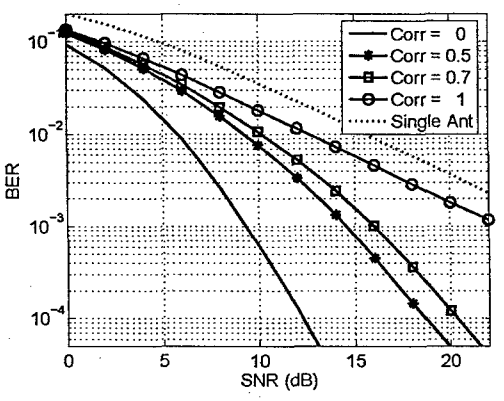

(b) $K = 1$

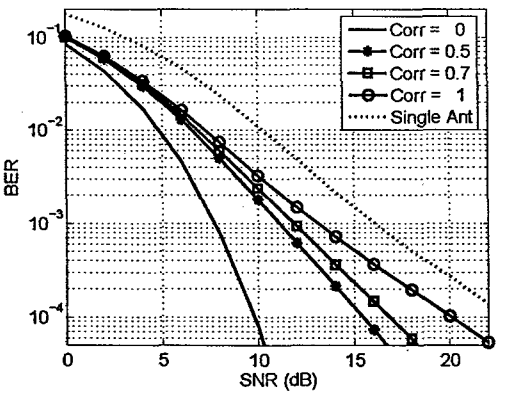

(c) $K = 5$

Figure 9: BER performance for a MIMO system (2 transmit antennas, 2 receive antennas).

REPORT DOCUMENTATION PAGE

Form Approved
OMB No. 0704-0188

PLEASE DO NOT RETURN YOUR FORM TO THE ABOVE ADDRESS.

1. REPORT DATE *(DD-MM-YYYY)*	2. REPORT TYPE	3. DATES COVERED *(From - To)*
05/08/2005	Final	June 2004 - June 2005

4. TITLE AND SUBTITLE

High Rate Multiuser Cooperative Diversity Systems

5a. CONTRACT NUMBER

5b. GRANT NUMBER

N00014-04-1-0617

5c. PROGRAM ELEMENT NUMBER

6. AUTHOR(S)

Zhang, Yimin (PI)
Amin, Moeness, G. (Co-PI)

5d. PROJECT NUMBER

5e. TASK NUMBER

5f. WORK UNIT NUMBER

7. PERFORMING ORGANIZATION NAME(S) AND ADDRESS(ES)

Villanova University
800 Lancaster Ave
Villanova, PA 19085

8. PERFORMING ORGANIZATION REPORT NUMBER

5-27730

9. SPONSORING/MONITORING AGENCY NAME(S) AND ADDRESS(ES)

Office of Naval Research
Ballston Centre Tower One
800 North Quincy Street
Arlington, VA 22217-5660

10. SPONSOR/MONITOR'S ACRONYM(S)

11. SPONSOR/MONITOR'S REPORT NUMBER(S)

12. DISTRIBUTION/AVAILABILITY STATEMENT

Approved for Public Release; Distribution is Unlimited.

13. SUPPLEMENTARY NOTES

14. ABSTRACT

The fundamental objective of this research project is to develop novel cooperative wireless network schemes and practical coding designs that provide unmanned surface vehicles (USV) swarm reliable wireless links with the overall data throughput and the communication quality significantly exceeding those of existing non-cooperative systems. Towards this end, we have made contributions in three areas: (1) We have developed a cooperation protocol that effectively constructs distributed space-time codes for cooperative diversity systems; (2) We have developed full-rate, large diversity product space-time codes with non-vanishing minimum determinant; (3) We have studied the channel modeling and spatial correlation between different antennas in sea surface environments.

15. SUBJECT TERMS

Cooperative diversity, multiple-input-multiple-output (MIMO), space-time code, unmanned surface vehicle (USV), diversity, channel model, spatial correlation

16. SECURITY CLASSIFICATION OF:			17. LIMITATION OF ABSTRACT	18. NUMBER OF PAGES	19a. NAME OF RESPONSIBLE PERSON
a. REPORT	b. ABSTRACT	c. THIS PAGE			19b. TELEPHONE NUMBER *(Include area code)*
U	U	U	UU	109	